Mobilization of radionuclides and trace metals in tailings at the Rautuvaara mining site

Mila Kristiina Pelkonen

Master's thesis

Supervisor Professor Jukka Lehto
University of Helsinki
Department of Chemistry
Laboratory of radiochemistry
June 2018

HELSINGIN YLIOPISTO
HELSINGFORS UNIVERSITET
UNIVERSITY OF HELSINKI

MATEMAATTIS-LUONNONTIETEELLINEN TIEDEKUNTA
MATEMATISK-NATURVETENSKAPLIGA FAKULTETEN
FACULTY OF SCIENCE

Tiedekunta – Fakultet – Faculty Faculty of science	Koulutusohjelma – Utbildningsprogram – Degree programme Degree Programme in Chemistry, radiochemistry	
Tekijä – Författare – Author Mila Kristiina Pelkonen		
Työn nimi – Arbetets titel – Title Mobilization of radionuclides and trace metals in tailings at the Rautuvaara mining site		
Työn laji – Arbetets art – Level Master's Thesis	Aika – Datum – Month and year 06/2018	Sivumäärä – Sidoantal – Number of pages 179

Tiivistelmä – Referat – Abstract

The old Rautuvaara mining area is located in North-West Finland, in the municipality of Kolari. Rautuvaara mine was operational between the years of 1962 and 1988 and the tailings field, located in the Niesajoki valley, was used to dispose of mine tailings from several different mines until 1995. Currently there are no mining activities at the Rautuvaara mining area, but it has become an object of interest, since an on-going mining prospect in Hannukainen is planning on transporting their produced tailings to Rautuvaara and depositing them above the existing ones. Sulphide-bearing ores and mine waste are known to form acid mine drainage (AMD) when sulphuric acid forms in the oxidative dissolution of sulphide minerals. The decreased pH in the area affected by AMD can further dissolve and mobilize harmful elements from the surroundings minerals, which may contaminate the natural water systems.

The aim of this study was to evaluate the occurrence and possible mobilization of the base metals Ni, Zn, Cu, Co, Fe, and Mn, potentially toxic metals As, Pb, Cr, and Cd, as well as the radioactive elements U-238 and Th-232, in samples collected from the Rautuvaara mining area. The collected samples included water samples from the mining area and its surroundings and four types of solid samples: enrichment sand samples from the tailings, sediment samples from the old settling pond, waste rock samples from the old mining area and acidic pond sand samples from the area of the tailings affected by AMD.

Measuring the total concentrations of metals and radionuclides in solid sample materials is not enough to understand the mobility and bioavailability of different elements and for this purpose a six-step sequential extraction procedure, with progressively increasing leaching reagents, was applied for all the solid samples. This was done in order to access the geochemical association of metals and radionuclides in the solid samples. The studied fractions were the exchangeable fraction I (pH 7,8), exchangeable fraction II (pH 5,0), mild acid-soluble fraction (pH 4,1), reducible fraction (pH 2,0), oxidizable fraction (pH 1,5) and strong acid-soluble fraction (pH 0). Gamma ray spectrometry was used to determine the total concentrations of radionuclides in the solid samples. The metal concentrations in the leaching supernatants and water samples from the mining area were determined by Inductively Coupled Plasma Mass Spectrometry. Furthermore, the behaviour of the mineral composition in the samples during extraction was studied by using Synchrotron Radiation X-ray Powder Diffraction (SR-XRPD) and by applying the Rietveld method for the acquired data.

Water analysis showed the metal concentrations in the settling pond and downstream river samples are comparable to the typical levels of the area, aside from slightly elevated base metal and uranium concentrations. The highest metal and radionuclide concentrations were seen in the acidic pond waters. Gamma ray spectrometry showed that the highest activity concentrations of U-238, Ra-226 and Pb-210 were found in the sediment samples. In the sequential extractions the total amounts of leached metals were in order of: enrichment sand, sediment, acidic pond sand and waste rock. The overall trend is that the highest amounts of metals are leached out in the oxidizable and strong acid-soluble fractions, indicating that the elements are tightly bound to the sample matrix. The dissolution of thorium and uranium was different: thorium mainly dissolved in the strong acid-soluble fraction, whereas uranium started dissolving in the mild acid-soluble fraction as the pH of the solution decreased. The sequential extraction test showed that the mobilization between the enrichment sand and acidic pond sand had been altered, possibly as an effect of AMD. The SR-XRPD data showed that the samples mainly consisted of albite, dolomite and quartz. A complete dissolution of dolomite, bassanite and calcite was seen, as well as a partial attack on pyrrhotite and pyrite, during the extractions. Also, gypsum formation happened in the mild acid-soluble leaching step as the pH decreased during the extractions.

The results can be used to evaluate the possible hazards the occurring metals and radionuclides pose to the surrounding environment and they also give a reference point of contamination for the future, if the use of the old tailings area continues.

Avainsanat – Nyckelord – Keywords
Rautuvaara, mining, mine tailings, acid mine drainage, AMD, NORM, sequential extractions, SR-XRPD, Rietveld

Säilytyspaikka – Förvaringställe – Where deposited
E-thesis

Muita tietoja – Övriga uppgifter – Additional information

Table of Contents:

1. Introduction

Mine tailings may contain high concentrations of base metals, as well as potentially toxic metals (e.g. Pb) and radioactive elements (e.g. ^{238}U). These elements constitute a threat to the surrounding environment if they are mobilized from the tailings, since they can be toxic even in low levels, and over-time bioaccumulate. Acid mine drainage (AMD) is known to increase the mobility of metals and metalloids from the sulphide-rich mine tailings. The overall aim of this master's thesis was to provide information about naturally occurring radioactive substances in the environment and the affect mining activities may have on their mobilization and bioaccumulation in the nearby ecosystems. The theory part of this master's thesis concentrates on the behavior of radioactive elements in the soils and mining tailings, their environmental effects and in some of they ways to study these properties.

The theoretical part of this master's thesis is a case study conducted at the old Fe-Cu mine of Rautuvaara. The aim of the case study was to study the occurrence and mobility of base metals Ni, Zn, Cu, Co, Fe and Mn, potentially toxic elements Pb, As, Cr and Cd, and radioactive elements ^{238}U, ^{226}Ra, ^{210}Pb and ^{232}Th, in the Rautuvaara tailings. The analytical methods used in this study consisted of gamma ray spectrometry, microwave assisted acid digestion, Inductively Coupled Plasma-Mass Spectrometry (ICP-MS), X-ray fluorescence (XRF) and Synchrotron Radiation X-ray Powder Diffraction (SR-XRPD).

The old Rautuvaara mining area was selected since an on-going mining prospect is planning on disposing their tailings waste on top of the old Rautuvaara tailings. This master's thesis is also giving a reference point of contamination for the future if the use of the old Tailings continues.

This master's thesis was done in co-operation with the Nuclear and Safety Authority of Finland (STUK), where some of the analyses were performed.

PART I: THEORY

2. Naturally occurring radionuclides

Naturally occurring radioactive nuclides are ubiquitously present in the environment and have always been a part of our world. Marie Curie discovered the first radioactive elements at the end of the nineteenth century and this led to the discovery of natural radioactive elements in the following century. There are three different kinds of naturally occurring radionuclides: primordial radionuclides, those that belong to the natural decay chains of uranium and thorium and cosmogenic radionuclides. (1) Three natural decay chains can be found in nature, and they are all headed by an isotope of uranium (^{235}U, ^{238}U) or thorium (^{232}Th). These parent nuclides were formed at the birth of the universe about 13.7 billion years ago and have such long half-lives that they are still present. (1) The parent nuclides of natural decay chains are presented in Table 1.

Table 1. Natural decay chains parent nuclides. (1) (2)

Radionuclide	**Half-life $t^{1/2}$ (years)**	**Decay mode**	**Decay energy (MeV)**	**Isotopic abundance (%)**
^{238}U	4,5 x 10^{9}	alpha	4,270	99,3
^{235}U	7,1 x 10^{8}	alpha	4,678	0,72
^{232}Th	1,41 x 10^{10}	alpha	4,081	99,9995

All these parent nuclides commence a chain of radioactive decay which end up with a stable isotope of lead: ^{207}Pb, ^{206}Pb and ^{208}Pb. Overall the decay chains consist of 42 radionuclides of 13 different elements and the most important ones in terms of radiation exposure to humans are the isotopes of radium, radon, lead and polonium in uranium decay series. (1) (2) All of the natural decay chain nuclides are alpha and beta emitters and their determination requires radiochemical separation. (1) Primordial radionuclides, which also include the parent nuclides of the natural decay chains, can be described as single occurring long-lived elements. The most common and easily detected of the primordial nuclides is ^{40}K ($t_{1/2}$ =1.26 x 10^{9} years), which is a gamma emitter and can be measured without chemical separation. Primordial radionuclides, like uranium and thorium, were created in the cosmic processes at the birth of the universe. (1) These radionuclides were present long before the formation of the solar system and when the earth's crust was formed they became trapped in rock minerals. (2) The third class of naturally occurring radionuclides is the cosmogenic radionuclides, which form in the upper parts of the

atmosphere due to cosmic radiation. These formed radionuclides either become trapped with particles in the air and get deposited on the ground or are in gaseous form (like ^{14}C in carbon oxide). (1)

2.1 Chemistry of naturally occurring radionuclides

The distribution and behavior of radionuclides depend greatly on their physical and chemical properties. This chapter describes some of the most important of the naturally occurring radionuclides and gives a description of their different properties and reactions.

2.1.1 Uranium

Uranium is part of the actinide group and has three isotopes in nature: ^{238}U, ^{235}U and ^{234}U with isotopic abundances of 99.28 %, 0.72 % and 0.005 %, respectively. All the natural uranium isotopes are alpha emitters. In solutions uranium has four oxidation states: +III, +IV, +V and +VI, of which the +IV and +VI states are the most stable. Due to the high charge of the elements +V and +VI states do not occur as free ions in the solutions and prefer to form uranyl species: UO_2^+ and UO_2^{+2}. The state +III occurs only under very reducing conditions and is oxidized quickly in aqueous solutions. The +V form of uranium has a very narrow redox potential range and is not thermodynamically stable; therefore, in nature it is either oxidized into +VI form or transformed through disproportionation into +IV and +VI. The tetravalent form of uranium is chemically immobile, but oxidizes slowly to the hexavalent form in solutions. The hexavalent form of uranium is the more stable one as can be seen from the Eh – pH diagram presented in Figure 1, which shows the occurrence of UO_2^{2+} with its hydrolysis species over a wide range of pH's in oxidizing conditions. It can also be seen that in reducing conditions the dominating species is the insoluble UO_2, which becomes unstable as the redox conditions become oxidizing. (1)

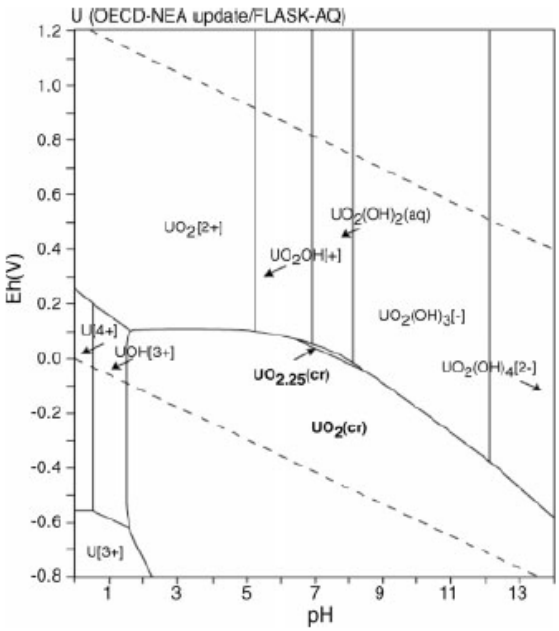

Figure 1. Eh – pH –diagram of uranium in 10^{-10} solution. (3)

Uranium forms strong complexes with fluoride and ligands containing free electron pair at oxygen or nitrogen. Complexes with other halides are also formed thus they are somewhat weaker. Oxyanion complex strength decreases in the order $PO_4^{3-} > CO_3^{2-} > SO_4^{2-} > NO_3^-$. (1) The dominant species of uranium complexes are carbonate species, which are formed in neutral and alkaline conditions. (1) (4) Different carbonate complexes of uranium in relation to pH are presented in Figure 2.

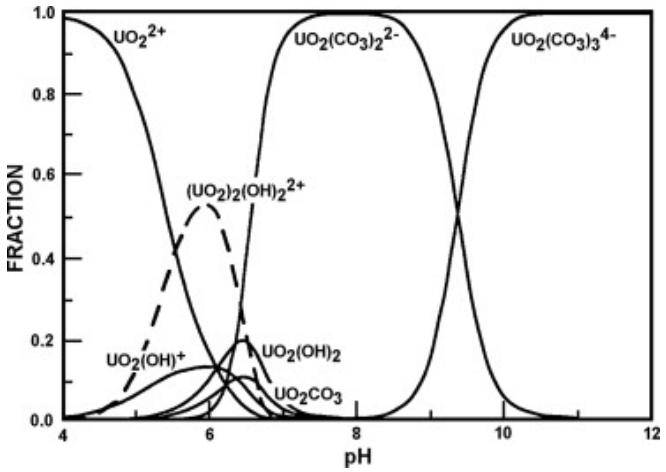

Figure 2. Distributions of uranium carbonate complexes in surface waters under normal atmospheric pressure at different pH. (2)

Between pH 6.5 to 8 the most prevailing species is $UO_2(CO_3)_2^{2-}$, which is also the dominant species in Finnish ground waters. (4) At pH 6 the most stable one is UO_2CO_3 and at a pH level higher than 8 the tricarbonate species start to appear. Anionic carbonate species are the most soluble and mobile ones. (1)

From the natural ligands, the most important complexing agents of uranium are humic and fulvic acids, which can solute, transport and reprecipitate it in natural waters. This complexation is pH dependent since the degree of ionization of humic and fulvic acids can be changed with varying pH. (4) The humic substances, for example, can be adsorbed onto clay soil particles forming organic coatings that can mask the original grain surface and its surface charge leading into altered reactivity with respect to metals, like uranium. U(VI)-humate complexes have such a high stability that they can make the humic colloids a rapid transport vehicle which improves the migration of uranium in nature. (5)

The global average concentration of uranium in the lithosphere is 2.3 ppm and its distribution is reasonably even. In Finland the corresponding concentration is 4 ppm and varies with the dominating rock type. In nature uranium forms over 200 minerals from which only few are found as ores. The most important ore minerals are uraninite (UO_2) and carnotite ($K_2(UO_2)_2(VO_4)_2 \cdot 3H_2O$). In the uraninite uranium can be partly oxidized forming a mineral called pitchblende (UO_{2+x}), which is a mixture of UO_2 and UO_3. The oxidization state of uranium in uraninite is +IV and in carnotite +VI. Uranium ores are formed when oxic ground waters carrying +VI uranium complexes meet more reducing anoxic conditions and uranium is reduced back to non-soluble +IV form, leading to an enriched geological barrier. Most common cause of reducing condition is the presence of pyrite mineral or organic matter. (1) Different uranium and thorium contents present in different rock types are described in Table 2.

Table 2. Varying uranium and thorium contents found in different rock types. (4)

Rock type	Name	Uranium (ppm)	Thorium (ppm)
Igneous	granites granodiorities, rhyolites	2,2 – 6,1	8 – 33
	gabbros	0,8	3,8
	basalt	0,1 - 1	0,2 - 5
Metamorphic	granulites	4,9	21
	gneiss	2,0	5 – 27
	schist	2,5	7,5 – 19
	slate	2,7	7,5
	phyllite	1,9	5,5
Sedimentary	shales (black)	3 – 1250	-
	bauxite	11,4	49
	phosphates	50 – 300	1 – 5
	peat	1 – 12	1 – 5
	limestone	2	0 – 2,4

The occurrence of uranium in ground waters in dependent on various factors e.g. the presence of uranium minerals in the bedrock. The concentrations vary throughout the world reaching as high as milligrams per liter. In seawater the usual concentration is between 2 - 4 ppb, while the reported values for other waters vary between 0.1 ppb to 1 ppm. (1)

2.1.2 Thorium

Thorium is also an actinide metal and has six naturally occurring isotopes: ^{227}Th, ^{228}Th, ^{230}Th, ^{231}Th, ^{232}Th and ^{234}Th. The half-lives of thorium isotopes in years are 0.051, 1.91, 75 400, 0.0029, 1.4×10^{10} and 0.066, respectively. (1) ^{232}Th is the most abundant species in the nature with close to hundred percentage abundance. From the natural isotopes of thorium ^{231}Th and ^{234}Th are beta emitters, while the others decay through alpha emission. The activity of ^{232}Th can be measured through its granddaughter ^{228}Ac by gamma spectrometry if they can be expected to be in secular equilibrium. (1)

The chemistry of thorium follows that of group 4 metals (e.g. Ti, Zr and Hf), therefore it only has one oxidation state +IV and can work as a chemical analog for other tetravalent actinide ions. Speciation of thorium is presented in Figure 3.

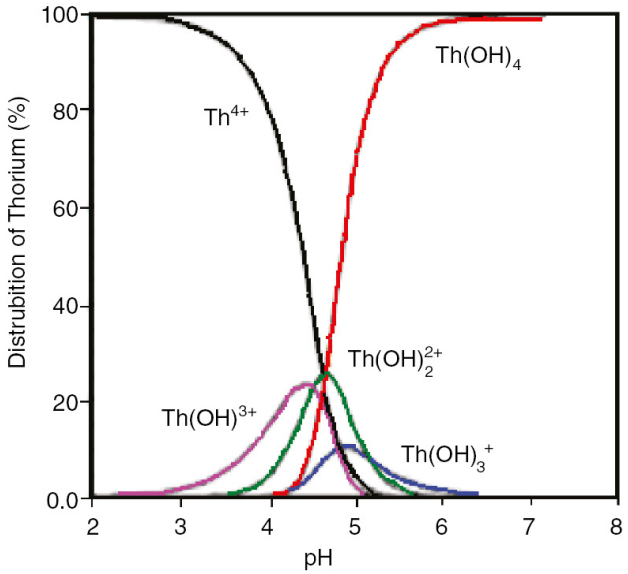

Figure 3. Different thorium species in 0.1 M solution. (6)

Thorium hydrolysis starts at pH 1 with the formation of mono-, di- and trihydroxy species. At pH 4, $Th(OH)_4$ becomes the predominant species in the solution. At high concentrations thorium forms polynuclear species, for example $[Th_2(OH)_2]^{6+}$, and colloidal complexes. (1) In general, thorium solubility is low: the most soluble element being the amorphous $Th(OH)_4$ and the least soluble - the crystalline ThO_2. Thorium is known to form complexes with fluoride, sulfate, phosphate and carbonate. (1)

The average concentration of thorium in the earth's crust is 8 ppm, which is about 4-5 times that of uranium and almost as abundant as lead. Thorium is mainly distributed evenly in the overburden and bedrock and only has two pure minerals, thorianite (ThO_2) and thorium silicate ($ThSiO_4$), which occur rarely and mostly mixed with uranium. Most of the thorium occurs in the lanthanide phosphate mineral called monazite. In natural waters thorium concentrations vary from 10^{-8} M to 10^{-9} M: in seawaters the concentration is approximately 1.5 ng L^{-1} and in oxic ground waters 1 µg L^{-1}. (1)

Overall, the chemistry of thorium is quite straightforward. However, factors like low solubility and strong absorption on surfaces makes its research rather demanding, when compared to other actinides. (1)

2.1.3 Lead

Lead is a post-transitional metal belonging to the 15th group in the periodic table of elements and has four stable isotopes ^{204}Pb, ^{206}Pb, ^{207}Pb and ^{208}Pb, the latter three being the final nuclides in the natural decay chains of uranium and thorium. Natural decay chains also contain four radioactive isotopes of lead, of which only one has a long half-life (^{210}Pb: $t_{1/2}$= 22y) and the others vary between 0.5 and 11 hours. (1) ^{210}Pb belongs to the uranium series and is a granddaughter nuclide of the gaseous ^{222}Rn, which can escape the bedrock and decay in the atmosphere. This leads to dry and wet depositions of ^{210}Pb and its daughter ^{210}Po to the top layers of soil. (7)

Chemistry of lead is fairly similar to that of tin. Normally lead exists at oxidization state +II, but under oxidizing conditions state +IV can occur. (1) Figure 4 presents the different species of lead over different Eh and pH range. Lead hydrolysis at the pH higher than 6 leads to the formation of $Pb(OH)^+$ and $Pb(OH)_2$. (4) In alkaline pH lead is precipitated as $Pb(OH)_2$ and then dissolved back into the solution as $Pb(OH)_4^{2-}$ when the pH of the solution reaches 13. (1)

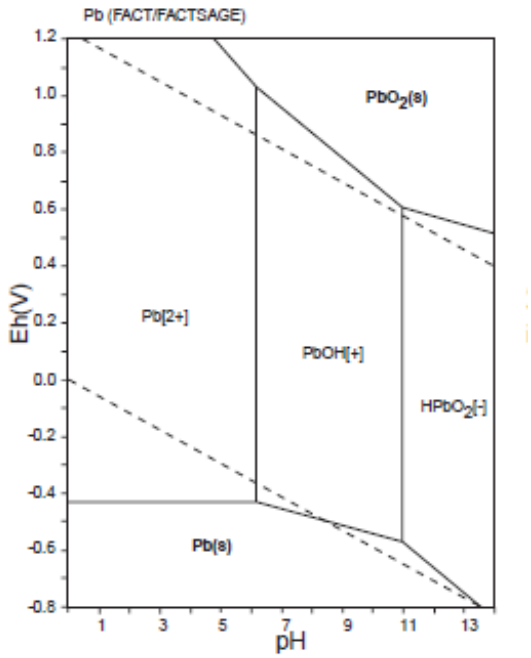

Figure 4. Eh – pH –diagram of lead in 10^{-10} solutions. (3)

Most of the formed lead compounds are sparingly soluble: $PbCO_3$, $2PbCO_3 \cdot Pb(OH)_2$, $PbSi_2O_3$, $Pb_2Si_2O_7$, PbS and $PbSO_4$. Only acetate, nitrate, chlorate and perchlorate compounds of lead can be dissolved in water. (1)

The average lead concentration in the earth's crust is 13 ppm meaning is it widely occurring. (1) In groundwater inorganic lead can form complexes with organic matter and thus get deposited onto particles. Organic compounds of lead are usually mobile in ground water. Only in very saline waters can lead form chlorine complexes, like $PbCl_2$ (aq), which are soluble over a wide pH range. (4)

2.1.4 Radium

Radium has four isotopes in nature which all belong to the natural decay series: ^{223}Ra, ^{224}Ra, ^{226}Ra and ^{228}Ra. The first three are alpha emitters and the last decays through beta emission. The most important of these are ^{226}Ra ($t_{1/2}$ = 1600 a) and ^{228}Ra ($t_{1/2}$ = 5,8 a), which belong to the decay chains of ^{238}U and ^{232}Th, respectively. In the periodic table of elements radium belongs to the alkaline earth metals (group 2), which are generally at oxidation state +II and form M^{2+} ions in aqueous solutions. (1) In waters of low salinity radium occurs as Ra^{2+} ions and it has weak complexing abilities with chlorine, sulphate and carbonate anions when the salinity increases. (4) Radium hydrolyses more readily than group 1 elements, while its hydroxides are soluble and do not precipitate. This property can be used in the separation of radium from other hydrolysable metals. Radium does not form coordination complexes with organic matter, due to the missing vacancies on its electron shells. (1) The chemistry of radium closely follows that of barium since they have similar ionic radii and, often when there is no data available for radium, barium can be used as a chemical analogue for it. (8) Predicted from the behavior of barium the colloidal transportation of radium should occur. (4) The solubility products of barium, which can be expected to correspond to those of radium, are presented in Table 3.

Table 3. Solubility products of barium, which acts as chemical analogue for radium due to the similarities in their ionic radii. (1)

Product	Solubility
$BaCO_3$	5.1×10^{-9}
$Ba(OH)_2$	soluble
BaC_2O_4	2.3×10^{-8}
$BaSO_4$	1.1×10^{-10}
$BaCrO_4$	2.2×10^{-10}
$Ba_3(PO_4)_2$	3×10^{-23}

In soils and ground waters the average concentration of radium varies according to the bed rock composition and the factors influencing its transport e.g. solubility, complexation and adsorption properties. (4)

2.1.5 Polonium

Natural decay chains contain seven polonium isotopes: ^{210}Po, ^{211}Po, ^{212}Po, ^{214}Po, ^{215}Po, ^{216}Po and ^{218}Po. The longest lived and most important of these is ^{210}Po, which has a half-life of 138 d. Polonium always occurs in nature since it is in equilibrium with its parent nuclide ^{210}Pb, which decays through ^{214}Bi by beta emission, as can be seen from Figure 5. Other naturally occurring isotopes of polonium have half-lives between 0.3 ps and 3 min. Due it's the short half-life the concentrations of polonium at the best are very small invisible amounts so the straight determination of its chemical nature is impossible and has been estimated from the elements that coprecipitate with it. Polonium in milligram amounts is also highly radiotoxic and had a high heat production. Polonium is pure alpha emitter and due to this its analysis needs separation. The only method used for the separation of polonium is its spontaneous deposition onto a silver or nickel disk. (1)

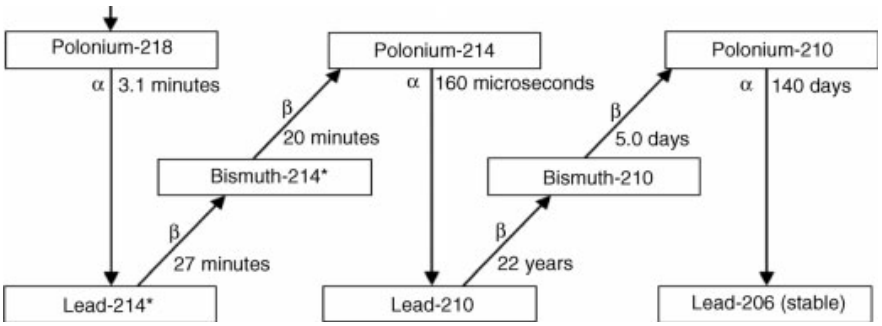

Figure 5. Polonium in natural uranium series after ^{222}Rn. (1)

Polonium has oxidation states –II, +II, +IV and +VI. The oxidation state of +IV is the most common and stable of them and can form oxides PoO_2 and $PoO(OH)_2$. The oxidation state +II only appears in reducing conditions. (1) The Eh – pH –diagram of polonium is presented in Figure 6.

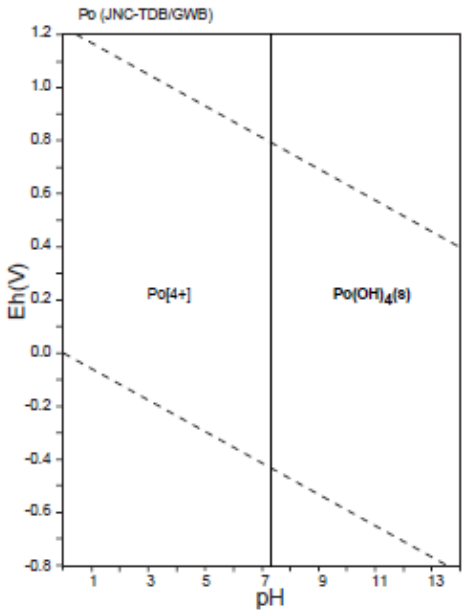

Figure 5. The Eh – pH –diagram of polonium in 10^{-10} solution. (3)

As can be seen from Figure 5 polonium appears as Po^{4+} in acidic solutions where it has the potential to form complexes with acid anions like $PoOCl_4^{2-}$. Hydrolysis of polonium starts at pH above 2.5, and $Po(OH)_4$ appears at pH 7. At pH's higher than this polonium can form negative colloidal hydrolysis products and eventually dissolve at pH 12 as PoO_3^{2}. (1) The hydroxyl species of polonium can be adsorbed into inorganic and organic colloids. (4)

In natural waters polonium is sparingly soluble due to its oxidation state +IV and it easily forms complexes and adsorbs onto different surfaces. (9) Polonium concentrations in the nature are so low that the formation of intrinsic colloids is not likely. (4) Polonium has a high boiling point of 962 ºC, however it becomes volatile quite easily due to reasons yet unknown to science. Due to this the only option to decompose a sample for polonium analysis is wet ashing. (1)

2.2 Binding mechanisms of radionuclides in soils

Soil is a complex heterogenic material that consists of solid material (minerals and organic matter) as well as liquid and gas phases. (7) In soils both the mineral and organic matter take part in retaining the anionic and cationic substances with their functional groups. Sorption reactions can vary depending on the retaining phase and the chemical properties of solute and soil solution. Sorption can happen through outer or inner sphere complexation. (10)

Organic substances can be divided into two groups, which are non-humic and humic substances. Non-humic substances consist, for example, of simple carbohydrates, proteins, lignin and amino acids and have a chemically identifiable composition. Humic substances have extremely complex structures, which cannot be identified, and they are only weakly affected by microbial degradation. Humic substances can be divided in to three categories: fulvic acids, humic acids and humins. (10) These three categories are presented in Table 4.

Table 4. Humic substances. (7)

Humic substance	**Properties**
Fulvic acids	1. Soluble in acidic conditions 2. Soluble in alkaline conditions 3. Slightly affected by microbial degradation 4. Smallest molecular mass
Humic acids	1. Insoluble in acidic conditions 2. Soluble in alkaline conditions 3. Middle range molecular mass
Humins	1. Insoluble in both acidic and alkaline solutions 2. Most resistant towards the microbial degradation 3. Largest molecular mass

The organic matter of soil has a large surface area (800 – 900 m^2 g^{-1}) and it holds most of the soil cation exchange capacity due to the wide range of neutral, acidic and basic functional groups. (7) (10) The neutral groups are often polar, not ionizing and contain oxygen, while the acidic ones have a negative charge from deprotonation. Basic groups normally contain nitrogen. Acidic and basic functional groups are able to attract cations or anions, respectively, from the solution by charge formation. Retention of cations and anions by soil organic matter happens through the unspecific outer sphere complexation,

excluding H^+ ions that retain specifically. As the charge/radius ratio increases so does the affinity of outer sphere complexed ions on soil organic matter functional groups. (10)

As was mentioned before, minerals also have the ability to retain cations and anions in soil. Minerals are inorganic components, which depending on their type can have either crystalline or amorphous structure. The retention ability of minerals depends on their surface properties (e.g. functional groups) as well as on the characteristic of the solutes. (10) Figure 6 represents the effect of solution pH on the minerals surface retention ability.

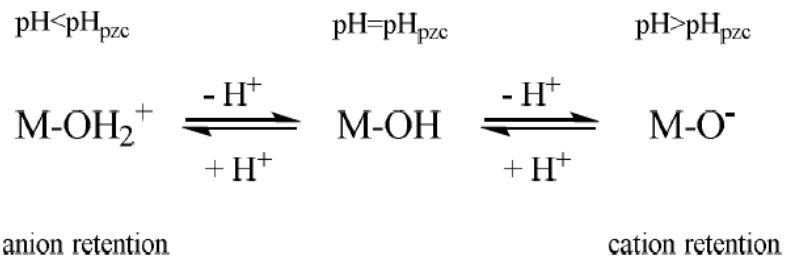

Figure 6. The effect of solution pH has on the mineral surface retention ability. (M = metal cation with hydroxyl group, pzc = pH point of zero charge) (10)

As can be seen from Figure 6 when the pH of a solution is low compared to the pH_{pzc} then the surface binds negatively charged anions and when it is higher than that of the pH_{pzc} it favors positively charged cations. When pH is equal to the pH_{pzc} the concentration of negatively and positively charged groups is equal. (10)

Ion retention happens through outer sphere complexation (ion exchange) when the interaction is due to electrostatic attractions between the opposite charges in the solute and the functional group on the mineral surface. In the solution the solutes have a hydration sphere around them that is made of water molecules, which are oriented in a way that their oppositely charged dipole points towards the solutes charge. This leads to a case where in outer sphere complexation the solute and the functional group on the mineral surface are always separated at least by the thickness of one water molecule (0.3 nm) and no direct bond is formed. Outer sphere complexation can be affected by changes in soil pH and composition leading into desorption reactions. (10)

Inner sphere complexation happens when a direct chemical bond is formed and the hydration sphere around the solute is partly or completely lost. Anions of weak acids form bonds between the oxyanions oxygen and metal cation of the surface. For the solute cations the inner sphere complexation happens between the solute metal cation and the

oxygen on the functional group on the mineral surface. Inner sphere complexation can retain anions stronger than outer sphere complexation, since the replacing oxyanions need to have a higher pK_a value than the species retained. Inner sphere complexation can also occur in the interlayer space of clay and mica minerals. (10)

Clay and mica minerals have a pH-dependent charge but also a permanent negative charge, due to isomorphic substitution of cations with lower positive charge (e.g. $Si^{4+} \rightarrow Al^{3+}$), and interlayer bonding of exchangeable cations balances it. (10) Clay minerals have a layered structure and they are especially good at retaining mono and divalent cations like $^{90}Sr^{2+}$ and $^{226}Ra^{2+}$. (7)

Soil minerals, together with weakly crystalline aluminum and iron oxides, have a significant amount of reactive hydrogen groups, which play an important role in soil sorption for oxyanions. The number of structural metal atoms affects the acidity of these hydroxyl groups as well as the bond strength of the M-OH bond and on the ability of the central metal cation to attract a shared pair of electrons (electronegativity). As the acidity decreases, with the decreasing variables, the ability of the functional group to stay protonated at higher pH values increases as well as their anion retaining ability when compared to ones with lower pK_a values. For example, Si-OH groups ($pK_a \approx 3$) in a naturally relevant pH range are exhibited as $Si\text{-}O^-$ and only take part in cation retention, as Fe-OH and Al-OH groups ($pK_a \approx 8\text{-}9$) take part in anion inner and outer sphere complexation reactions over a wide pH range. (10) Radionuclides and metals can also be retained in soils by precipitation from the supersaturated soil solution. Supersaturation can occur due to pH, temperature or redox condition changes. (7)

2.3 Radionuclides speciation and transfer in the environment

Over the years radionuclides have been released into the environment from radiological and nuclear sources. (11) When this happens, the ecosystem is affected by radioactive contamination. The impact of the contamination depends on the source and release conditions (e.g. nuclear and radiological sources), deposition and ecosystem transport, which includes the biological uptake of radionuclides by organisms and the following effects that they may cause. (12) In order to assess the total impact it is necessary to obtain information about speciation and mobilization instead of just measuring the whole concentrations of pollutants. (13) Radionuclides are often released with other pollutants (e.g. heavy metals) causing multiple stressor situations for the ecosystem that can cause a wide variety of interactions leading to various combined biological effects. (14) The different variables influencing the "exposure – biological effect" -outcome are presented in Figure 7.

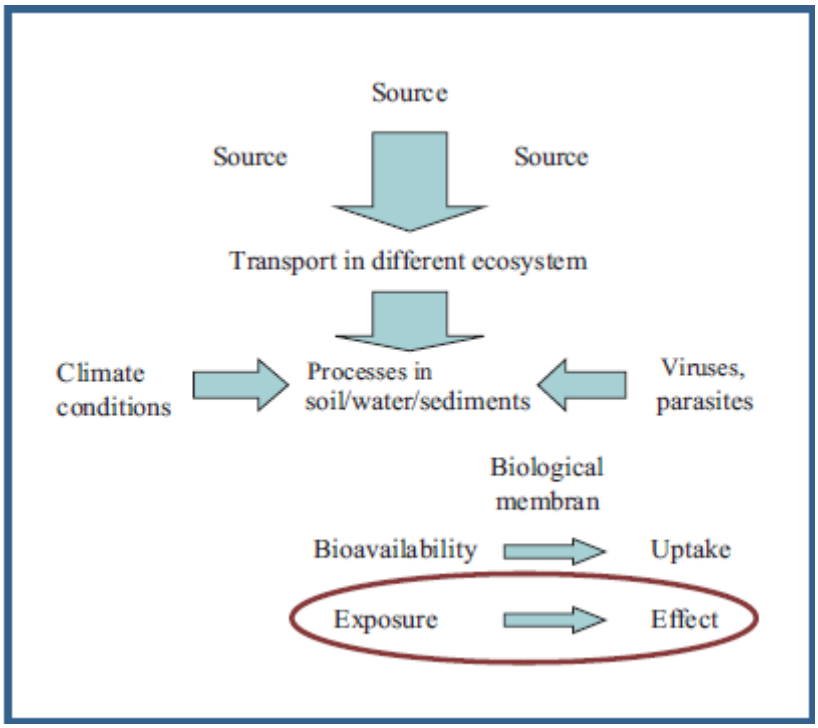

Figure 7. Variables affecting the "exposure - biological effect" -relationship in radionuclide contamination. (15)

2.3.1 Speciation

Radionuclides may be present in the contaminated area in different physico-chemical forms, which are low molecular mass (LMM) species (e.g. ions), high molecular species (e.g. colloids) and particles or fragments. The latter two can vary greatly in their size, shape, structure, morphology, density, valence and charge properties. (11) IUPAC 2000 has defined the speciation of radionuclides as the "distribution of radionuclide species in a system" and their analysis as "the analytical activities of identifying and/or measuring the quantities of one or more individual chemical species in a sample" (16). Most of the particles are from severe nuclear events, like nuclear weapon testing or the Chernobyl accident, and their chemical and nuclear properties vary depending on the source term and release conditions. This master thesis focuses on the radionuclides deriving from naturally occurring radionuclide-bearing sources so those derived from man-made nuclear sources are not discussed further.

Particles are often buried in soils and sediments by gravity. LMM species are referred as the mobile species, since they are soluble in soil water and are reversible bind to the solid surfaces, and they can penetrate biological membranes in active uptake. (15) HMM species on the contrary can be retained in filtering organisms. (11) The different size distribution of elements is presented in Figure 8.

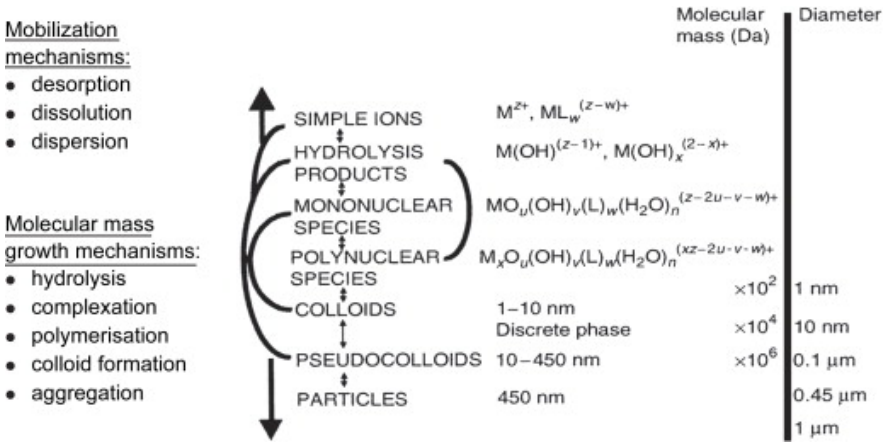

Figure 8. Elements categorized by their molecular mass and physico-chemical form. (17)

Overall it can be said that the ecosystem transfer of radionuclides is rapid if mobile species are presents and slow if the main concentration is retained by particles. (12) Distribution in the soil/water and sediment/water systems in radioecology is often studied using the

distribution coefficient K_d (Bq kg^{-1} soil or sediment per Bq L^{-1} or Bq m^{-3} water) (18). K_d calculations are based on equilibrium assumption in the studied environment, although it is a time dependent variable, which will change overtime as the interactions with components in soils and sediments take place. (17) The initial mobility of radionuclides may change due to the remobilization processes that include weathering of particles, redox processes and reactions caused by interaction with organic matter. For example if the soil or sediment is acting as a sink for radionuclides originally then over time it can become a source of contamination. (12) Figure 9 presents the distribution coefficient K_d as a function of contract time in sediment – sea water system and it can be seen that reaction of radionuclides with sediment happens rapidly leading into high K_d -values.

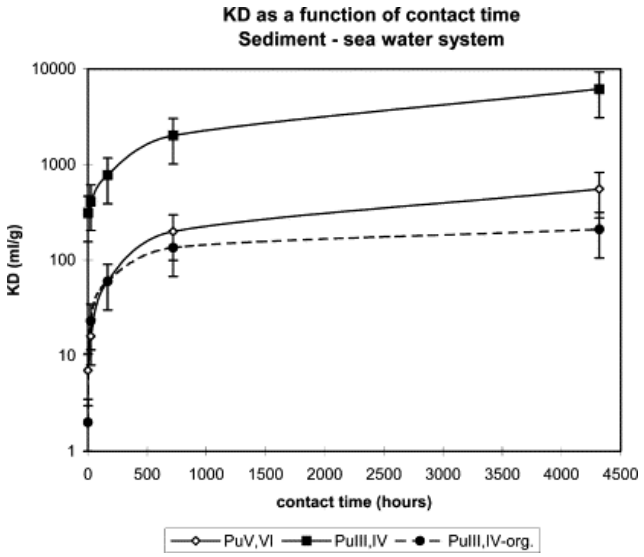

Figure 9. Distribution coefficient (K_d) presented as a function of time for Pu species in Kara Sea sediment. (17)

Biological uptake, accumulation and biomagnification of radionuclides happen through the speciation. (12) It has been proven that ligands and carrier molecules in the biological membranes act as carrier of LMM species, either directly or indirectly, leading to an active uptake. This is often studied using transfer coefficients, assuming that equilibrium has been achieved. Transfer of radionuclides from soils, sediments or water to vegetation, animals and fish are often modeled using a transfer coefficient TC (Bq kg^{-1} vegetation per Bq m^{-2} soil), sometimes also referred as aggregated transfer coefficient T_{ag}; a transfer factor TF (Bq kg^{-1} vegetation d.w. per Bq kg^{-1} soil); a concentration factor CF (Bq kg^{-1} animal per Bq kg^{-1} fodder) or a concentration ratio CR (Bq kg^{-1} animal per Bq m^{-2} soil). (12) (15) In an aquatic environment bio concentration factor BCF (Bq kg^{-1} fish w.w. per Bq m^{-3} water)

is often used instead of CF. (12) These coefficients are based on the total concentrations of radionuclides and do not take into account of the fraction of mobile and bioavailable species. Also, TC, TF and CF all have large seasonal variations leading to large differences in the reported data. The mobile species in soils or sediments, which are available for root uptake, can be modeled with mobility factor MF (Bq m^{-2} mobile species per Bq m^{-2} total deposition). Mobility factor has less seasonal variation due to the vegetation growth since it usually includes species taken up by vegetation. (18) All of the coefficients mentioned are also influenced by factors like soil type, microbial activities, used plant and animal species and their dietary customs and food chain level. (12) For example uptake of radionuclides in invertebrates happens when ionic species (LMM) interact with external organs such as skin or as a consequence of digestive uptake. On the contrary, filtering organisms on the contrary can retain HMM species such as colloids that can lead into accumulation of radionuclides, as their bioavailability is changed by digestion or phagocytosis. (12) Different radionuclide species can be separated according to different molecular masses by fractionation techniques. Table 5 presents the different *in situ*, at the site and in lab fractionation techniques, that are commonly combined to gain more information.

Table 5. Different fractionation techniques used *in situ*, at the site and in lab. ([a] = Applied in situ or at site) (18)

Size-fractionation	**Charge fractionation**	**Solid state speciation**
- Filtration[a]	- Exchange chromatography (cation, anion, adsorption)[a]	- Electron microscopy techniques (SEM, TEM)
- Tangential flow/hollow fibre ultrafiltration[a]	- Liquid – liquid extraction	- X-ray-induced spectrometry (μ-XRD, μ-XANES, EXAFS, μ-tomography)
- Continuous flow centrifugation	- Sequential extractions	- Laser-induced spectrometry (LIPAS, LITLS, LAMMA)
- In situ dialysis (small volumes)[a]	- Electrochemical methods	- Mass spectrometry (SIMS, ICP-MS, AMS)
- Ultracentrifugation	- Crown ether chromatography	-Electron energy loss spectroscopy
- Density centrifugation		-Raman spectroscopy
- Dialysis		-Nuclear magnetic resonance spectroscopy
- Gel chromatography		

Combined techniques:

- Filtration / Ion-exchange chromatography[a]
- Tangential flow ultrafiltration / Exchange chromatography[a]
- In situ dialysis with exchange resins (small volumes)[a]
- Electrodialysis (small volumes)
- Chromatographic methods (HPLC, LC) and mass spectrometry (LC/MS/MS, HPLC/ICP-MS)

2.3.2 Radionuclide speciation in water

In aquatic systems radionuclides can be present in LMM species or they can be associated with colloids and particles. (18) This difference can be distinguished by performing a size and charge fractionation of radionuclides using methods presented in Table 5. (12) The fractionation should take place *in situ* or at site since storing the samples may change the physico-chemical phases (as sorption, aggregation or sedimentation may occur), pH or redox condition and bacterial growth might influence the distribution of different species. (11) In the fractionation rinsing the equipment with sample material prior to collections can reduce the sorption. Stirring should be avoided in order to maintain the aggregates in their physical forms. No chemical components should be added before fractionation, as it would lead to changes in radionuclide distribution. While fractioning the aggregation of colloids and particles may lead to clogging of the membranes and this should be supervised at all times in order to obtain defined samples.

The generally used methods in size fractionation of water samples are filtration and ultrafiltration. Filtration can be done by using 0.45-µm millipore membranes that are able to separate particles with a diameter over 0.45 µm from other radionuclide species. In filtration the uncertainties are formed by LMM sorption on the materials, clogging of the membrane, concentration polarization and salt formation. (11) It has been shown that slow filtration rates are often caused by clogged membranes and lead to undefined fractioned samples. (11)

Ultrafiltration can be done either by using the tangential cross flow (TCF) system or the hollow fibre system (HF). Both TCF and HF are capable of separating colloids from LMM species by membranes with nominal mass ranging from 1 – 100 kDa. Ultrafiltration systems have a large surface area, when compared to traditional filters, and hundreds of litres of water can be processed *in situ* or at site. Clogging of the ultrafiltration system is unlikely due to high internal fibre flow. (11)

Of the different charge fractionation techniques the commonly used one is chromatography for retaining cation, anions and neutral species from natural waters. This technique can be easily combined with size fractionation and performed in field. (11) Figure 10 presents a combined size and charge fractionation system, which is applicable in the field. The presented system, in Figure 10, can be easily combined with 0.45-µm filtration system that would be located before the HF. Separation of cationic, anionic and neutral species is

essential for the evaluation of mobility and bioavailability of radionuclides in the aquatic environment. (18) (11) Also *in situ* measurements of water pH, temperature and ionic strength should be made for the characterization purposes. (12)

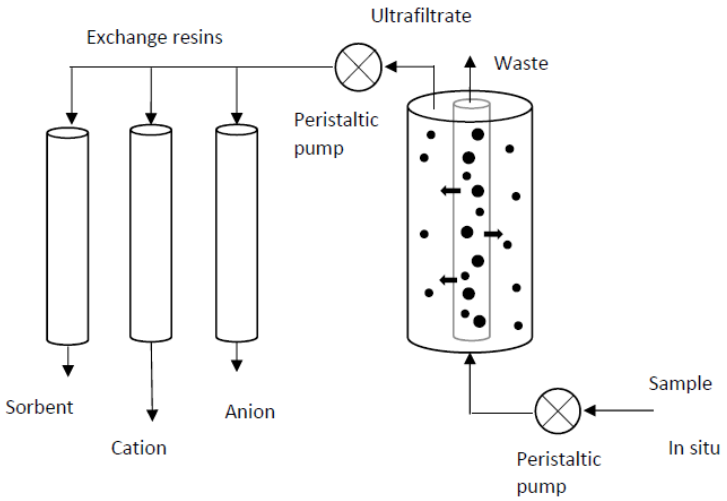

Figure 10. Combined size and charge fractionation system with a hollow fibre ultrafiltration and on-line chromatography fractioning cations, anions and neutral species. (18)

2.3.3 Radionuclide speciation in sediment and soils

Soil-water and sediment-water systems have been intensively studied in the past years for the processes influencing the mobility and bioavailability of radionuclides. Traditionally the fractionation has been done by sieving or grain size analysis, thus the research is still lacking a well-defined method for speciation of radionuclides in heterogeneous systems. In soil and sediment systems the mobile fraction is the LMM species, which consist of soluble ions and complexes and reversibly bound elements in solid surfaces. The inert fraction in these systems refers to radioactive colloids and particles, which are deposited in soils or sediments, and to irreversibly bound elements on solid surfaces or in mineral matrixes. Soil-water and sediment-water systems are dynamic and the equilibrium may or may not be established upon sampling. LMM species in these systems reach equilibrium fast, but for the species penetrating diffuse douple layers at mineral surfaces equilibrium is reached slowly. (15)

The different soil and sediment water -systems are often described with K_d values to assess the environmental impact, thus most published values vary significantly indicating large uncertainties in the methods. Variation in the K_d values is caused, for example, by used soil type and pH and the percentage of organic matter. Mobile species in these systems have a fast ecosystem transfer, while for the inert ones it is slow, however this can change overtime due to the weathering of solid material.

Different radionuclide species can be determined from soil and sediment samples by solid-state speciation techniques or indirectly by chemical reagents. Chemical extractions, either with single or sequential method, differentiate between reversible and irreversible bounds elements in soils and sediments. (11) Extraction methods are further discussed in Chapter 4 of this master's thesis. Solid-state techniques can be used for particles with a diameter higher than 1 μm. In soil and sediment systems colloids and particles act as a sink for radioactivity and are distributed heterogeneously over the ecosystem forming so called hot spots. These localized heterogeneities in the field can be observed with portable alpha, beta and gamma detectors or in laboratories by autoradiography. The most useful ways of characterizing the hot spots are electron microscopy and synchrotron radiation X-ray micro techniques. Electron microscopy techniques include transmission electron microscopy (TEM) and scanning electron microscopy (SEM), which can both be used for structure and elemental analysis of particles, colloids and nanoparticles. (11) SEM technique with energy dispersive X-ray spectroscopy (SEM/EDX) is most widely used method for characterization of the surface structures of particles. (19)

Synchrotron based X-ray techniques include:

- **μ-XRF**: X-ray fluorescence for 2D and 3D analysis of elemental distribution within particle;
- **μ-XRD**: micro-X-ray diffraction for analysis of crystallographic structure spectrometry;
- **μ-XANES**: X-ray absorption near edge structure spectrometry for the analysis of oxidation state within the matrix;
- **EXAFS**: X-ray absorption fine structure analysis for studying the coordination number and distance to neighboring atoms within the matrix.

Information about distribution of elements in the particle can be acquired by μ-PIXE and SIMS techniques. Structural information can be studied using μ-RAMAN and electron

diffraction techniques while the information about different oxidization states can be obtained by energy loss spectroscopy (EELS). All the mentioned techniques have their uncertainties and it has been noted that there are no proper standard materials for oxidation state measurements. In order to assure quality results all of the measurements should be confirmed by using two different techniques. (11)

2.4 Naturally occurring radioactive materials

Naturally occurring radionuclides can be found in almost every material in trace amounts and the most important ones from the radiation point of view, are those belonging to ^{238}U and ^{232}Th decay series and ^{40}K. Most of these materials have radiation level that is close to the normal background levels and some are subjected to regulation due to their higher activity levels. If human activities increase the exposure for these materials then they are referred as naturally occurring radioactive materials (NORM).

Over the years there has been a lot of confusion about the correct definition of NORM and it has been widely used even with non-radioactive minerals containing natural radionuclides. One attempt to clarify the broadly used definition was the introduction of TENORM, which is an acronym for technologically enhanced naturally occurring material describing elevated concentrations from human activities, but it caused even more confusion. (20) This master's thesis follows the IAEA guidelines of the definition and uses the term NORM for describing the naturally occurring radioactive material where human activities, e.g. mining, have increased the risk of potential exposure, when compared to unaltered situation, whether concentrations have been increased or not. (21) Depending on the radiation level NORM material may or may not need control and regulation. (22)

Human activities, such as mining and milling, can enhance the radionuclide concentrations in materials creating NORM. (23) Other potentially significant industries for NORM waste and residues are fossil fuel power stations, the oil and gas industry, metal processing plants, the phosphate industry, titanium oxide pigment production plants, zirconium and REE processing plants and cement production. (24) It has been proposed that when NORM pose a risk to humans or biota, they should be regulated with the same rules as the nuclear industry or use of radioactive sources. (25) The European Council Directive 96/29EURATOM first recognized the risk caused by NORM and this lead to creation of Basic Safety Standards (BSS), which are meant to protect the health of workers and the

general public from the effects caused by ionizing radiation. (26) In 2014, a numerical criterion for exemption and clearance of NORM (1 Bq g-1 for U and Th series and 10 Bq g-1 for 40K) was included to BSS, which has elucidated the problem to a certain level. (27)

2.4.1 NORM in mining

The mining and milling industry is known to be an important source of NORM materials, which are created when ores containing naturally occurring radionuclides are extracted and/or processed. The radiological concern has been recognized since the industrial activities may lead to the radioactive contamination of products, by-products, wastes and plant installations. (28) Depending on the extraction procedure, initial concentration and chemical form of radionuclides the NORM wastes produced will contain varying concentrations of uranium, thorium and their daughters, which may end up in the surrounding ecosystem through leaching and dust dispersion from rock waste and tailings. (29) (30)

The chemical behavior of radionuclides in the waste rock and tailings vary from site to site. Uranium is known to occur in ores and tailings with different physico-chemical forms e.g. with different oxidization states with different solubilities. (30) Daughters of the uranium decay chain will be present with varying concentrations depending on the transport history of the parent nuclide. (31) The mobility of radionuclides also depends on the mineralogy of the ore body e.g. uranium can be leached out from minerals like uraninite (UO_2) and calcite ($CaCO_3$) under suitable conditions. (30) Acid leaching techniques of ore may results in waste with elevated levels of NORMs, trace metals and sulfates. (30) If the waste is not neutralized prior to deposition to the final disposal place the leaching process may continue and mobilize the radionuclides to bind to the solid tailings. (30) (31)

Mobilized radionuclides from tailings may stay soluble in tailings solutions or become precipitated as the conditions change. Secondary minerals containing high levels of NORMs may be formed locally in the geochemical barriers. (30) Oxides formed by manganese and iron as well as by secondary sulphate mineral jarosite are known to host important environmental pollutants, like radionuclides. In the fresh acid leached/lime-neutralized uranium mill tailings Ra-226 is most likely hosted by gypsum, and in the aged tailings by iron-oxyhydroxides as well as barium and lead sulphates. Po-210 and Pb-210

are able to co-precipitate with sulphates also. The physico-chemical forms of radionuclides in NORM waste can also be changed by chemical and microbiological mechanisms. (30)

Understanding of the chemical behavior and final disposal of NORM wastes, produced by mining and milling industries, is important for the selection of appropriate rehabilitation techniques. (30) In Finland, the termination of NORM-bearing mining activity has to be approved by the Radiation and Nuclear Safety Authority in order to assure that the procedure is appropriately completed. (32)

2.4.2 Former NORM studies – examples of typical cases

In recent years an increasing awareness of the radiological impact from NORM industries has made research of the phenomena possible. (26) Each case is a unique complex where the radionuclide concentrations originating from the same source can differ enormously. (15) This chapter presents few of the previous NORM related studies.

2.4.2.1 Kurday uranium mining site, Kazakhstan

Strømman et al. (33) and Salbu et al. (34) have studied the concentrations of radionuclides and trace metals at and around the Kurday uranium mining site in Kazakhstan. *In situ* gamma and ^{222}Rn measurements were performed as well as at the site water fractioning. Samples were collected from water, fish, sediment, soil and vegetation. In the lab sequential extractions were performed and the radionuclide and trace metal concentrations were measured from the acquired samples. The results showed elevated concentrations of trace metals and uranium in the Pit Lake (1 ppm) and in the artesian water. Water fractionation proved that U, As, Mo and Ni were mostly as mobile LMM species, while Cr, Mn and Fe were found associated with colloids and particles. It was established that most of the radionuclides and trace metals were associated in mineral matrixes in soils and sediments. Sequential extractions showed that significant fractions of U (50 %), Pb and Cd were found in reversibly bound fractions indicating possible mobilization. Most of the Th, Zn and Co were bound in the irreversible fractions and can be considered as immobile. The significant amount of trace metals retained in particles was considered to pose a hazard under strong wind events. Distribution coefficients (K_d) showed that the transfer of radionuclides and metals from soils and sediment to water was minor. The transfer between soils or sediments and vegetation was slow according to the transfer factors (TF),

and the transfer between water and vegetation was seen to be faster. Biological concentration factor (BCF) showed that the transfer of Cd, Pb and As from water to fish liver was high. Also, the concentrations of uranium in gill, liver, muscle and bone of fish collected from the Pit Lake were elevated. BCF indicated that the highest accumulation of uranium was in bones and the lowest in muscles. The total gamma and radon dose rate from to humans reached 6 mSv/y. The ERICA Assessment Tool evaluated the highest dose for non-human biota to be for aquatic plants (700 μGy/y). Overall, it was concluded that measures such as restriction of the Pit Lake and dietary guidelines should be presented to reduce the risk posed to the environment. (33) (34)

2.4.2.2 Former uranium sites Taboshar and Digmai, Tajikistan

Salbu et al. (35) and Skipperud et al. (36) (37) studied the environmental impact of radionuclides and trace metals at former uranium sites Taboshar and Digmai in Tajikistan. *In situ* radon and gamma dose measurements were performed and sampling of water, fish, sediments, soils and vegetation was conducted. Radionuclide and trace metal concentrations were analyzed using alpha spectrometry and ICP-MS. Water samples collected from both locations showed elevated levels of uranium, Taboshar having the peak at 3 ppm in the Pit Lake waters. All the water samples also had high concentrations of As, Mo, Mn and Fe. Water fractionation showed that U, As, Mo and Ni were present in LMM species and could be considered to be mobile and bioavailable. Taboshar Pit Lake sediments had the highest concentrations of uranium (6 kBq kg^{-1}), while Digmai soil expressed the highest soil concentrations of radium (17 – 32 kBq kg^{-1}). In sequential extraction U and Pb were leached out from Pit Lake sediment samples in exchangeable and reducible fractions indicating high mobility. In tailings samples the mobility of U was found to be high, while Pb was irreversibly bound and inert. In all of the samples the highest concentrations of Th, As and most trace metals were found to be immobile as they were leached out in the residual fraction. Distribution coefficient (K_d) showed the mobility of radionuclides from sediment to water to be low. Transfer factors for soil – plant systems were also low. Biological concentration factors (BCF) showed a high accumulation of U, Pb and Cd in fish collected from Taboshar Pit Lake. The highest amounts of uranium were found in the fish bones. The direct uptake of unsupported ^{210}Po into the fish liver was also concluded in the results. Overall the Taboshar Pit Lake fish samples also had elevated levels of ^{210}Po and ^{210}Pb although the distribution varied between the organs as ^{210}Pb was

found to be a "bone seeker ", while ^{210}Po accumulated mostly in the liver. Finally, it was concluded that both legacy sites contained high levels of pollutants which may lead to radiological and chemical effects on man and biota and measures to prevent this should be taken into consideration. (35) (36) (37)

2.4.2.3 The Fen region, Norway

Speciation of radionuclides and metals were studied by Popic et al. (38) and Skipperud et al. (15) in southeastern Norway in the Fen area. This area is rich in NORM and has been the target of several mining activities before the 1960s and thus elevated concentrations of NORM occur there. The annual total effective dose to population in the area is estimated to be four times higher than the average of 2.9 mSv per annum elsewhere. The study concentrated on getting an overall picture of the radionuclide and metal distribution in the environment and determine the concentrations of radionuclides ^{232}Th, ^{238}U and metals As, Cr, Cd, Cu, Ni, Pb and Zn. Sampling of rocks, soils, vegetation species (moss, lichen, birch leaves, fern, spruce, pine needles) and water was conducted and analytical methods included at the site gamma measurements, sequential extractions and elemental analysis of the collected and extracted samples by ICP-MS. Gamma measurements varied between 0.07 – 9.24 μGy h^{-1} between the different locations and the highest values were found around the former NORM mining sites. The values exceed the world average of 0.059 μGy h^{-1} exhibiting the presence of radionuclide bearing minerals in volcanic rocks from the terrain. Depending on the location, the annual effective dose from outdoor external exposure was estimated to range between 0.18 – 9.82 mSv. The soil concentrations of ^{232}Th were higher than the average Norweigian soil values and were found to correlate with the occurrence of certain ^{232}Th bearing rock types. No correlation was seen between ^{232}Th and ^{238}U from which it was concluded that they have different and separate type of carrier minerals. The soil concentrations of radionuclides and metals were found to be higher in the vicinity of the former mining sites. ^{232}Th has a strong positive correlation with As and Ni, and a moderate one with Cd, Cr and Zn, suggesting that they are present in the same minerals. The values of As, Cd, Pb, Cr, Ni and Zn in soils partly exceeded the criteria for non-polluted soil in Norway. The water samples showed elevated levels of radionuclides and metals but still fulfilled the criteria for clean water. The vegetation was found to have high concentrations of ^{232}Th and ^{238}U despite the low reported transport factors. Sequential extractions were performed for different soil fractions in order to access

mobility and the possible bioavailability of radionuclides and metals. The results were in good agreement with former studies and showed that thorium was irreversibly bound in the soils, as most of it (77-94 %) was leached out in the residual fraction. Uranium mobility was higher than that of thorium in all of the samples, which was also consistent result with previous studies conducted in well-aerated superficial environments. On average 50 percent of total uranium was found to be tightly bound to soils. All the mining sites had higher concentrations of mobile lead (9-13 %) and one of them had elevated levels of mobile Cr (14 %) and As (8 %), when compared to the undisturbed site (2 %). The size fractionation of water samples from a nearby lake indicated that radionuclides and trace metals could accumulate in the living organisms, since they were mostly associated as colloids and LMM species. (38) (15)

2.4.2.4 Former coal mining sites, Poland

Leopold et al. (39) have studied radium and heavy metal contamination from Polish hard coal mining in the Upper Silesian Coal Basin. These industries produce highly mineralized brines with elevated levels of radium and heavy metals, which in the past were pumped to the surface and released into tailing ponds. This was done in order to allow suspended loads to settle in the bottom before the brines were mixed up with river waters. Nowadays this cleaning of the brines is done underground, but the former ponds with sediments contaminated with radioactivity and trace metals still exist and may pose a risk to the environment without proper land reclamation. To investigate the mobilization of these pollutants samples were collected from two sites affected by coal mining discharges. Samples consisted of tailings from a former tailing pond and of scale from an abandoned tailing pond site. The mobility of radium and trace metals was studied with a three-step extraction procedure created by the Standards Measurements and Testing Programme of the European Union (BCR). The radionuclide concentrations were determined by gamma spectrometry and trace metal concentrations by ICP-AES. The results showed a difference in the leaching behavior of different radium isotopes. Tailings that were characterized with surface absorbed radium had 25 % of the initial ^{226}Ra content in a mobile fraction, as the corresponding figure for ^{228}Ra was 15 %. No radium mobilization from the scales were observed and it was shown that radium was tightly bound in radiobaryte, $Ba[Ra]SO_4$. Heavy metal mobilization was seen to be similar to radium: Mn, Ni and Zn are readily dissolved by water from the tailings and no mobilization can be seen from the scales.

Overall, it was concluded that the water soluble fractions of radium and heavy metals pose a risk to the surrounding environment and might lead to antagonistic (1+1=0) or synergistic (1+1=3) effects which must be taken into consideration. (39)

2.4.2.5 Former phosphoric acid processing plant, England

The nature and concentrations of NORM at a decommissioned phosphoric acid processing plant on the North West coast of England was studied by Beddow et al. (28). The plant was in use from 1954 to 2001 and it produced waste with elevated levels of radioactivity and trace metals, which, in the early years, were discharged to sea and later landfilled on site. To characterize the different waste materials scale samples were collected from four different locations at the site, which represented the different stages of the process in chemical composition, mineralogy and radioactivity. The scale samples were found to mainly consist of fluorides, calcium sulphate and a mixture of different fluorides and phosphates. Measured metal and radionuclide concentrations were compared to the original processed ore from Morocco. Elevated levels of chromium, lead, copper, zinc and nickel were found in the different parts of the plant and most of them originated from the plant, installations which were exposed to phosphoric acid. Radioactive contamination consisted mainly of ^{238}U and its progenies, which were found retained in installations over the areas where the process flow consisted of mainly fluorides and phosphates. The highest ^{226}Ra concentrations were found in the calcium sulphates in the precipitates. Levels of ^{210}Po exceeded those of its parent's ^{226}Ra in many materials due to the chemical composition of the waste and the purification process of the plant. Leaching experiments showed that substantial amount of the solid waste was water-soluble and that leaching processes can mobilize uranium and radium isotopes leading to radioactive contamination of the solutions. (28)

2.4.2.6 Paukkajanvaara pilot-scale uranium mining, Finland

Tuovinen et al. (40) studied the release of naturally occurring radionuclides from waste rocks and tailings produced by Paukkajanvaara, a former pilot mining of uranium located in Eastern Finland. The mining operations were conducted between 1958 and 1961 and the Radiation and Nuclear Safety Authority in Finland supervised the rehabilitation of the site in the early 1990s. In total 40 000 tonnes of ore with a uranium grade of 0.14 % was mined and treated on site. The processing of ore generated 12 000 m^3 of fine-grained tailings material and 7 300 m^3 of waste rock, which were deposited in a small pond near the mine without further action. The aim of the study was to see if any further mobilization of radionuclides took place after remediation. For this purpose, soil, sediment and water samples were collected near the waste rock pile and the mill tailings. Water samples were also collected from a stream that flows from the tailings into Iso Hiislampi Lake. Water and sediment sampling was also conducted for the lake itself. Uranium and thorium concentrations in water, soil and sediment samples were analyzed with ICP-MS. Prior to the measurement the solid samples were acid digested with conc. HNO_3. Radionuclide concentrations were also determined with gamma spectrometry. Leaching of ^{226}Ra was seen from the waste rock pile as it had accumulated in the nearby soils. In sediment samples from the former streambed next to the waste rock the concentrations of ^{238}U and ^{226}Ra were higher than in the reference samples. Elevated levels of uranium were seen in the water samples collected from the stream that flows from the mill tailings into the lake. It was proposed from the radionuclide concentrations measured in the soil samples collected from between the mill tailings and the stream that ^{238}U and ^{226}Ra are leaching out with surface water flow. The sediment samples collected from the Iso Hiislampi Lake showed disequilibrium in the uranium series nuclides since fractionation of ^{210}Po and ^{210}Pb nuclides relative to their parent ^{238}U had happened. Overall, it was concluded that the leaching of the waste rock, and possibly even the mill tailings, is an ongoing process, which may lead to further mobilization of radionuclides in the Paukkajanvaara area. (40)

3. Environmental effects of radionuclides and trace metals

Radioecology studies a wide range of subjects varying from the source term to the environmental impacts caused by radiation. In order to gain a full understanding a knowledge of radiobiology, ecotoxicology and radioecotoxicology is needed. Radiobiology can give information about the responses in living organisms exposed to radiation, while ecotoxicology evaluates the early biological responses, toxicity or harmful effect for non-human organisms after exposure to pollution. Radioecotoxicology is the study of negative and harmful effects caused by radiation exposure for different species. (41) When assessing the environmental impacts it is crucial to include information from all these different fields. This chapter describes a few of the topics needed to make an accurate environmental assessment when radiological hazards are considered.

3.1 Radioecotoxicology

When radionuclide contamination occurs, it is important to take into account the possibly radiation characteristics, mobility and bioaccumulation properties. Also, the receiving ecosystem must be considered since there are differences in how tolerant the native species are. Studying the relationship between different "exposure – effect" -pathways has proved to be a challenge and it is extremely difficult to document and quantify them in nature. Laboratory experiments for different test organisms have been more successful and have determined biological responses to radiation from molecular to ecosystem levels. In living organisms ionizing radiation can cause the formation of harmful free radicals and reactive oxygen species (ROS), which can have an effect on membrane integrity and damage biomolecules e.g. nucleic acids. These effects can cause downstream responses in sensitive biological endpoints like infertility, weakened immune system response, mutagenesis, morbidity and mortality. Some of the organisms are less susceptible to the radiation and can even reverse the negative effects by stimulated DNA repair and by developing adaption and higher stress tolerance. (12)

Effect assessments caused by different doses are based on dose distribution and on the different biological endpoints. Dosimetry measurements for non-human organisms are still based on the assumption that the dose would be evenly distributed and they do not take into account the difference between external and internal radiation. (12) The relative

biological effectiveness (RBE) can be used to describe the differences in the required doses of different types of ionizing radiation to produce an equal biological response. (42) The RBE values are often based on calculations done for humans and it is important to note that the values for flora and fauna are different. (12)

The downstream effects of radiation in man, which leads to cancer, can be described by effective dose (unit Sv). The biological endpoints for flora and fauna are different and the effects are currently evaluated by using absorbed dose (unit Gy). An effect unit for non-human organisms has not been developed yet. (12) (41) Also the data lacks information about the threshold limits for low dose chronic exposures of ionizing radiation leading to biological responses for both human and non-human organisms. (41)

Extrapolation of toxicity data is a commonly used method for the lack of information since the biological systems are complex and the experiments are hard to execute. Single experiment data can be used for extrapolation in-between e.g. multiple stressor situations, different organisms, effect concentrations, acute and chronic effects and different test conditions. However, this leads to uncertainties, which are difficult to assess so defined safety factors are used as substitutes for error propagations. (12)

The International Commission on Radiological Protection (ICRP) has proposed guideline levels for radionuclide activities in drinking water. These levels are conservative and do not represent mandatory limits. When radionuclide concentrations exceed these levels, it should act as a trigger for further investigation instead of classifying the drinking water unsafe for use. (43) The levels proposed by ICRP for naturally occurring radionuclides studied in this work are presented in Table 6.

Table 6. Guidance levels for radionuclides in drinking water proposed by ICRP. (43)

Radionuclide	**Guidance level** $Bq\ l^{-1}$
^{238}U	10
^{226}Ra	1
^{228}Ra	0,1
^{232}Th	1

3.2 Multiple stressors

In laboratory experiments it is possible to limit the number of stressors into one, however this is not the case in the field. In nature, organisms can be exposed to a mixture of stressors e.g. radionuclides, heavy metals and organics originating from the same or different sources. (12) Together these harm-causing substances are called multiple stressors and they can lead to different types of interactions and react with multiple targets sites. The effects caused by multiple stressors can differ from those caused by a single one. Multiple stressors are capable of causing additive (1+1=2), synergistic (1+1=3) and antagonistic (1+1=0) effects. Although more research is needed since there are still huge gaps in the knowledge concerning multiple stressors. Also, environmental quality standard (EQS) values, used for evaluating the toxicity of substances, should consider the risk caused by multiple stressors instead of being restricted to single ones. (41) Multiple stressors and their possible downstream and endpoint effects are presented in Figure 11.

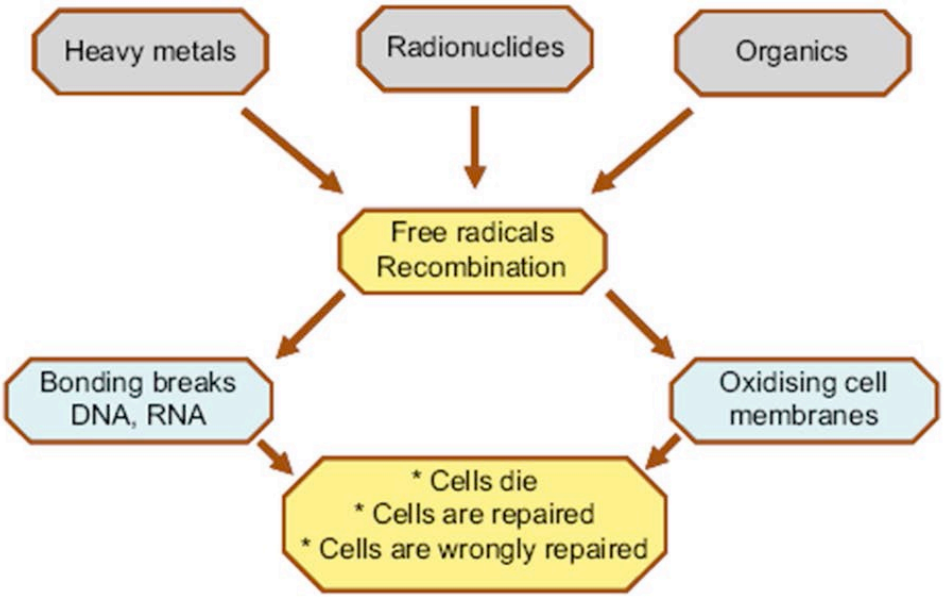

Figure 11. Downstream effects on organisms caused by free radicals induced by multiple stressors. (12)

3.3 Trace metals

Trace metals are naturally occurring elements in the earth's crust with a concentration less than 100 mg/kg, e.g. cadmium, copper, manganese, nickel and zinc. Sometimes these elements are referred to in literature as toxic or heavy metals, however these terms are often inaccurate. The toxicity of trace metals depends on many factors, including concentration and mobility, while heavy metals are classified as substances with a density greater than 5 g cm^{-3}. Many of the trace elements are essential nutrients for plants and animals and others can be toxic even at low concentrations. (44)

Globally, different human activities, like mining, manufacturing industry and waste disposal, have elevated the trace element concentrations locally, leading to increased levels in the surrounding ecosystems. (44) Mining industry often produces waste with high levels of cadmium, mercury, lead, chromium, copper, nickel, zinc and arsenic, which are all important in terms of water pollution and mobility. (45) (46) Trace metals, like radionuclides, can accumulate in organs of human and non-human organisms in the exposed ecosystem, especially in the liver, kidneys, bones and muscles. (46)

In soil, sediment and aquatic systems trace metals are affected by the same reactions as radionuclides, which were discussed in Chapter 2. Soils and sediments can act as a sink leading to long-term risks, since trace elements are non-degradable and can be mobilized through weathering of the solid materials or plant uptake. From the ecotoxicology point of view, elevated levels of arsenic, cadmium, mercury, lead and selenium in soil and sediments pose the highest risk to the ecosystems. (44) The World Health Organization (WHO) has set safe drinking-water guidelines in order to protect the public health. The given values for metals represent the calculated maximum concentrations that do not pose a risk to health in daily consumption. The guideline values are given as provisional values when there is a lack of research data in the toxicology and health records. The guideline values for different metals in drinking water set by WHO are presented in table 7. (43)

Table 7. Chemical guideline values for metals for drinking water set by WHO. (43)

Chemical	**Guideline values** μg/l
As [A,T]	10
Cd	3
Cr [P]	50
Fe*	-
Mn	400
Cu	2000
Pb [A,T]	10
Ni	70
U [P, **]	30
Zn	3000

[A] = Provisional guideline value since the calculated one is below the achievable quantification level

[P] = Provisional guideline value due to the uncertainties is research data

[T] = Provisional guideline value since the calculated one is below the level which can be achieved through practical treatment methods, source protection etc.

* = Not a health concern at levels causing acceptability problems in drinking-water

** = Based on the chemical toxicity for the kidney

3.4 Evaluation of environmental risks

Environmental impacts and risks are assessed by combining information from several levels, which are the source term, exposure pathways, ecosystem mobility and bioavailability and whether these encountered risks, under different conditions, pose a risk to living organisms. In risk management strategies the mentioned factors are usually the first to go under consideration when important risk-lowering measures are proposed and implemented. To achieve an effective risk management there must be a balance between benefit-cost and risk, and the possible stakeholders must be informed thoroughly about risk communication activities. In general, the risks are identified by combining the information of hazards identification, possible known effects and exposure pathways. A hazard is described as a possible source of danger that could have a negative effect on a living organism's health. In environmental protection the focus in normally on the possible effects of chronic radiation exposure at population level. (12)

In the case of radionuclides, it is also important to find the source term, deposition of material, transfer within ecosystems, biological availability and uptake and the effects caused in exposed organisms. In environmental impact and risk assessments the source term is evaluated from the source inventory as a released percentage and it gives qualitative and quantitative description of released nuclides, which can be modeled to give information about air and water transport, dispersion and deposition of different radionuclides. The activity of the released pollutants can be evaluated from the source term as well as from developments over time, plume height and energy content of the released nuclides, while it lacks information about their physico-chemical forms. In general, radiological risk and impact assessments assume that the contamination is distributed homogeneously over the area and they often lack the ability to consider particle contamination, which poses a long-term risk due to the delayed mobilization of radionuclides. (12)

Ecosystem transfer is often modeled by using dynamic constants, which can be changed with time, like distribution coefficient (K_d), concentration ratio (CR) or transfer factor (TF), which have been calculated using the total radionuclide concentrations in bulk samples and by assuming that equilibrium has been reached. This leads to large variations in the values reported in literature as the system dynamics and kinetics of the process have been ignored. (12)

4. Sequential extraction

Sequential extractions are selective techniques commonly used to give information about metal distribution in solid samples, when the total concentrations of metals cannot be considered to accurately represent their bio- and physicochemical availability and toxicity. (47) Numerous articles have been published on the extraction of metals and radionuclides from soil (18) (48) (15) (7) (49) (50). Extraction methods are designed to divide metals into different fractions that are likely to occur in nature due to various environmental conditions. (51) Single step extractions can be used to rapidly provide an estimate of the exchangeable metal fractions in samples as a more complicated multistep extraction procedure gives detailed information about the different metal associations and possible mobility. One of the major objectives in the invention of the extractions was to obtain a fraction that could mimic the uptake of metals and radionuclides by plants. Nonetheless, this task still seems to be open to improvements as the current methods all contribute to large uncertainties when plant uptake is considered. (15)

4.1 Reversible and irreversible sorption processes

Sequential extractions can be used to acquire information on whether the metals and radionuclides associated are bound reversibly or irreversibly and about their remobilization potential as the reagents are changed. The reversible physical sorption is induced by indifferent inert non-reacting electrolytes. The reversible electrostatic sorption on the contrary is pH affected or caused by competing or complexing ligands. The irreversible chemical sorption happens as a result of redox reactions in increased temperatures. All of these can be afflicted in the sequential extraction procedure when the dissolution and the displacement power of reagents are increased. (12) Metals and radionuclides bound with reversible reactions are normally estimated to be environmentally available in soils and sediments. Sequential extraction fractions that contribute towards the environmentally available fractions are considered to be the water-soluble fraction, exchangeable fraction and mild acid soluble fraction. (14)

4.2 Sequential extraction fractions

This chapter describes the different extraction fractions, their chemical properties and some of the most well-known problems. The presented fractions are based on the procedure proposed by Tessier et al. (47), which in literature seems to be the most popular and widely applied one (51) (45) (15).

4.2.1 Exchangeable fraction

Exchangeable fraction is designed to extract metals that are retained in the solids by weak electrostatic interactions and can be leached out by ion exchange. The most widely used reagent in this fraction is 1 M $MgCl_2$, since it combines the cation exchange ability of Mg^{2+} with weak complexing capability of Cl^-. (51) It has also been seen that this reagent does not react with organic matter, silicates and metal sulphides. (47) Acetate salts, such as NH_4Ac, have also been used regularly in sediment and soil extractions. Metal complexes formed with acetate ions are more stable than those formed by Cl^- favouring the ion exchange and decreasing the re-adsorption. Ammonium salts have buffering properties, however they are known to attack the carbonates leading to overestimates of leached metals in the first fractions. (51) The metals in this fraction normally represent a small fraction of the total metal concentrations, being generally only 2 %. (45)

4.2.2 Mild acid-soluble fraction

In the mild acid-soluble fraction metals are leached out from pH sensitive matrixes when the pH of the solution turns slightly acidic. In this fraction the most widely used reagent is a buffered acid/sodium acetate solution, which reacts with calcium carbonates. Although it is known that the dissolution of dolomite might not be complete in this step. This step also leaches out the residual absorbed metals that were not extracted the previous fraction. (51) Tessier et al. (47) concluded that iron and manganese leached out at this state derive from divalent salts, most likely from the ferrous and manganous carbonates. Also partial dissolution of pyrrhotite and lead sulphates can occur. The dissolution of carbonates is highly affected by the used solid:liquid –ratio: a ratio of 1:25 has been suggested for a high percentage of dissolution. (51)

4.2.3 Reducible fraction

The reducible fraction is designed to dissolute some or all of the metal-oxide phases present by changing the Eh/pH –properties of the solution. This step is especially designed for reduction of the Fe(III) and Mn(IV) in soils. The metals leached out in this fraction are usually bound to hydrous oxides of Fe and Mn, which are oxides [MO_x], hydroxides [$M(OH)_x$] and oxyhydroxides [MO_xOH_y]. The hydrous oxides of Fe and Mn are capable of retaining a large amount of metals due to coprecipitation, adsorption, surface complexation and ion exchange reactions. (7) An effective reagent needs to have a reducing agent, to attack the crystalline forms of oxides, and a ligand capable of keeping the released ions in the soluble form. (51) The most commonly used extraction reagent is hydroxylamine ($NH_2OH \cdot HCl$). This step can be done in one, two or three steps, which gives a change to separate the Mn and Fe oxides. Dissolution of Mn oxides is rather fast and not affected by the agitation time or the used reagent concentration. Oppositely, the dissolution of Fe oxides favours a long agitation time, increased reagent concentration and decreased pH. (51)

4.2.4 Oxidizable fraction

This faction attacks the organic matter mainly in the solid materials, including living organisms (and their remaining organic coatings), humid substances and, in a lower degree, products like carbohydrates, proteins, peptides, amino acids, fats or waxes and resins. Metals are released from organic matter by introducing oxidising conditions. One of the mostly used reagents is H_2O_2 in dilute nitric acid; however there has been great criticism of its inablity to totally destroy the organic matter. Hydrogen peroxide is also known to partially dissolve the sulfides. (51) Generally the metals bound in the organic matter are assumed to stay in soils and sediments for a long period of time and can only become mobile through the decomposition processes. (45)

4.2.5 Strong acid-soluble fraction

Metals in the strong acid-soluble fraction are mainly leached out from primary and secondary minerals that contain metals in their crystalline lattice. The reagents commonly used are strong acids like HCl, HF, $HClO_4$ or HNO_3. (51) From these HCl, HF and weak $HClO_4$ are non-oxidizing acids and they are able to dissolve metals that have reduction

potential higher than that of hydrogen. Furthermore, HNO_3 and strong $HClO_4$ are oxidizing acids. Nitric acid is the most commonly used one, because it has good oxidizing properties when the used concentration is > 2 M and it can dissolve organic matter. (30) A dissolution of the silicate matrix by nitric or hydrochloric acid is not likely so the residual phase only gives an estimation of the potentially mobile species. (45) This step cannot be used for quality control, since the dissolution of metals is only partial, however it serves as a useful tool in the evaluation of the long-term risk caused by the dissolved metals in the biosphere. (51) (45)

4.2.6 Total concentration of leached metals

The total concentration of metals in solid samples can be acquired from complete digestion of samples. This can be done using e.g. by using microwave digestion, which has become the standard method as it has clear advantages when compared to the traditional acid digestion: shorter digestion times, better recoveries of the volatile elements and compounds, lower contamination levels, smaller volumes of reagents and reproducible yields. (30) The total concentration of metals can be compared to the combined concentrations of the leached metals from all the extraction fractions ($F_1 + F_2 \ldots + F_{(1+n)}$). (52) The digestion for total concentration of metals can be done with either non-oxidizing acid (HCl, HF, weak $HClO_4$ or weak H_2SO_4) or oxidizing acid (HNO_3, concentrated H_2SO_4 or concentrated $HClO_4$). HNO_3 can mostly dissolve clay minerals, biotite and amorphous iron oxides, while silicates and most of the oxides are not affected. HCl alone does not reduce organic matter, thus it is commonly used with HNO_3 in aqua regia, which can dissolve some elements of the silicates although the silicate framework is inert to it. Sulphuric acid has a high boiling point of 338 °C, thus it cannot be used with Teflon vessels (melting point of 260 °C) in microwave digestion. HF can be used for the dissolution of silicates with another acid with a higher boiling point e.g. HNO_3. However, it is not always practical to use HF since it can affect the laboratory glassware and damage the torch of an ICP-MS machine. (30) Tuovinen et al. (30) concluded that for environmental samples mineral acid digestion can be considered sufficient, because components that do not dissolve in strong mineral acids are most likely not harmful biologically or environmentally.

4.3 Sequential extraction techniques

This chapter describes three of the commonly used sequential extraction techniques: extraction by Tessier et al. (47), extraction by Outola et al. (53) and extraction by Oughton et al. (48). The latter two have been optimized to extract radionuclides from soil and sediment samples.

4.3.1 Sequential extraction technique by Tessier et al.

In literature the most commonly used and modified sequential extraction technique was developed by Tessier et al. (47) in 1979. The selected fractions were exchangeable, bound to carbonates (acid-soluble fraction), bound to Fe-Mn oxides (reducible fraction), bound to organic matter (oxidizable fraction) and residual faction. The aim was to propose a method that could selectively extract the specific trace metals, which are likely to be released due to changing environmental conditions. They studied the dissolution of Cd, Co, Cu, Ni, Pb, Zn, Fe and Mn from layered bottom sediment samples. The outline of Tessier et al. (47) procedure is presented in Table 8.

Table 8. Sequential extraction procedure proposed by Tessier et al. (47)

FRACTION	EXTRACTION
1. Exchangeable fraction	8 mL **1 M $MgCl_2$** (pH 7.0) → extraction at room temperature, 1 h, continuous agitation required
2. Bound to Carbonates	8 mL **1 M CH_3COONa** (pH 5.0 with CH_3COOH) → extraction at room temperature, 5h, continuous agitation required
3. Bound to Fe - Mn oxides	20 mL **0.04 M $NH_2OH{\cdot}HCl$** (in 25% CH_3COOH, pH≈2) → extraction at 96 °C, 6h, occasional agitation
4. Bound to organic matter	3 mL **0.02 M HNO_3** + 5 mL **30% H_2O_2** (pH 2.0 with HNO_3) → extraction at 85 °C, 2 h, occasional agitation 3 mL **30% H_2O_2** (pH 2.0 with HNO_3) → extraction at 85 °C, 3 h, occasional agitation 5 mL **3.2 M CH_3COONH_4** (in 20% HNO_3) → extraction at 25 °C, 30 min, continuous agitation required
5. Residual fraction	Digestion with $HClO_4$-HF mixture

Between the different fractions the supernatants were separated from the residual solids by centrifuging at 10 000 rpm for 30 min and then removed by pipetting. Washing of the samples between the extraction steps was done with ionised water. In the residual fraction, after addition of reagents, the samples were evaporated to dryness and dissolved in hydrochloric acid. The resulting solutions were analysed using flame atomic absorption spectrophotometry to define their metal concentrations with a standardized technique.

4.3.2 Sequential extraction by Outola et al.

Outola et al. (53) propose a sequential extraction technique which is a modified version of the one proposed by the National Institute of Standards and Technology (NIST). The NIST technique was based on that developed by Tessier et al. (47). The technique was tested by extracting IAEA ocean sediment material and by analysing a wide selection of elements from the extracts, including radioactive Am, Pu and U. Outola et al. (53) have optimized the extraction conditions from that of Tessier et al. (Ref. Tessier) for ^{239,240}Pu and ^{238}U by changing the extraction temperatures, concentrations of the leaching reagents and leaching times. The outline for Outola et al. (53) is presented in Table 9.

Table 9. Sequential extraction fraction proposed by Outola et al. (53)

FRACTION	EXTRACTION
1. Exchangeable fraction	**0,1 M $MgCl_2$** → extraction at 25 °C, 1 h
2. Acid-soluble fraction	**1 M Ch_3COONH_4** (in 25 % CH_3COOH) → extraction at 50 °C, 2 h
3. Reducible fraction	**0,1 M $NH_2OH \cdot HCl$** (in 25 % CH_3COOH) → extraction at 70 °C, 6 h
4. Oxidizable fraction	**30 % H_2O_2 and 0,05 M HNO_3** → extraction at 70 °C, 3h, pH has to be adjusted below 2
5. Residual fraction	**4 M HNO3** → extraction at 90 °C, 4 h

In the Outola et al. (53) technique the used solid:liquid –ratio was 1:15. Before the commencement of extractions the samples were kept wet in ionised water for 24 hours. Between the steps the supernatants were separated by centrifuging and removed by pipetting. The stable concentrations of metals from the extracts were analysed using ICP-OES or ICP-MS and the radionuclide concentrations by alpha spectrometry. It was

concluded that the method does not dissolve all of the solid material e.g. the metals bound to silicate phases. (53)

4.3.3 Sequential extraction by Oughton et al.

The sequential extraction procedure proposed by Oughton et al. (48) was created to study the speciation of radionuclides originating from the Chernobyl accident, in the soil samples collected from Norway, Belorussia and the countries from the former USSR. This method is based on the work of Tessier et al. (47). The optimization has been made by the addition of the water soluble fraction and by changing the extraction times and reagent concentrations. Also, all the solid samples were washed with deionised water in-between the steps. The supernatants were separated by high-speed centrifuging (11 000 g). The total radionuclide concentrations in the original soil samples was measured and it was used as standardising method for the evaluation of the extraction results. The outline of the Oughton et al. (48) procedure is presented in the Table 10.

Table 10. Sequential extraction procedure by Oughton et al. (48)

FRACTION	EXTRACTION
1. Water soluble	**H_2O** → extraction at room temperature, 1 h, pH 5,6
2. Exchangeable	**1 M NH_4OAc** → extraction at room temperature, 2 h, pH 7
3. Bound to carbonates	**1 M NaOAc** → extraction at room temperature, 6 h, pH 5 (adjusted with HOAc)
4. Easily reducible Fe/Mn oxides	**0,04 M $NH_2OH \cdot HCl$** (in 25 % v/v HOAc) → extraction at 80 °C, 6 h, pH 2
5. Oxidizable organic matter	(1) **30 % H_2O_2** → extraction at 80 °C, 5,5 h, pH 2 (adjusted with HNO_3) (2) **3,2 M NH_4OAc** (in 20% v/v HNO_3) → extracted at 80 °C, 0,5 h
6. Acid-digestible	**7 M HNO_3** → extracted at 80 °C, 1 h, pH 1
7. Residue	**Total activity of fractions 1 - 6**

It was concluded that the method gives good reproducibility for ^{137}Cs and ^{90}Sr and it has been used in various studies afterwards (15) (14) (11) (54).

4.4 Factors contributing to uncertainties in sequential extractions

Sequential extractions have been widely used for determining the possible mobile fractions of trace metals and radionuclides in soil and sediment samples for years. Although, the method has been extensively criticised since its creation. One of the major differences between the methods is that some of the authors refer to presumed mineral phases, like bound to carbonates, without proofing that the actual phases exists and are taking part in reactions. Therefore it is recommended to refer to the displacement or dissolution power of used reagent e.g. oxidizable fraction. Selection of the used method must be done carefully in order to obtain the highest quality for the analytical results. It has been proposed that all the used methods should be standardized using appropriate standard materials in order for the results to be comparable. Standardization of solid:liquid –ratio, agitation type and rate, temperature, separation of phases and time of contact is most essential and by doing this the uncertainties of the extraction method are evaluated to be within 10%. (11) Most of the used extraction techniques include extraction with each reagent only once, as it is in the Tessier et al. (47) procedure, though it has been concluded that yield of the reversibly bound species reaches 50 % only if extracted once. In order to get higher percentages and to avoid the overlapping fractions the steps should be successfully repeated as is presented in Figure 12.

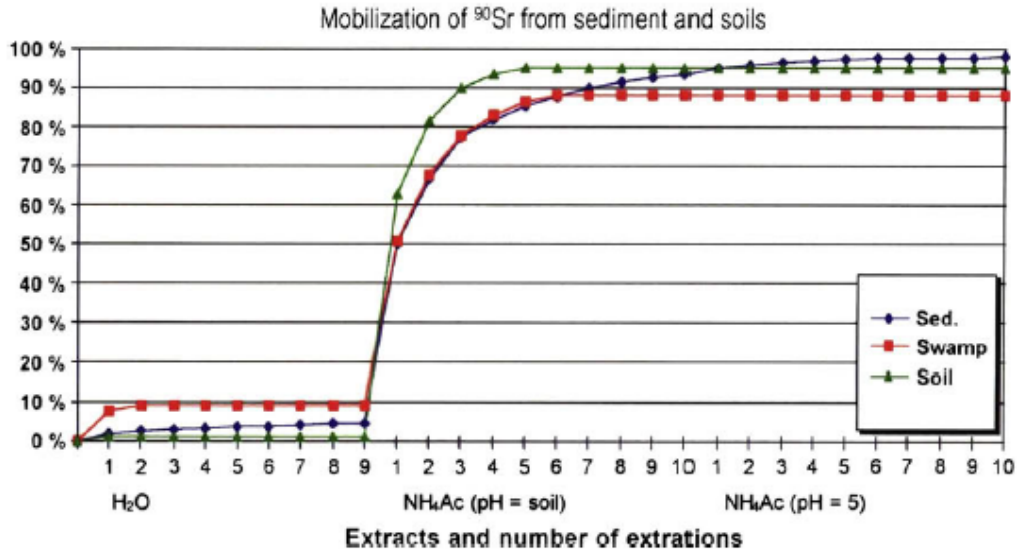

Figure 12. Repeated extractions of Sr-90 in soils and sediment from Mayak, Ural. (11)

The other contributing factors would be the lack of selectivity reagents, re-adsorption and redistribution of metals solubilised during the extraction and sample pre-treatment. For example Tessier et al. (47) specified that the dissolution of carbonates can be incomplete in the second and third extraction steps, due to different metal solubilities, leading to over-estimations in the reducible fraction. The incomplete dissolution is also one of the factors causing redistribution and re-adsoprtion of metals, as it was noted by Kheboin and Beuer (55), when they evaluated the problem by extracting synthetic models, which were spiked with specific trace elements. The results showed a significant redistribution of Cu, Pb and Zn. Lead was continuously re-adsorbed in each step and finally appeared in the residual fraction. The re-absorption of lead is a known problem as it has the potential to distribute on iron oxides and humic substances. (51) Metal distribution has also been reported due to the lack of selective reagents: as was seen by Martin et al. (56), when pyrrhotite ($Fe_{1-x}S$) dissolution in the acid-soluble step precipitated the dissolved metals with sulphide ions. Sample pre-treatment was studied by Bordas and Bourg (51) and it was noted that air and freeze drying caused less damage to the original distribution of metals than oven drying and suggested that in order to get environmentally relevant information the extractions should be applied to wet and sieved samples immediately after sampling. (51) Tessier et al. (47) noted that all of the different procedures suffer the lack of selectivity for example from sediment samples with freshly formed sulphides the leaching tends to be rather progressive than selective. It has been stated that all the different extraction schemes and reagents have advantages and disadvantages and that there is no ideal protocols for general use. Taking into account the nature of the samples (sediment, soil, sludge or industrially-polluted soil) and the studied elements is very important while selecting the procedure and should be given a major consideration. (51) Also combining size and charge fractionation techniques with sequential extractions gives a better view into elemental transfer from samples to environment, since the speciation of radionuclides can change overtime e.g. due particle weathering processes. Sediments and soils can act as a sink for LMM species and later on become a diffuse source of contamination. (11)

4.5 Environmental risk assessment from sequential extractions

Environmental risk caused by heavy metal pollution can be estimated by using a risk assessment code (RAC), which is based "on the strength of the bond between metals and the different geochemical fractions in sediment or soils and the ability of metals to be released and enter into the food chain" (57). The RAC is calculated by combining the extracted metals concentrations in exchangeable and acid-soluble steps and calculating the percentage with the total concentrations acquired from all the extraction steps. The formula for calculating the RAC percentage is presented in Formula 1.

$$RAC(\%) = \frac{c(exchangeable\ fraction\ I) + c(exchangeable\ fraction\ II) + c(mild\ acid - soluble\ fraction)}{c(total\ from\ all\ fractions)} * 100 \qquad [1]$$

RAC can give a good estimate of the bioavailability when sequential extractions are performed. (13) It is estimated that there is no risk when the RAC percentage is lower than 1 % of the total concentration, low risk at 1-10 %, medium at 11-30 %, a high risk at 31-50 % and an extremely high risk for higher percentages. The RAC method does not take into account the total metal concentrations found in the soils, however, it can be used as an evaluation of the environmental risk when using sequential extractions as a characterization method. (57)

5. Case study: Rautuvaara mining area

Rautuvaara mining area is located in Northwest Finland in the municipality of Kolari (67º29'N, 23º56'E). (58) Rautuvaara is a former iron-copper mine that was operated between the years of 1962 and 1988 by Outokumpu Oy. The mining complex consisted of one underground and two open pit mines. Rautuvaara has palaeoproterozoic bedrock with the main minerals being quartz, quartzite monzonite, diorite, skarn and amphibolite. (59) The extracted ore was enriched at the mining site and the used methods consisted of traditional crushing, grinding and magnetic separation techniques as well as flotation technique for the separation of copper. (60) Due to a lack of information available it is not possible to accurately describe the mining and enrichment processes at Rautuvaara mine. The total amount of extracted material from the mines was 12.86 Mt with 11.56 Mt of it being enriched. The Rautuvaara concentrator plant continued to work after mining had already concluded until 1996 under Rautaruukki Oy. (61) All of the enriched and deposited ores at Rautuvaara mining area are presented in the Table 11.

Table 11. Enriched and disposed ores at Rautuvaara tailings 1962 to 1996. (61)

Deposit	Ore metals	Deposited enrichment sand
Rautuvaara, Kolari	Fe, Au, Cu	4,68 Mt
Hannukainen, Kolari	Fe, Au, Cu	2,38 Mt
Saattopora, Kittilä	Cu, Au	2, 05 Mt
Laurinoja, Kolari	Cu, Au	0,13 Mt
Pahtavuoma, Kittilä	Cu, Ag	0,26 Mt
Juomasuo, Kuusamo	Au, Cu, Co	16 kt
Kirakkajuppura, Keminmaa	Pt, Pd	2,14 kt

According to the Geological Survey of Finland, the bearings from the Juomasuo deposit in Kuusamo have elevated levels of uranium, rising as high as 500 ppm, and the corresponding levels in water surrounding the deposit being 100 – 500 ppb. (32) Currently, there are no mining activities in the Rautuvaara area, however an on-going mining prospect in Hannukainen is planning to locate their concentration mill and tailings wastes to the old waste area in Rautuvaara. Hannukainen mining is planning on producing magnetite (Fe_3O_4) as their main product – in addition gold and copper enrichments would be

produced as by-products. The produced enrichment waste would contain elevated levels of pyrrhotite, reagents, lime, iron oxides and possible also other contaminants. (59) The plan is to dispose 65 Mt of low sulphur waste on top of the old tailings and 11 Mt of high sulphur waste into new tight-based waste ponds isolated with dams. The Hannukainen mine is estimated to be in production for 18 years. (62)

The Rautuvaara mining area was selected as a case study in this master's thesis since it has been an object of interest in the past and will continues to be so if the new mining facility at Hannukainen continues to use it. The aim of this case study was to evaluate the occurrence and mobility of trace metals and radionuclides from Rautuvaara tailings and estimate the possible hazards they pose to the surrounding ecosystems. The results will also give a reference point for contamination for the future if the use of the old tailings area continues.

5.1. Rautuvaara tailings area

Rautuvaara tailings are located next to the former Rautuvaara mine as is presented in Figure 13.

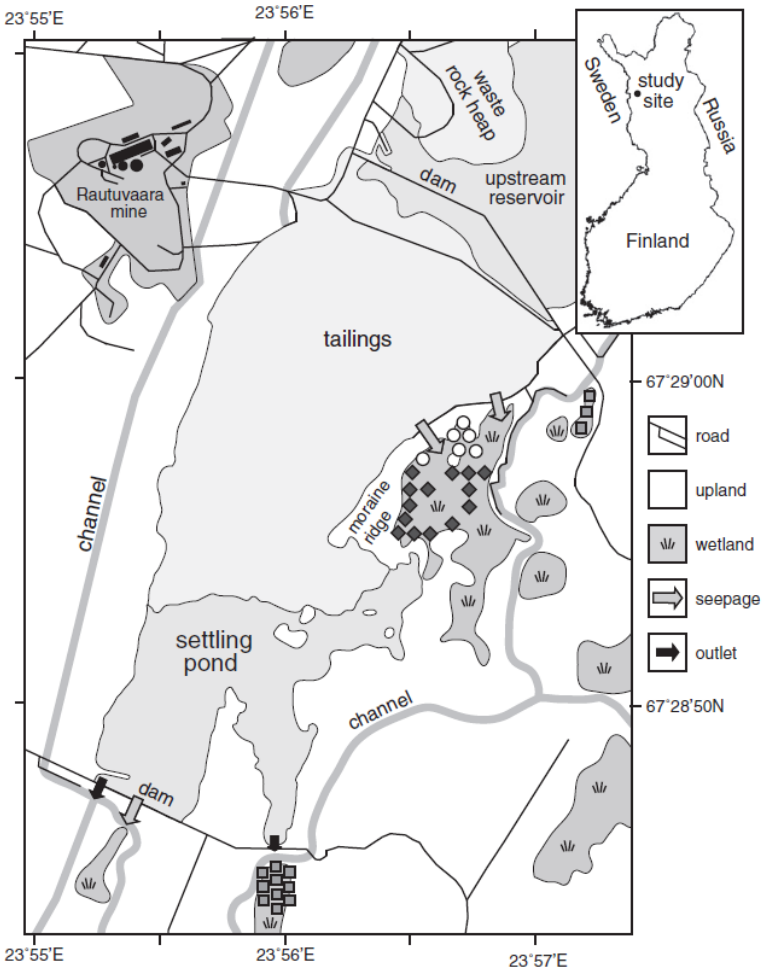

Figure 13. Location of Rautuvaara mine and tailings. (58)

The Rautuvaara tailings area is approximately 135 hectares and consists of 9.53 Mt of enrichment sand. (61) The tailings are located in the former valley of the river Niasa, on top of a compressed peat foundation, which has a declining topography towards the south. At the beginning of mining the former river was re-directed into the river Äkäs and the valley protected with three dams in order to keep the contaminated waters in a settling pond. (58) (61) Currently, approximately 30 hectares of the tailings are under water at the area of the former settling pond. Originally the enrichment sand was pumped to the tailing area from the north of the valley and this has caused the grain size to decrease towards the south as the water has separated the fine aggregates and carried them downhill. (61)

According to Räisänen et al. (61) this can still be seen at the site where the wet fine aggregate at the northern part of the sand pit is still slowly moving towards the south. The northern parts of the tailings are located on top of sandy or gravel moraine, instead of peat, which exposes the nearby aquifers to the leached elements from the waste. Detailed pictures of the tailings area are presented in Figures 14, 15 and 16.

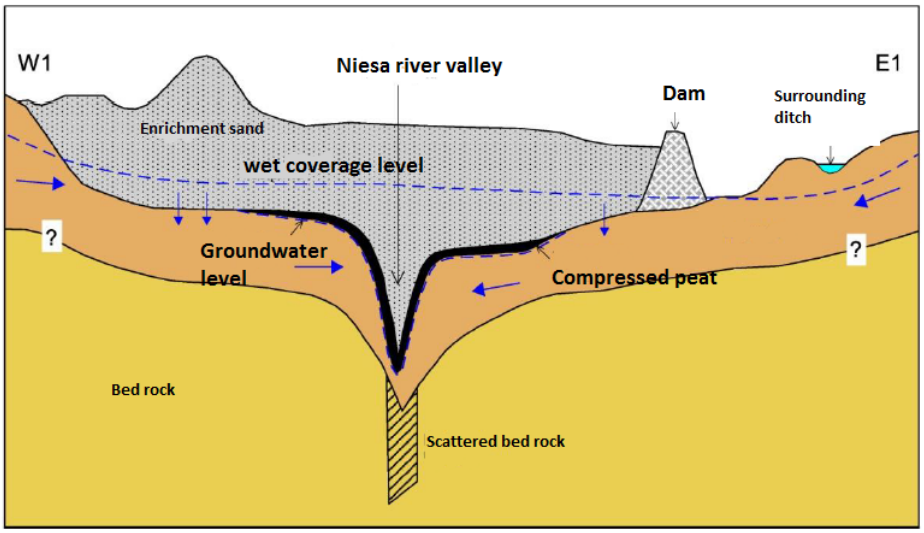

Figure 14. Cross-section of the northern tailings area in West-East direction. (61)

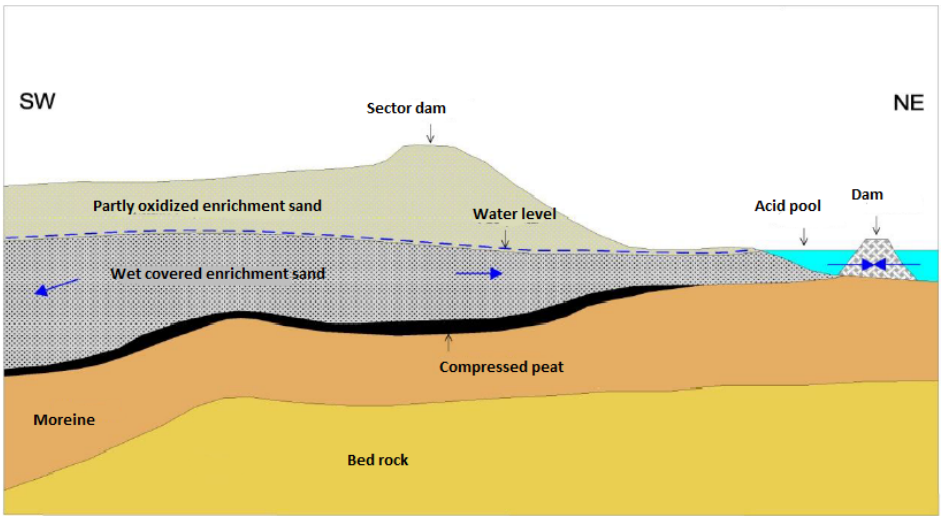

Figure 15. Cross-section of the northern tailings area in Southwest-Northeast direction. (61)

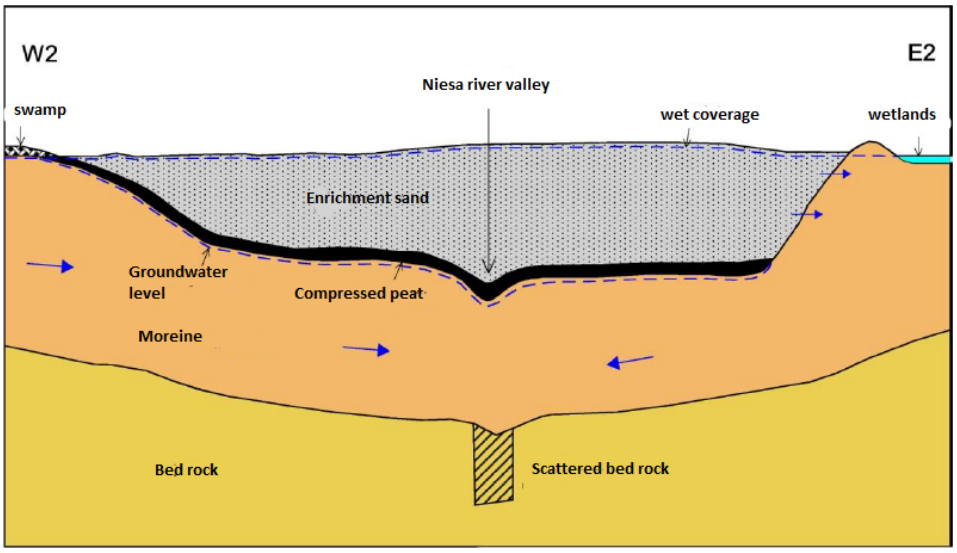

Figure 16. Cross-section of the middle tailings area in West-East direction. (61)

5.2 Former environmental studies at Rautuvaara

In the past Rautuvaara has been studied on several different occasions and still continues to be an object of interest. The Geological Survey of Finland studied the site between the years of 2005 – 2006. The aim was to study the possible chemical changes in tailings and water quality in the surrounding areas. The study included collection of water and enrichment sand samples, gamma-ray monitoring and test pits and core samples in order to get a full idea of the stratification and lithology of basal sediments. The results indicated that only the northern parts of the tailings were chemically changed due to oxidization of the sulphide minerals, also known as acid mine drainage (AMD). Oxidization happens when the wet covering of the area gets lowered as an outcome of seasonal changes and the sulphide bearing iron minerals are exposed to air. The produced sulphuric acid and ferric iron in the oxidization reaction can act as oxidants and further continue the reaction. This can lead to the leaching of metals (e.g. As) from other metal sulphides, uranium from uranium oxide and at the further stage aluminium and other elements from silicates. Some of the leached elements precipitate as secondary minerals and some are carried outside the tailings area by seepage waters. The results showed that sulphide weathering was progressing slowly and visible primarily in the surface sections (2-3 meters). No chemical alteration was seen in the southern parts of the tailings. The most serious changes had happened in the surface waters of the northern parts of the tailings, between the tailings

and the dam, where a pool of acidic water had formed. No alteration was seen in the groundwater samples collected from the area and the waters at the former settling pond were concluded to fulfill the requirements in the standard for drinking water recommended by the Ministry of Social Affairs and Heath. Also, some of the enrichment sand had spread at the bottom of the former settling pond since sediments with high levels of arsenic were found. (61)

In 2012 Närhi et al. (58) studied the wetland around Rautuvaara mining area that is influenced by tailings effluents. The study focused on soil chemical variables, wetland vegetation compositions and in identification of the plant species that could tolerate elevated levels of toxic elements from Rautuvaara tailings. They found out that the tailings contain elevated levels of copper, zinc, arsenic, nickel and cobalt when compared to the surrounding tills and can be classified as acid generating waste due to high Fe-sulfide concentrations. It was concluded that the weathering of tailings had increased the toxic elements concentrations in surrounding wetlands causing the plant diversity to decrease more than 50 %. Although it was also seen that elevated levels of Ca, originating from flotation chemicals lime and xanthates, decreased the uptake and toxicity of metals and that some of the plant species had adapted to high concentrations of As, Co, Cu, S and Zn. (58)

Savolainen (59) conducted a study about the hydrogeological and environmental state of the Rautuvaara mining area and its suitability as a future tailings disposal area. The study revealed that the surrounding waters represent the baseline of the Kolari area. A change was seen in the contaminated northern parts of the tailings and in a few close groundwater observation wells which were influenced by the acid mine drainage. The groundwater flow patterns were found to follow the topography of the area while forming a hydraulic gradient in the direction of the Niesa River valley. Enriched metal concentrations were found in a confined aquifer under the tailings area, in the southern part of the tailings, indicating that the peat layer that the area was built on is almost impermeable. Study suggests that the tailings area has its own water system that reduces the contamination to the surrounding area. The results were in good agreement with the former study made by The Geological Survey of Finland in 2005. (59)

5.3 Possible environmental effects caused by mining

Mining activities include ore prospecting, mine and mill plant constructions, production and mine closure with rehabilitation of the area. All of these stages can affect the surrounding environment and the outcome depends on the used methods, ore type and exposed ecosystem. (59) Even a small mining project can have a large impact on the surroundings. (63) One of the biggest concerns when it comes to environmental contamination caused by metal mining is acid mining drainage, also known as AMD. (63) It is produced when sulphite-bearing materials are exposed to oxygen and water leading to oxidization. (64) The most common of the sulphite minerals is pyrite (FeS_2) and its oxidation (AMD) is presented in Equation 1. (64)

$$FeS_2 + \frac{7}{2}O_2 + H_2O \rightarrow Fe^{2+} + 2{SO_4}^{2-} + 2H^+ \quad (1)$$

This reaction will produce an increase in the total dissolved solids and a decrease in the pH value of water. If the conditions remain oxidizing long enough then the ferrous iron will oxidize to ferric iron, which is presented in Equation 2. (64)

$$Fe^{2+} + \frac{1}{4}O_2 + H^+ \rightarrow Fe^{3+} + \frac{1}{2}H_2O \quad (2)$$

Also the ferric iron produced in Equation 2 can oxidize additional pyrite, which is presented in Equation 3. (64)

$$FeS_2 + 14Fe^{3+} + 8H_2O \rightarrow 15Fe^{2+} + 2{SO_4}^{2-} + 16H^+ \quad (3)$$

All of the Equations 1 – 3 assume that the oxidized mineral is pyrite and the oxidant is oxygen. (64) The lowered pH then dissolves metals from the surrounding materials that are then spread across the area by surface and ground waters. (59) (63) In general, AMD waters can be identified from low pH (between 2.1 - 6.6), elevated electrical conductivity when compared to the baseline (800 – 6 500 μS cm^{-1}), high redox potential and high leached metal concentrations. In order for the AMD to form the amount of sulphate rich minerals has to be large in comparison to neutral ones and the grain size and porosity of the solid material must allow the penetration of oxygen-bearing waters. The formation of

AMD can be prevented by moist covering the tailings that will preclude the oxidization processes. (59) If left untreated, the AMD process can continue a long time after the mine closure and cause significant contamination to the surrounding ecosystem. In Rautuvaara tailings pyrrhotite has the highest potential for AMD production. (59) It has been proposed that if the use of Rautuvaara tailings site continues the new storage for high sulphur waste should be located so that the seepage waters can be collected and treated, since it can be presumed that the constructed lining structures will not be completely leak-proof. An optimal place for a southern dam would be at the narrow passage at the southern end of the valley, since it would be possible to collect all surface waters and contaminated ground waters within a single area. This would separate the mine impacted waters effectively from the surrounding nature and allow their treatment in a ideal way. (63)

PART II: EXPERIMENT

6. Sampling

The samples used in this work were collected from the former Rautuvaara mining area between the 29th of June and the 1st of July in 2016. The sampling was performed by MSc student Mila Pelkonen and Research Scientist Pirkko Hölttä. Collected samples consisted of five different sample matrixes, which were water, sediment, enrichment sand, "acid pool" sand and waste rock. Sampling permits were acquired from different landowners for the collection of the tailings samples. Sediment and water sampling did not require any specific permits.

6.1 Sediment samples

Sediment sampling took place on the 29th of June 2016 in the old settling pond of Rautuvaara mining area. Sampling was performed from a boat with Limnos sediment sampler and after numerous attempts one core sample was successfully transferred to land and divided into subsamples. The collected sediment subsamples are presented in Table 12 and their sampling location in Figure 17. Picture of sediment sampling is presented in Figure 18.

Table 12. Sediment samples from Rautuvaara settling pond. Sampling location was in the southern part of the settling pond. Sample depth: 6.4 m. (R = Rautuvaara, S = Sediment)

Sample code	Location coordinates (WGS 84)	Core depth (cm)
R-S-1	N 67°28,775'' E 023°55,361''	0 – 1
R-S-2	N 67°28,775'' E 023°55,361''	1 – 2
R-S-3	N 67°28,775'', E 023°55,361''	2 – 7

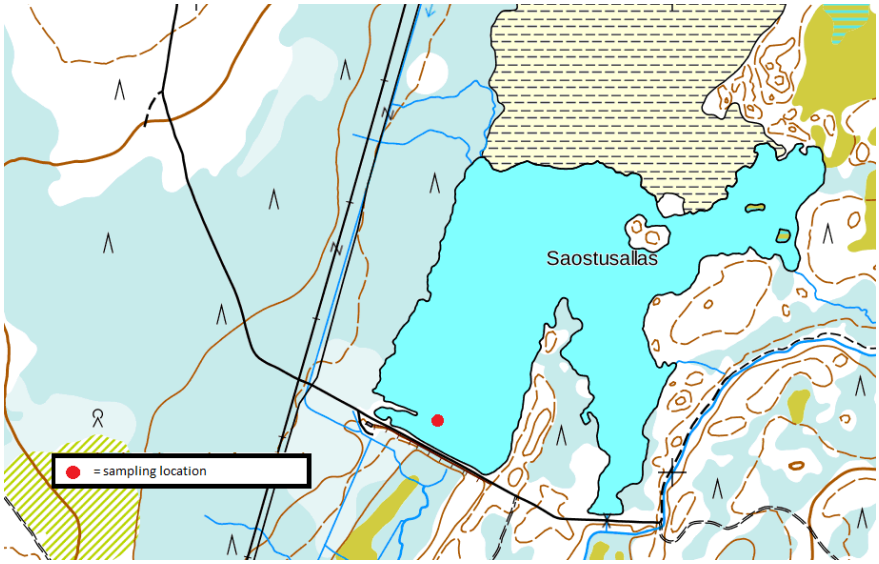

Figure 18. Sediment sampling location in the Rautuvaara settling pond. (65)

Figure 19. Sediment sampling in Rautuvaara settling pond and Limnos sediment sampler. Picture by Mila Pelkonen.

6.2 Water samples

Water samples were collected from the 29th of June until 1st of July 2016. Samples were collected using 25 ml syringes and filtered through a syringe filter (22 mm w/ 0.45 µm polypropylene membrane) into 25 ml centrifuge tubes. Syringes and centrifuges were acid-washed overnight in advance with 5 % HNO_3. Syringes were rinsed three times with water from the sampling location prior to sample collection. Two duplicate samples were collected from each location. The collected samples were preserved by adding 0.1 ml of 70 % suprapure HNO_3 into the centrifuge tubes. Reference water samples (nro 15) were collected for quality assurance purposes from upstream of the old mining area of Rautuvaara. All the collected water samples are presented in table 13 and the maps of the sampling locations in Figures 20, 21, 22 and 23. Pictures from the water sampling are presented in Figures 24, 25 and 26.

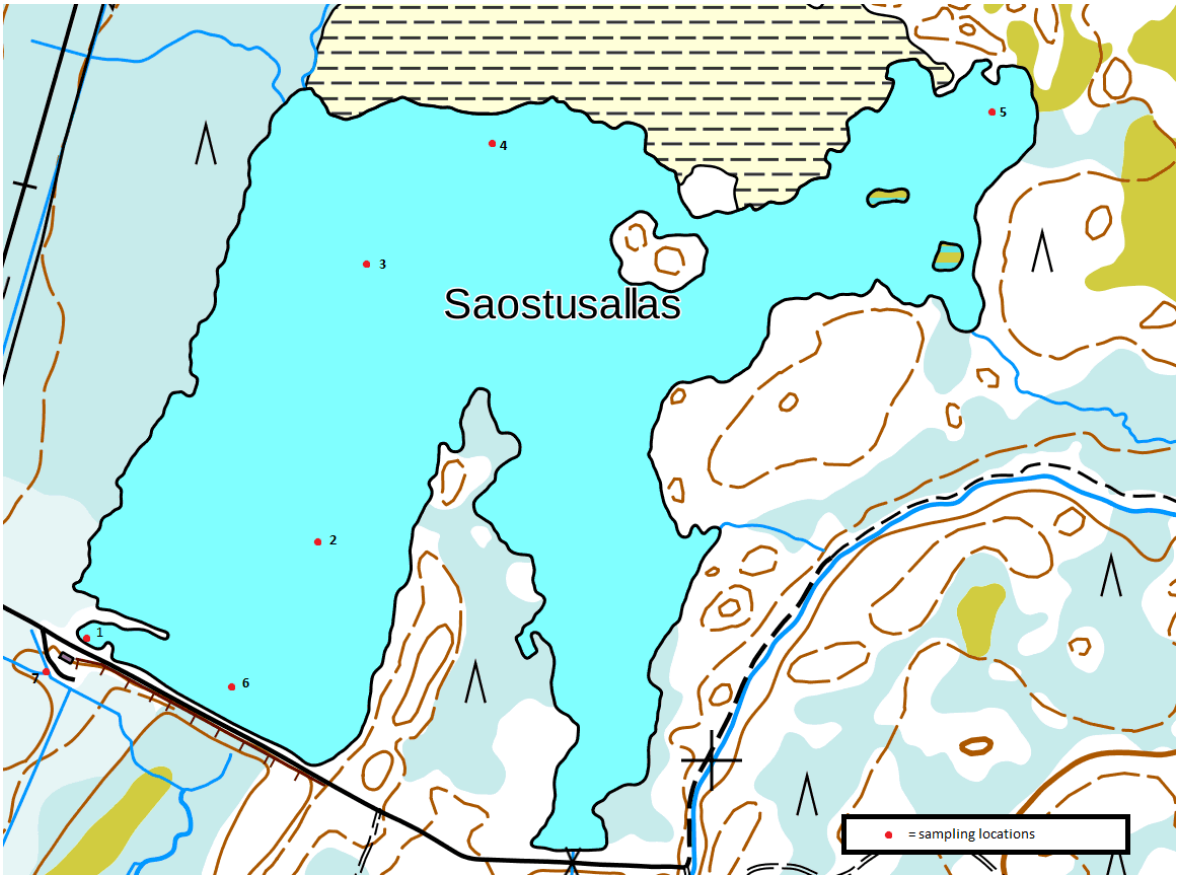

Figure 20. Water sampling locations in the former settling pond of Rautuvaara mine. (65)

Table 13. Water samples from Rautuvaara mining area and its surroundings. (R = Rautuvaara, W = Water, A/B = duplicates, No. = sampling location)

No.	Sample code	Location (WGS 84)	Location coordinates	Time of sampling
1	R-W-1A R-W-1B	Settling pond (South)	N 67˚28,752'' E 023˚55,386''	29.6.2016
2	R-W-2A R-W-2B	Settling pond (middle)	N 67˚28,832'' E 023˚55,474''	29.06.2016
3	R-W-3A R-W-3B	Settling pond (middle)	N 67˚28,985'' E 023˚55,534''	29.06.2016
4	R-W-4A R-W-4B	Settling pond (North)	N 67˚29,048'' E 023˚55,701''	29.06.2016
5	R-W-5A R-W-5B	Settling pond (North)	N 67˚29,078'' E 023˚56,399''	29.06.2016
6	R-W-6A R-W-6B	Settling pond (South)	N 67˚28,777'' E 023˚55,169''	29.06.2016
7	R-W-7A R-W-7B	Downstream from settling pond	N 67˚28,761'' E 023˚55,135''	29.06.2016
8	R-W-8A R-W-8B	Acidic pond	N 67˚29,476'' E 023˚56,983''	29.06.2016
9	R-W-9A R-W-9B	Acidic pond	N 67˚29,494'' E 023˚56,930''	29.06.2016
10	R-W-10A R-W-10B	Acidic pond	N 67˚29,522'' E 023˚56,847''	29.06.2016
11	R-W-11A R-W-11B	Acidic pond	N 67˚29,544'' E 023˚56,763''	29.06.2016
12	R-W-12A R-W-12B	Upstream water reservoir	N 67˚29,546'' E 023˚56,879''	29.06.2016
13	R-W-13A R-W-13B	Upstream water reservoir	N 67˚29,664'' E 023˚56,586''	29.06.2016
14	R-W-14A R-W-14B	Niasa river (downstream from mining area)	N 67˚25,622'' E 023˚49,800''	30.06.2016
15	R-W-15A R-W-15B R-W-15C R-W-15D	Niesa river (upstream mining area) *Reference water samples*	N 67˚31,087'' E 024˚02,975''	30.06.2016
16	R-W-16A R-W-16B	Upstream water reservoir, next to waste rock	N 67˚29,733'' E 023˚56,830''	01.07.2016

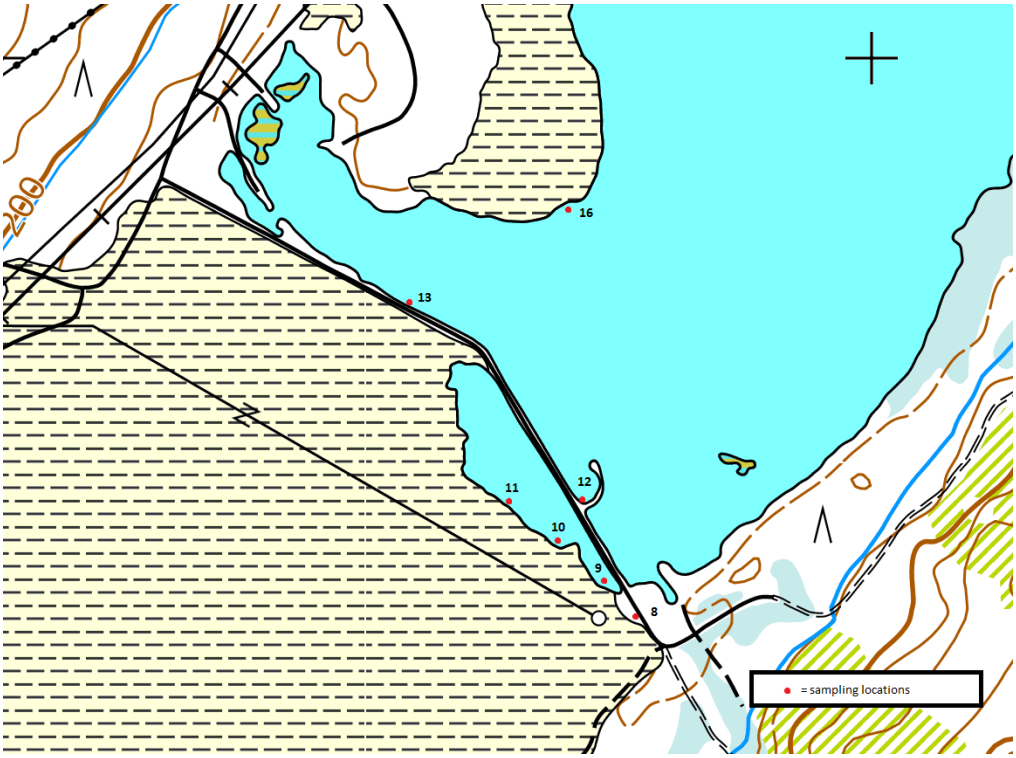

Figure 21. Water sampling locations on the north side of the tailings in Rautuvaara mining area. (65)

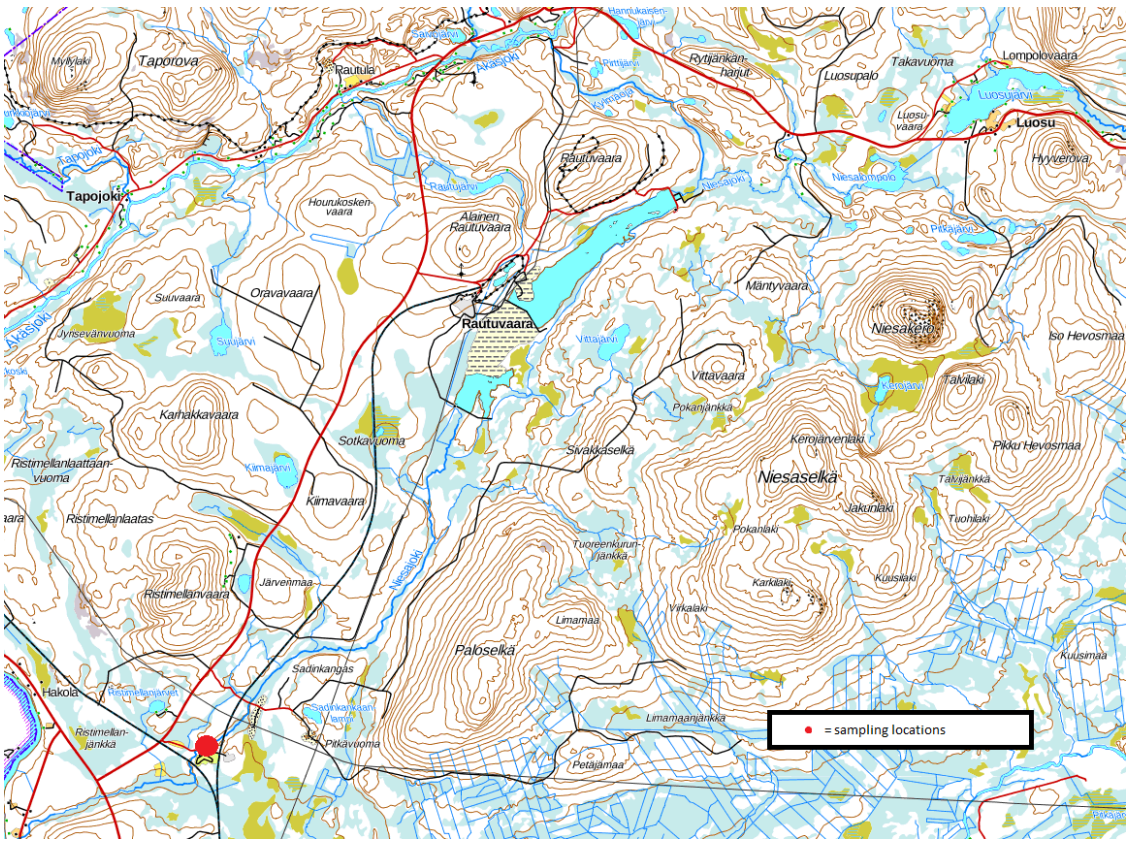

Figure 22. Water sampling location in Niesa River. Located downstream from Rautuvaara mining area. (65)

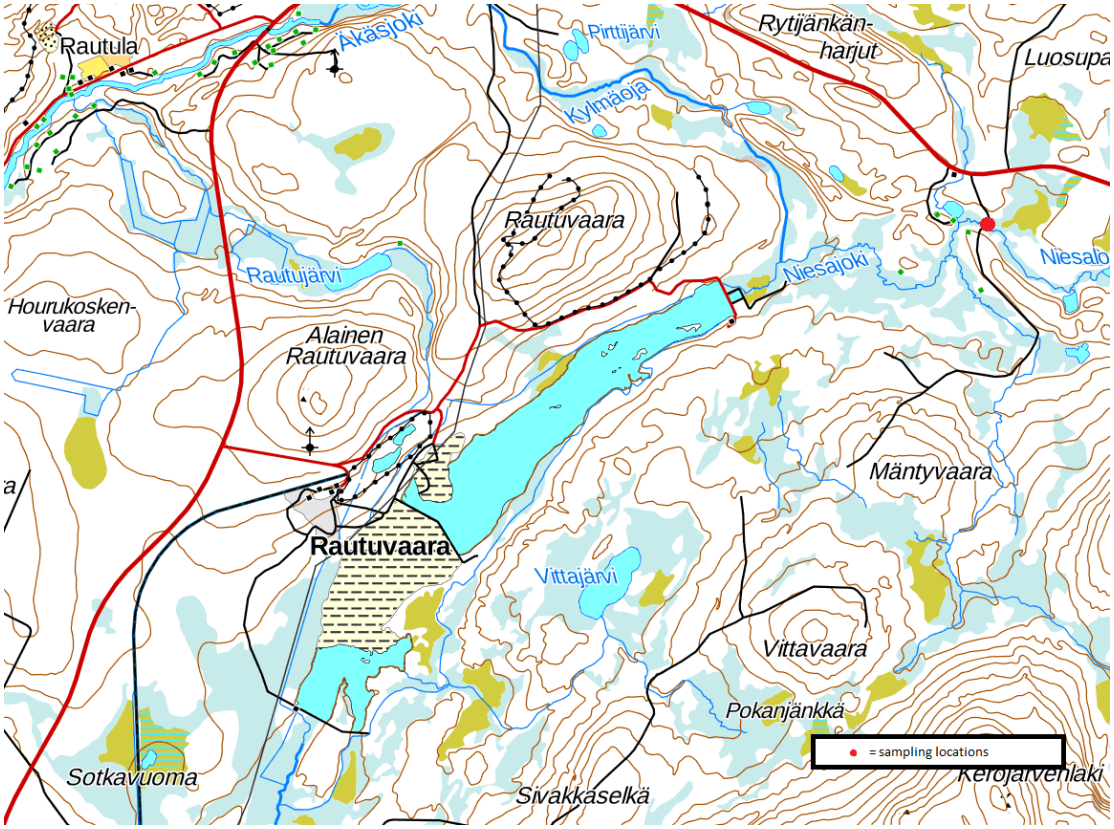

Figure 23. Water sampling location of the reference water samples (No. 15) upstream from Rautuvaara mining area. (65)

Figure 24. Water sampling equipment (syringe, syringe filter and centrifuge tube) at Rautuvaara settling pond. Picture by Pirkko Hölttä.

Figure 25. Acidic pond water at Rautuvaara tailings. Picture by Pirkko Hölttä.

Figure 26. Sampling of the reference water samples (No. 15). Picture by Pirkko Hölttä.

A sample for pH measurement of the acidic pond water was also collected. Accurate pH measurements could not be taken at the sampling site due to the lack of a pH meter. The acidity of acidic pond was measured on site using pH paper and it was seen to be between 2 - 3. Precise pH measurement was done in the laboratory after sampling. The pH of the acidic pond was proved to be 2.79 (Orion pH meter model 430A with Orion 8157BNU Ross Ultra pH/ATC Triode).

6.3 Tailing samples

Tailings samples were collected between the 30th of June and the 1st of July 2016 and they consisted of enrichment sand and acidic pond sand. Enrichment sand samples were collected by digging a hole with a spade and taking the sample from the depth with the highest αβ –activity count. Originally sediment samples were aimed to be collected from the acidic pond as well, but due to the acidity of the water sampling was done from the shore of the pond with a spade. Enrichment sand samples are listed in Table 14 and acidic pond sand samples in Table 15. Figures 27 and 28 present the maps of sampling locations. Figure 29 present pictures from the enrichment sand sampling. The sampling locations for enrichment sand samples were selected according to the former studies made at the area, which showed the total activity concentrations at the area. (61) Figure 30 presents a map of the measured total activity concentrations at the Rautuvaara enrichment sand area. (61)

Table 14. Enrichment sand samples. (R = Rautuvaara, E = Enrichment sand, A/B = duplicate samples, No. = Sample location)

No.	Sample code	Location coordinates (WGS 84)	Sampling time	Sample depth (cm)	αβ (cps)
1	R-E-1	N 67°29,125'' E 023°56,005''	30.06.2016	30	2,0
2	R-E-2	N 67°29,149'' E 023°55,867''	30.06.2016	30	1,8 - 1,9
3	R-E-3	N 67°29,191'' E 023°55,689''	30.06.2016	30	1,5 - 2,0
4	R-E-4	N 67°29,218'' E 023°55,727''	30.06.2016	30	1,6
5	R-E-5	N 67°29,199'' E 023°55,872''	30.06.2016	20	2,3
6	R-E-6	N 67°29,188'' E 023°56,020''	30.06.2016	30	1,8
7	R-E-7	N 67°29,201'' E 023°56,156''	30.06.2016	30	1,8
8	R-E-8	N 67°29,251'' E 023°56,031''	30.06.2016	30	1,8
9	R-E-9	N 67°29,321'' E 023°55,871''	30.06.2016	40	1,9
10	R-E-10	N 67°29,361'' E 023°55,924''	30.06.2016	30	2,3
11	R-E-11	N 67°29,318'' E 023°56,078''	30.06.2016	40	1,8
12	R-E-12	N 67°29,270'' E 023°56,233''	30.06.2016	40	2,8
13	R-E-13	N 67°29,319'' E 023°56,392''	30.06.2016	40	2,2
14	R-E-14	N 67°29,342'' E 023°56,445''	30.06.2016	40	2,4
15	R-E-15A R-E-15B	N 67°29,237'' E 023°56,207''	01.07.2016	20 40	2,0
16	R-E-16	N 67°29,271'' E 023°56,301''	01.07.2016	40	2,4

Table 15. Acidic pond sand samples. (R = Rautuvaara, S = Sediment/Sand, No. = Sampling location)

No.	Sample code	Sampling coordinates (WGS 84)	Sampling time
1	R-S-4	N 67°29,476'' E 023°56,983''	29.06.2016
2	R-S-5	N 67°29,494'' E 023°56,930''	29.06.2016
3	R-S-6	N 67°29,522'' E 023°56,847''	29.06.2016
4	R-S-7	N 67°29,544'' E 023°56,763''	29.06.2016

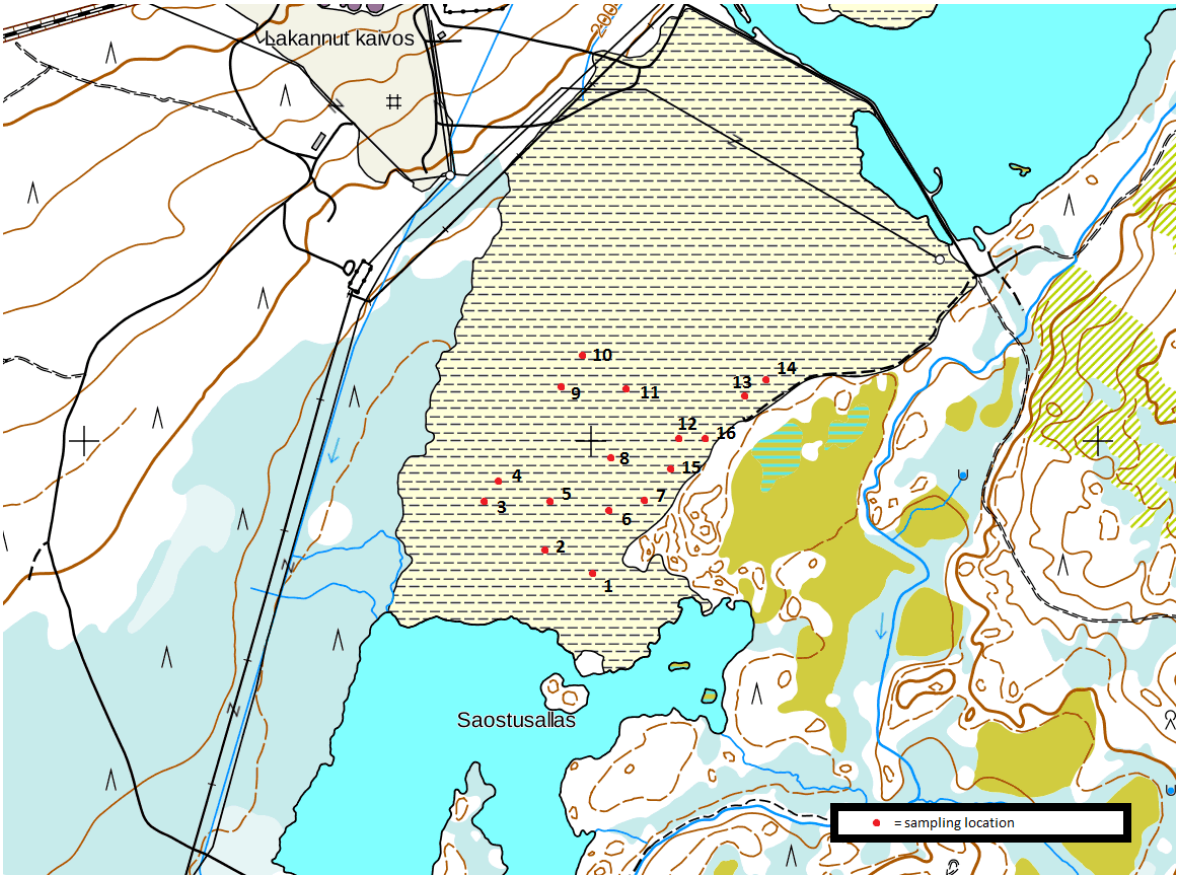

Figure 27. Enrichment sand sampling locations at Rautuvaara mining area. (65)

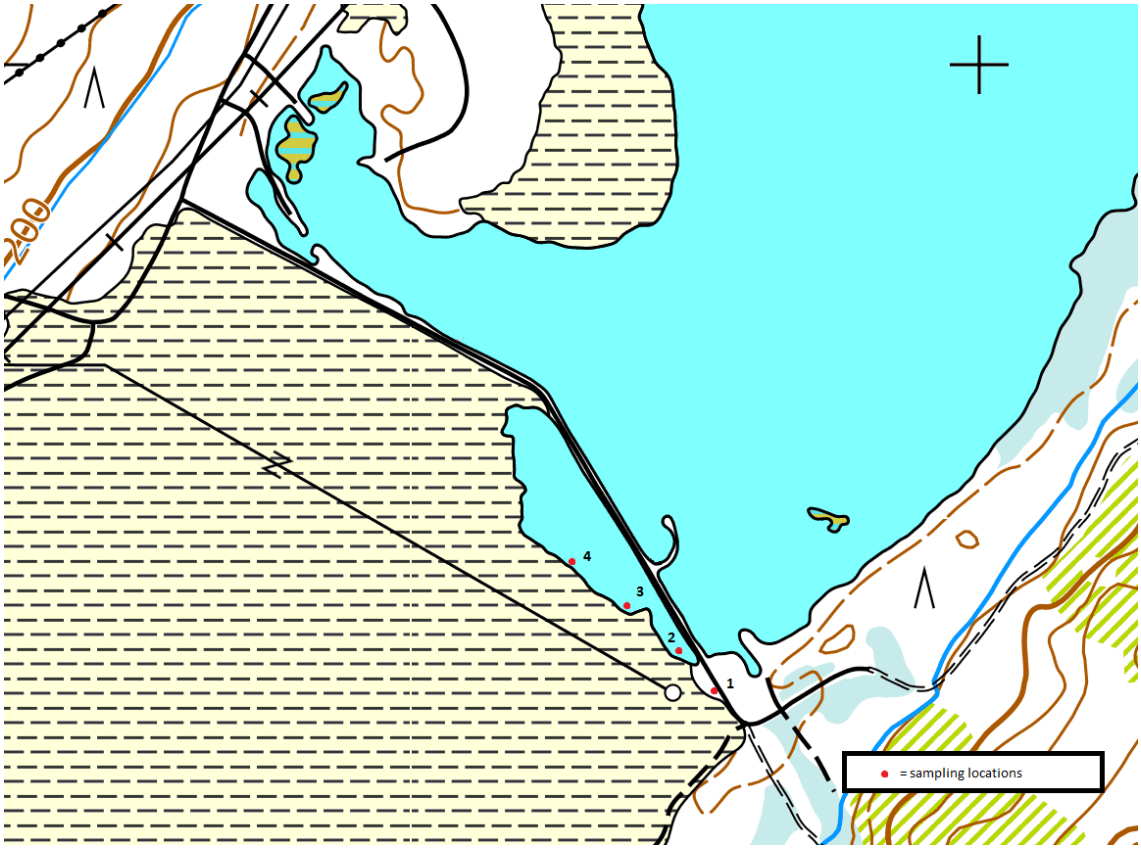

Figure 28. Acidic pond sand sampling locations at Rautuvaara mining area. (65)

Figure 29. Start of the enrichment sand sampling at Rautuvaara mining area (left) and the different enrichment sand layers (right). Picture by Pirkko Hölttä.

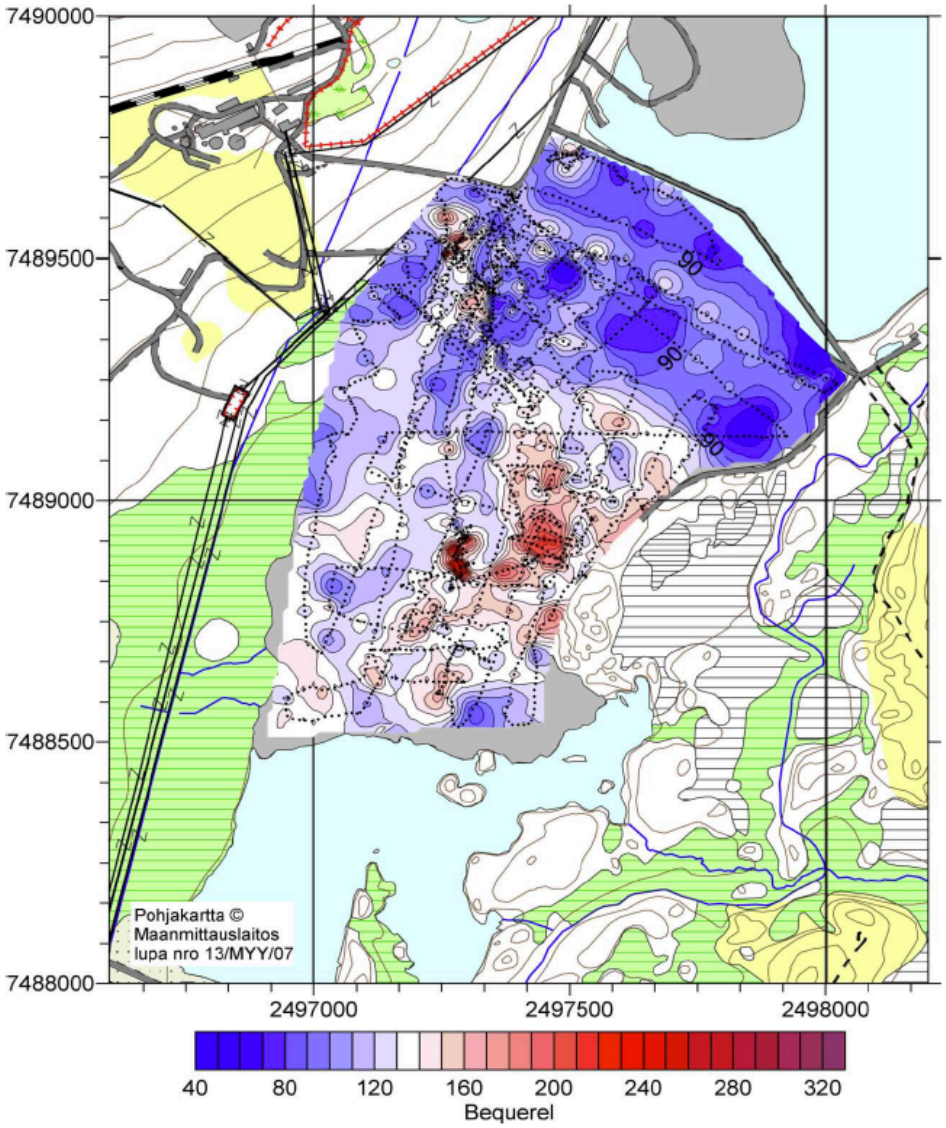

Figure 30. Total activity concentrations (Bq) measured in the old Rautuvaara enrichment sand. Blue areas refer to areas where the activity is below 130 Bq and red to those where it is over 130 Bq. (61)

6.4 Waste rock samples

Waste rock samples were collected on the 1st of July 2016 from a waste rock pile next to the old Rautuvaara mine. Sampling of waste rock was done using a spade. Waste rock samples are presented in Table 16 and the sampling location in Figure 31.

Table 16. Waste rock samples. (R = Rautuvaara/ Rock, A/B = duplicates)

Samle code	Location coordinates (WGS 84)	Sample depth (cm)	Sampling time
R-R-1A	N 67°29,757'' E 023°56,807''	10	1.7.2017
R-R-1B	N 67°29,757'' E 023°56,807''	10	1.7.2017

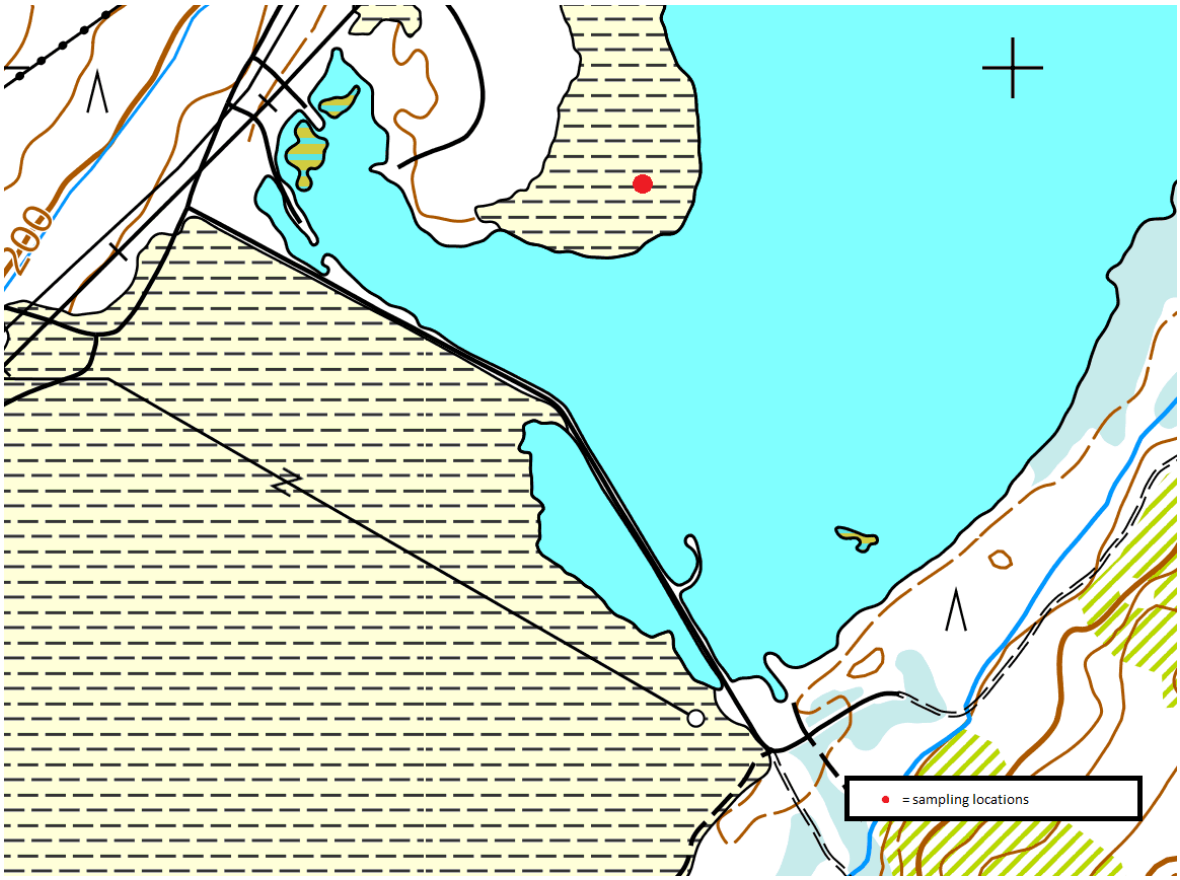

Figure 31. Sampling location of waste rock at Rautuvaara mining area. (65)

7. Solid sample pre-treatment

Four different kind of solid samples were collected from the Rautuvaara mining area. These were tailings samples, including enrichment sand and acidic pond sand, sediment samples and waste rock samples. This chapter explains the pre-treatment techniques used for solid samples.

7.1 Tailings and waste rock samples

Tailings and waste rock samples were processed according to Finland's Radiation and Nuclear Safety Authority's guide for Pre-treatment of soil and sediment samples. (66) Pre-treatment was done in order to find out the dry weight of samples.

The procedure started with weighing approximately 100 g of wet sample on a tared 0.5 l evaporating dish. Then the dish was weighed once more and placed into the heating oven at 105 ºC overnight. Crushing of the samples was not necessary since the material had been crushed in the mining processes before reaching the tailings area. After removal of the dishes from the oven they were left to cool at room temperature for an hour before weighing. Dried samples were homogenized in a mortar and afterwards stored in 0.5 l plastic bags for further experiments. Dry weight results for the tailings and waste rock samples are presented in Tables 17 and 18.

Table 17. Dry weights for tailings. (R = Rautuvaara, E =Enrichment sand, S = Acidic pond sand, No. = Sampling location, A/B = Subsamples)

Sample	Dry weight (%)	Sample	Dry weight (%)
R-E-1	75,3	R-E-12	80,6
R-E-2	77,9	R-E-13	76,4
R-E-3	76,5	R-E-14	77,9
R-E-4	78,9	R-E-15A	78,1
R-E-5	78,5	R-E-15B	76,8
R-E-6	79,1	R-E-16	78,0
R-E-7	76,4	R-S-4	79,2
R-E-8	76,9	R-S-5	70,1
R-E-9	80,8	R-S-6	76,7
R-E-10	78,7	R-S-7	75,5
R-E-11	78,9		

Table 18. Dry weights for waste rock samples. (R = Rautuvaara/Rock, No. = Sampling location, A/B = Subsamples)

Sample	Dry weight (%)
R-R-1A	92,8
R-R-1B	94,5

All the dry weights for the tailings samples stayed between 70-80 percent. Dry weights for the waste rock samples were above 90 percentages due to their coarser grain size.

7.2 Sediment samples

Sediment samples were treated according to Finland's Radiation and Nuclear Safety Authority's guide for Pre-treatment of soil and sediment samples. (66) Due to the high percentage of clay in the sediment the samples were freeze dried (Lobogene ScanVac CoolSafe PRO freeze dryer) instead of oven drying in order to avoid clodding of the samples. Sediments samples were dried for gamma spectrometry measurements. Calculating dry weight percentage for sediment samples was impossible due to the high water content of the samples.

The drying started by spreading the wet samples on to metal plates designed to fit into the freeze drier. Then these plates were covered with tinfoil and placed into the freezer overnight. The next day the frozen samples were placed inside the freeze drier and drying was commenced. Samples were taken out from the machine after 48 hours and they were left to stabilize in room temperature for an hour before weighting. The dried samples were homogenized in mortar and afterwards stored into 0.5 l plastic bags for further experiments. Due to the small sizes of the sediment samples the whole mass was dried.

8. Determination of pH of soil and sediment samples

Sample quality was studied by measuring the pH of the solid samples using an ISO standard method. (67) For this purpose, four samples were chosen: two enrichment sands, one acidic pond sand and one sediment sample. Chosen samples were air-dried at room temperature overnight, except the sediment sample, which was freeze-dried as is described in chapter 7.2.

The pH of the solid samples were measured with a pH meter from a suspension, which was prepared by mixing 5 ml of the solid sample into 25 ml 0.01 M calcium chloride. Calcium chloride solution was prepared by dissolving 1.47 g of calcium chloride dehydrate ($CaCl_2 \cdot 2H_2O$) in water and diluting the total volume into 1000 ml. The water used was purified with Millipore Milli-Q system (Millipore, USA). Before taking the measurements the suspensions were shaken for an hour. The pH meter was calibrated with buffer solutions of 4, 7 and 10 (ORION pH meter model 420A with ORION 8157BNU Ross Ultra pH/ATC Triode). Each sample was measured three times in order to reduce the error. The results are presented in Table 19 on the next page.

Table 19. pH of solid samples. Measurement temperatures were between 21 – 22 ˚C.

Sample	**pH**
R-S-3 (Sediment)	1. 6,54 2. 6,57 3. 6,53
R-S-7 (Acidic pond sand)	1. 4,15 2. 4,18 3. 4,11
R-E-2 (Enrichment sand)	1. 7,02 2. 7,01 3. 6,95
R-E-11 (Enrichment sand)	1. 6,80 2. 6,71 3. 6,73

Used ISO standard defines acceptable difference for the measured pH values in different pH range. Below pH 7 the accepted difference is 0,15 and above pH 7 it is 0,20. All the measured values are in between the accepted ranges.

9. Sequential extractions

Sequential extractions were performed for all solid sample materials in order to evaluate the mobility and bioavailability of trace metals and radionuclides. The extraction method used was modified from that of Outola et al. (53) and is presented in table 20.

Table 20. Applied sequential extraction method. (RT = room temperature)

No.	Fraction	Reagents	Leaching time and temperature	pH
I	*Exchangeable fraction I (pore water model solution)*	0,01 M $NaNO_3$ 0,1 M $MgCl_2$ 0,01 M KCl 0,1 M $CaCl_2$	1 h, RT	7,8
II	*Exchangeable fraction II*	1 M NH_4Cl	1 h, RT	5,0
III	*Mild acid-soluble fraction*	1 M CH_3COONH_4 (in 25% CH_3COOH)	2 h, 50 ºC	4,1
IV	*Reducible fraction*	0,04 M $NH_2OH{\cdot}HCl$ (in 25% CH_3COOH)	6 h, 70 ºC	2,0
V	*Oxidizable fraction*	30 % H_2O_2 and 0,05 M HNO_3	3 h, 70 ºC	1,5
VI	*Strong acid-soluble fraction*	4 M HNO_3	4 h, 90 ºC	0

The procedure was modified by adding of extraction step at the beginning (Exchangeable fraction I) and changing the solvent in the step 2. The first step was added in order to study the metal concentration in the pore waters of solid samples. At the step 2 the solvent was changed from $MgCl_2$ into NH_4Cl. This was done in order to lower the pH of the exchangeable fraction II. The pH of the extraction solutions were measured using a pH meter (Orion 4 Star pH meter D0 Benchtop with ORION 9103APWP AquaPro Semi Micro Ph Prode). The solid : reagent ratio used in the extractions was 1 g of solid material to 15 ml of solution (1:15). Extractions were performed in Sorvall® P.P. 50 ml centrifuge tubes in order to reduce the loss of solid samples. For the quality and repeatability purposes duplicate samples were processed and one chemical blank was added to each extraction set. Sequential extractions were performed for tailings, sediment and waste rock samples. Extractions were performed for samples in their original form, without drying or crushing,

since the metal concentrations in the pore waters were studied. The only exception was sediment sample R-S-3, which was freeze dried before the extractions.

9.1. Reagents

The reagents used in this study had a standard of purity of Purissimum Pro Analysis (p.p.a, >98 %) or higher. The water used in the solutions was acquired from the Millipore Milli-Q system (Millipore, USA). The pH of every solution was measured before use. These are the reagents used in the extractions II – VI:

- **1 M NH_4Cl:** 53,45 g of solid NH_4Cl was weighed into a volumetric flask and diluted to the 1000 ml mark with MilliQ-water.
- **1 M CH_3COONH_4:** 77,87 g of CH_3COONH_4 was weighed into a 1000 ml volumetric flask and dissolved in 250 ml of MilliQ-water. Then 250 ml of 100% CH_3COOH was added to the flask and the solution was diluted to the mark.
- **0,04 M $NH_2OH{\cdot}HCl$:** 2,78 g of solid NH2OH·HCl was weighed into a 1000 ml volumetric flask and dissolved in small amount of MilliQ-water. Then 250 ml of 100% CH_3COOH was added to the flask and the solution was diluted to the mark.
- **0,05 M HNO_3:** 3,5 ml of 65% HNO_3 was added to 500 ml of MilliQ-water in a 1000 ml volumetric flask and diluted to the mark.
- **4 M HNO_3:** 279 ml of 65% HNO_3 was added to 500 ml of MilliQ-water in a 1000 ml volumetric flask and diluted to the mark.

Reagent for Exchangeable fraction I is presented in the chapter 9.1.1.

9.1.1 Pore water model solution for exchangeable fraction I

Exchangeable fraction I was added to the procedure in order to study the composition of pore water in the sample matrixes. For this purpose a specially designed reagent was prepared with macro elements composition matching that of the untreated samples. The pore water composition of the samples was studied by leaching them with water and measuring the macro element concentrations in the supernatants by ICP-MS. In the leach test three enrichment sand samples were extracted with MilliQ-water as follows. The

extractions were performed in 50 ml SORVALL® centrifuge tubes and then the extracted samples were on stored in VWR 50/15 mL PP Centrifuge Tubes. The used solid : reagent ratio was 1:15 and two duplicate samples were analyzed.

The leach test was started by weighing 2 g of solid material into a centrifuge tube. Then 30 ml (30 g) of MilliQ-water was added to the tubes and samples were placed in a mechanical agitator for 1 hour at room temperature. Afterwards the samples were centrifuged (12 000 rpm, 15 min) and the supernatant was removed using a pipette and filtered using a funnel and a filter paper (Whatman® ashless 41) into a 50 ml centrifuge tube. These extraction supernatants were analyzed with ICP-MS in semi quantitative mode. The macro element concentrations in the sample pore waters were calculated using the dry weight percentages of the samples, which are presented in chapter 7.1. The weighted mass was multiplied with the dry weight percentage of the sample to get the amount of water in them and this allowed the calculation of the original pore water concentrations. The calculated pore water concentration results are presented in the table 21.

Table 21. The calculated pore water concentrations for the Rautuvaara enrichment sand samples.

Sample	**Na (ppm)**	**Mg (ppm)**	**K (ppm)**	**Ca (ppm)**
R-E-7 I	174	755	200	998
R-E-7 II	176	792	203	709
R-E-8 I	292	2310	276	5387
R-E-8 II	282	2155	292	6188
R-E-11 I	124	3128	214	8196
R-E-11 II	158	3458	225	6833
Average	201	2100	235	4719
STD	69	1137	39	3133

Using the results from Table 21, the power water model solution was prepared as follows:

- 0,74 g of solid $NaNO_3$; 17,56 g of solid $MgCl_2 \cdot 6H_2O$; 0,45 g of solid KCl and 17,31 g of solid $CaCl_2 \cdot 2H_2O$ were weighed into a 1000 ml volumetric flask and dissolved into 800 ml of MilliQ-water. After dissolution was finished the water volume was diluted to the mark.

9.2 Method of extraction

This chapter will present the whole sequential extraction procedure used in this study. All the laboratory glass wear, centrifuge tubes, syringes, syringe filters and pipettes used in this work were acid washed with 5% nitric acid before use. This was done in order to avoid contamination. All the heating and cooling of the samples took place inside a fume cupboard. In the procedure "A" refers to an extraction step and "B" to a washing step. Washing steps were only performed after extraction steps III – VI.

9.2.1 Exchangeable fraction I

The procedure was started by adding 30 ml of pore water model solution into the centrifuge tubes which contained 2 g of solid sample. Then the tubes were shaken for 1 hour at room temperature inside a mechanical agitator. After that the tubes were centrifuged for 15 min at 12 000 rpm (SORVALL® RC-5B Refrigerated Superspeed Centrifuge, rotor SS-34) and the supernatant was removed using a pipette into a 50 ml centrifuge tube. There after, 5 ml of the sample was filtered at 0,45 µm (VWR 25 mm Syringe Filter w/ 0,45 µm Polypropylene Membrane) into a 15 ml centrifuge tube and acidified with 50 µl of 70 % HNO_3 in order to preserve the samples for later use. At the end the residual sample was moved to the second extraction step.

9.2.2 Exchangeable fraction II

In the second extraction 30 ml of 1 M NH_4Cl was added to the centrifuge tubes, after which the samples were placed in a mechanical agitator for 1 hour at room temperature. After this the supernatant was centrifuged, removed, filtered and stored as is described in chapter 9.2.1. Lastly, the residual sample was moved to third extraction step.

9.2.3 Mild acid-soluble fraction

A. In the third extraction step 30 ml of 1 M CH_3COONH_4 was added to the centrifuge tubes and the tubes were placed inside a fume cupboard in a water bath at 50 ºC for 2 hours. Shaking of the samples was done manually every hour. After cooling the supernatant was centrifuged, removed, filtered and stored as is described in chapter 9.2.1 The residual samples were moved to the washing step.
B. Samples were washed by adding 30 ml of MilliQ-water into the tubes and shaking them for 1 hour inside a mechanical agitator. The washing liquid was centrifuged, removed and filtered like the extraction solutions as is described in chapter 9.2.1. The left-over samples were moved to the fourth extraction step.

9.2.4 Reducible fraction

A. In the fourth extraction step 30 ml of 0,04 M $NH_2OH \cdot HCl$ was added to the tubes and the tubes were placed in a water bath at 70 ºC for 6 hours. Shaking of the samples was done manually every hour. The supernatant was centrifuged, removed and filtered, as is described in chapter 9.2.1. Acidification of the samples was not necessary since the pH of the solutions reached 2. (7) The residual samples were moved to the washing step.
B. Samples were washed by adding 30 ml of MilliQ-water into the tubes and shaking them for 1 hour inside a mechanical agitator. The washing liquid was centrifuged, removed and filtered, like the extraction solutions, as is described in chapter 9.2.1. The left-over samples were moved to the fifth extraction step.

9.2.5 Oxidizable fraction

A. In this step 11 ml of 0,05 HNO_3 and 19 ml of 30% H_2O_2 were added to the residue samples from the fourth step. The reaction between the solid samples and hydrogen peroxide was vigorous so the addition of reagents had to be made step-by-step. At first 5 ml 0,05 HNO_3 was added to the tubes, followed by 19 ml of hydrogen peroxide, added 1 ml at the time. It proved necessary to perform the addition of hydrogen peroxide at room temperature for the reaction to start. Ice bath was used

to cool down the samples after the reaction had started. The remaining 6 ml of HNO_3 was added after the reaction had reached completion. In total the addition of both reagents took approximately 2 hours. Thereafter the tubes were placed in a water bath at 70 ºC for 3 hours. Shaking of the samples was done manually every hour. The pH of the solutions was measured with pH paper before, during and after heating, and it was observed that the pH stayed the same. The supernatant was centrifuged, removed and filtered as is described in chapter 9.2.1. Acidification of the samples was not necessary since the pH of the solutions reached a value below 2. (7) The residual samples were moved to the washing step.

B. Samples were washed by adding 30 ml of MilliQ-water into the tubes and shaking them for 1 hour inside a mechanical agitator. The washing liquid was centrifuged, removed and filtered, like the extraction solutions, as is described in chapter 9.2.1. The left-over samples were moved to the sixth extraction step.

9.2.6 Strong acid-soluble fraction

A. The final extraction step 30 ml of 4 M HNO_3 was added to the tubes, which were then placed in a water bath at 90 ºC for 4 hours. Shaking was done manually hourly. The supernatant was centrifuged, removed and filtered as is described in chapter 9.2.1. Acidification of the samples was not necessary since the pH of the solutions reached below 2. (7) The residual samples were moved to the washing step.

B. Samples were washed by adding 30 ml of MilliQ-water into the tubes and shaking them for 1 hour inside a mechanical agitator. The washing liquid was centrifuged, removed and filtered, like the extraction solutions, as is described in chapter 9.2.1. After washing the residual solids were stored in empty scintillation vials in a case of further experiments.

10. Solid sample digestion by Microwave Accelerated Reaction System

All solid sample materials (the enrichment sand, acidic pond sand, sediment and waste rock) were digested in order to assess the total concentrations of elements with ICP-MS. The samples were digested by using a 5th edition of Microwave Accelerated Reaction System (MARS) with OMNI/XP-1500 vessels. Digestion was performed according to Finland's Radiation and Nuclear Safety Authority's manual for Microwave digestion of Environmental samples as follows. (68) Approximately 0.5 g of dried sample was weighed into pre-cleaned OMNI vessels, followed by 10 ml of concentrated nitric acid. Then the vessels were left to react in a fume cupboard overnight. The addition of concentrated hydrofluoric acid was not done since it is only recommended for ICP-MS analyses when samples containing Ti, Zr, Hf, Nb, Ta, Mo, W, Si, Ge, Sn or Sb are analyzed. (69) The next day the vessels were closed by sealing the frame with a torque wrench and placed on a turntable inside the microwave system. For quality purposes, triplicate samples were digested and two chemical blank samples were included. The digestion program settings were based on that used by Tuovinen et al. (70) and is presented in Table 22.

Table 22. Used settings for MARS 5 digestion (Ramp to temperature for 12 vessels).

Stage	Max Power	% Power	Ramp (min)	Pressure (bar)	Temperature (ºC)	Hold (min)
1	1600 W	100	20:00	55.19	165	00:00
2	1600 W	100	10:00	55.19	200	20:00

After cooling, the sample was transferred from the OMNI vessel into a glass beaker with 10 ml of MilliQ-water. The digest was separated from the residue by using a filter paper (Whatman 42 ashless). Then the glass beaker and the filter paper were rinsed with 10 ml of MilliQ-water. The undigested residue on the filter papers were left to air-dry in fume cupboard, and then weighed before storage for further use. The digest was filtered with a 0.45 μm polypropylene syringe filter and then stored for ICP-MS analyses. The quantities of undigested and digested sample materials are presented in Appendix A. Since there was a residual sample left after the digestion the measured concentrations do not represent the total concentrations of elements in the sample matrixes. However, they the results can be used in this study since the residual sample is likely to consist of minerals phases that are unlikely to become mobile under environmental conditions.

11. Analysis of radionuclides and trace metals

In this work the trace metal and radionuclide concentrations were studied using several different methods. Gamma-ray spectrometry was performed, for all the solid samples, with a germanium semiconductor detector in order to obtain information of the naturally occurring radionuclides. Trace metal, uranium and thorium concentrations, from liquid samples, were analysed using inductively coupled plasma-mass spectrometry (ICP-MS). And finally, the elemental composition and mineral phases of the enrichment sand samples were also studied using X-ray fluorescence (XRF) and X-ray diffraction (XRD) methods.

11.1 Gamma-ray spectrometry of radionuclides

11.1.1 Principles of gamma-ray spectrometry

Gamma-ray spectrometry is based on the fact that every radionuclide has their own gamma-ray energy distribution, which can be identified. Gamma-ray photons are uncharged and weightless and the interactions that they have with surrounding media happen rarely, giving them a long range and pervasive nature. Gamma-ray photons can only be measured once they undergo an interaction, which transfers all or some of the energy they carry to the surrounding target atoms. These interactions consist of five different processes that are coherent scattering, photoelectric effect, Compton scattering, pair formation and photonuclear reactions. (71) The first four of these are presented in Figure 31.

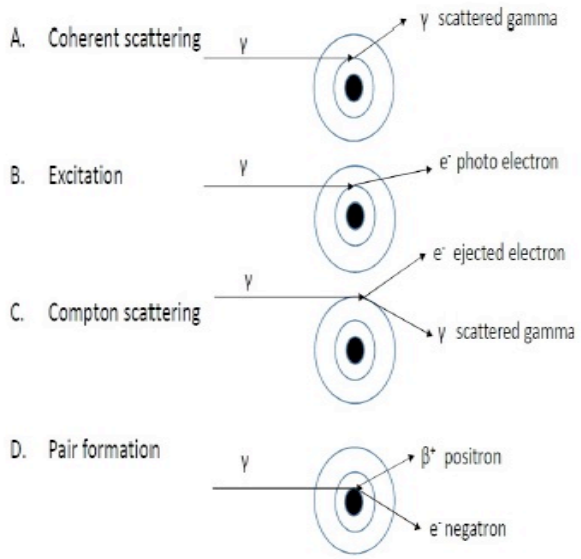

Figure 31. Gamma-ray photon interactions with matter. (71)

Photonuclear reactions and coherent scattering have a minor role in the overall reactions of gamma rays so in this master's thesis they are not discussed any further. The other three mechanisms are significant in the measurements of gamma rays. In photoelectric effect the gamma ray interacts with an orbital electron. All of the energy the photon carries is transferred to the electron, which is then emitted out from the atom, leaving a vacancy on electron orbit. This vacancy is then filled with a higher energy electron, which causes X-ray and Auger electron formations. In Compton scattering the emitted electron only receives part of the original gamma photon energy, which continues forward with less energy and a changed direction. Compton scattered photons are able to cause new interactions as long as their energy is higher than the electron binding energy. Pair formation is a process in which the nuclear electric field of an atom transfers the whole gamma photon energy into electron-positron pair. The energy of the gamma photons needs to be at least 1.022 MeV since in the pair formation both electron and positron require 0.511 MeV. If the gamma photon energy exceeds the requirements the rest is shared as kinetic energy for the forming pair. Further on the formed electron is absorbed by the interacting matrix and the positron is annihilated after sufficient energy loss. (71) The occurrence of different gamma photon interactions depends on gamma photon energy and atomic number of the interacting media as is presented in Figure 32.

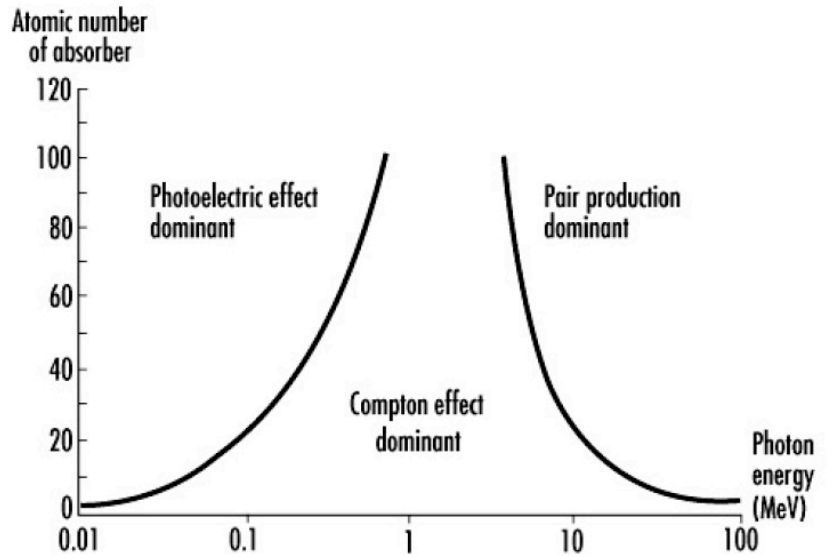

Figure 32. The effect of gamma photon energy and the density of the media on gamma interactions. (71)

Gamma radiation can be measured with two different kinds of detectors: solid scintillators and semiconductors. Previously described gamma photon interactions release energy into the detector material, which is then transformed into electrical pulses and can be counted using computers. In this master's thesis the gamma measurements were done using a semiconductor detector so the scintillation detectors are not discussed any further.

11.1.2 Gamma-ray spectrometry with semiconductor detector

In gamma spectrometry the most commonly used semiconductor material is germanium. The semiconductor consists of two different parts: n-type semiconductor and p-type semiconductor. The n-type part produces mobile electrons, which are created by introducing phosphorus atoms (+V) into the germanium matrix (+IV). In the p-type semiconductor indium atoms (+III) are added into the germanium matrix to produce positive holes. When a bias electric field is introduced to the system an area depleted of both holes and electrons is formed at the interface of the two different parts. This interface becomes conducting when a gamma photon hits it and produces electron-hole pairs. The produced electric pulse can be recorded and measured. Germanium semiconductor detectors have a very good energy resolution, which allows the detection of multiple gamma emitters from the same sample, for example, from complex nuclear waste samples.

Traditionally germanium detectors are shielded with an aluminium cover that makes the detection of the low-energy gamma emitters (etc. ^{210}Pb) impossible, as they get absorbed into it. This can be avoided using a design with a very thin window of either beryllium or carbon composite, which allows the incoming photons to reach the germanium. (1)

11.1.3 Analysis of radionuclides with gamma spectrometry

In this study the gamma spectrometry measurements were done using Canberra high purity germanium detectors at the Radiation and Nuclear Safety Authority of Finland (STUK), in Helsinki. In order to obtain the activities of ^{210}Pb, ^{238}U, ^{226}Ra, ^{232}Th and ^{228}Ra, the natural radionuclides ^{210}Pb ($t_{1/2}$ = 22,3 a), ^{228}Ac ($t_{1/2}$ = 6,15 h), ^{214}Bi ($t_{1/2}$ =19,9 min), ^{214}Pb ($t_{1/2}$ = 26,8 min) and ^{234m}Pa ($t_{1/2}$ = 1,17 min) were measured and determined from all the solid samples using UniSampo-Shaman (USS) spectral analysis software. Prior to analysis the detectors had been calibrated according to STUK's standards. The activity of ^{238}U was assumed to be in equilibrium with its progeny nuclide ^{234m}Pa. (28) The activity of ^{226}Ra was in secular equilibrium with its granddaughter's ^{214}Bi and ^{214}Pb, since the samples were vacuum packed in aluminium covers in order to enable the growing in of the granddaughter nuclides. The activity concentration of ^{226}Ra was calculated as a weighted mean of the ^{214}Bi and ^{214}Pb activity concentrations. (72) The activities of ^{232}Th and ^{228}Ra are in secular equilibrium (± 5 years) with their daughter nuclide ^{228}Ac, since the mining activities at the Rautuvaara mine terminated 30 years ago. (28) Thus the assumption for ^{232}Th/^{228}Ra is tentative since more enrichment sand was added to the Rautuvaara tailings area later on. (72) The results were given in unit Becquerel's per kilogram of dryweight (Bq per kg d.w.). In order to compare the gamma measurement results of ^{232}Th and ^{238}U to those derived from ICP-MS the results were converted into concentrations using the next two relations (73):

$$1\ Bq\ ^{238}U\ kg^{-1} = 81 \cdot 10^{-3}\ mg\ U\ kg^{-1}$$

$$1\ Bq\ ^{232}Th\ kg^{-1} = 246 \cdot 10^{-3}\ mg\ Th\ kg^{-1}$$

Figure 33 presents the measured gamma spectrum of one of the enrichment sand samples from Rautuvaara tailings area.

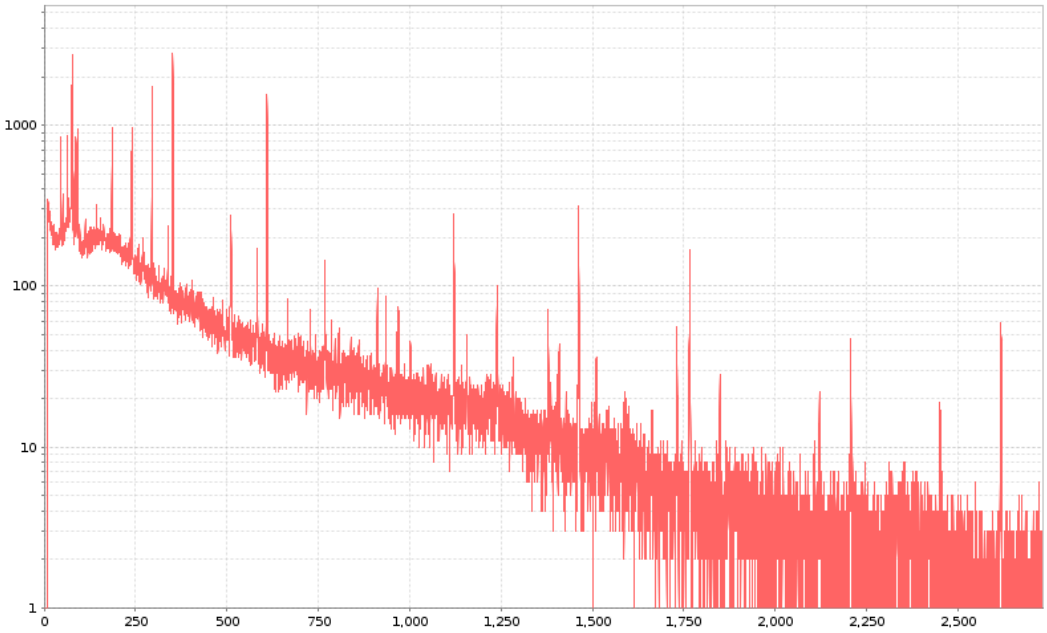

Figure 33. Measured gamma spectrum of the enrichment sand sample (R-E-1) from the Rautuvaara tailings area.

11.2 Elemental analysis by ICP-MS

11.2.1 Principles of ICP Mass Spectrometry

Inductively coupled plasma-mass spectrometry (ICP-MS) can be used to measure low concentrations of elements from the sample solutions. In the method a high temperature plasma splits the compounds into elements and furthermore into positively charged ions, which are then identified by their mass-charge –ratio (m/Z). Concentrations are counted from the total count of identified ions. (74) The basic principle of ICP-MS is presented in Figure 34.

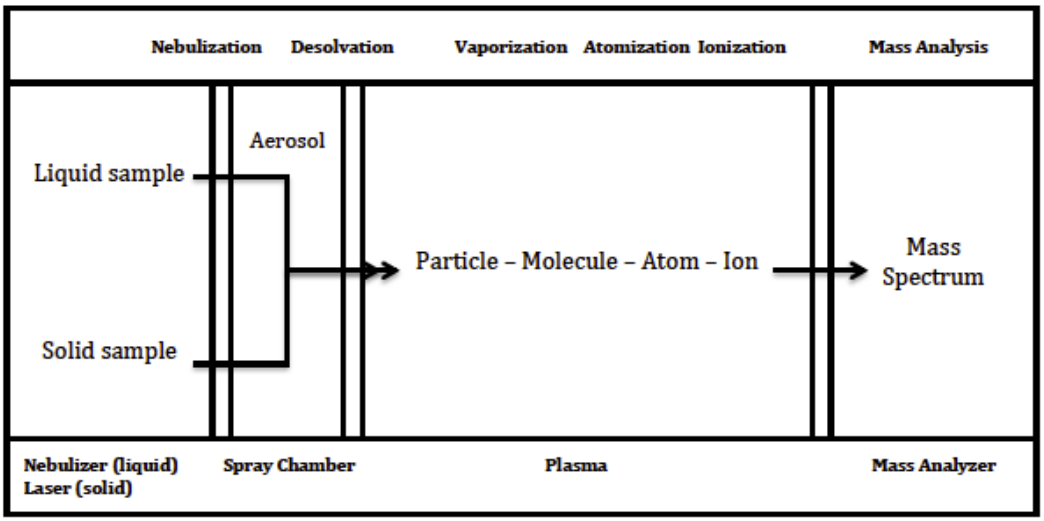

Figure 34. Basic principle of mass spectrometry.

ICP-MS analysis can be divided into four steps that are sample introduction, ICP torch, interface and mass-analyzer. Samples can be introduced in various ways depending on the physical features of the sample (liquid or solid), however the aim is to get the sample into the torch in a gaseous or aerosol form for analysis. Typically, the samples used are in liquid form and can be used in the analysis after nebulization in the argon gas flow in the gas chamber. Nebulization does not separate any compounds of interest and therefore all the nebulized elements will be introduced to the torch and detected. The torch itself is a concentric quartz structure with a copper induction coil wrapped around it and a continuous argon gas flow (12 – 20 l/min) running through it. The coil is coupled with a magnetic field at a frequency of 27,12 MHz and a power of 1000 W. Flowing argon is ionized with a spark from a Tesla unit and the produced cations and electrons are subjected to an accelerating rotation movement in the magnetic field. Plasma generation occurs when

the collision of the particles in the rotation movement produces enough heat. (75) When plasma has reached equilibrium it remains at a temperature between 6 000 – 10 000 K. (7) In the plasma, samples are dried of their solvents and atomization occurs via gas formation, producing monovalent positive ions that will eventually come to the interface. The purpose of the interface is to connect the ICP part of the instrument to the mass analyzer part. From plasma the samples are led to a water-cooled sample cone at the interface, which leads to a depressurizing chamber. At this point the gaseous sample cools downs and expands, which allows a fraction of it to pass through another cone into the mass analyzer chamber that is maintained at a vacuum. Then the stream of ions is directed into single ion lenses, which focuses it for the quadrupole region. The quadrupole consist of four parallel cylindrical rods of which the opposites are connected similarly: two to the positive side of a variable current source and two to the negative terminal. This system separates the ions with desired m/Z –ratio and allows them to reach the transducer, while the undesired are pumped out of the system. The quadrupole system is suitable for resolving ions with mass numbers differing by one unit. Measuring with the quadrupole unit is fast and the measurement in the 2 – 206 AMU region can be done in 0,1 s. After the quadrupole unit the separated ions enter the detector. Typically, the detectors are electron multipliers, which are capable of converting the positive ions into electrical impluses. (75) A simplified structure of ICP-MS machine is presented in the figure 35.

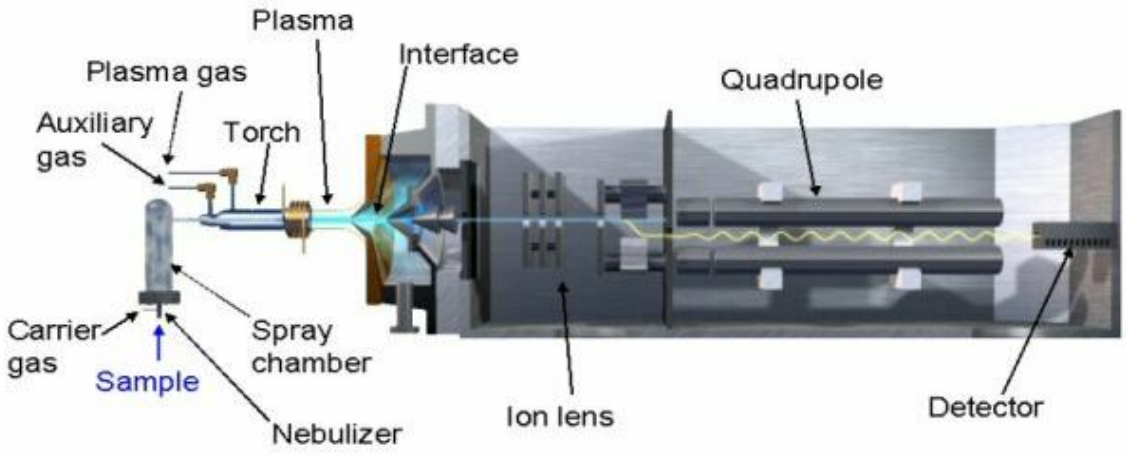

Figure 35. The structure of ICP-MS. (76)

These days the ICP-MS instrument control system has been almost completely computerized. (75) There are many benefits in ICP-MS analysis, such as a high sensitivity

of 0,5 AMU and wide linear measurement range, though the method has its downsides which can be divided into spectral and non-spectral interferences. (75) Spectral interferences are caused by the limited resolution of the mass spectrometer when the detected ions differ less than 0,5 AMU in their mass units. Spectral interferences can also be caused by overlapping isotopes of different elements (isobaric interferences), by double charged ions (M^{2+}) with low second ionization energy forming oxides or by formation of polyatomic species at the plasma. With the right instrumental parameters it is possible to reduce these interferences to 1 – 2 percent. Non-spectral interferences can be classified in two categories, which are reversible and irreversible interferences. Reversible interferences are formed while the samples are being measured. Irreversible interferences are matrix effects that occur when the nebulizer gets clogged or when the sample deposits on the torch or in the ion lenses. Non-spectral interferences can be reduced by using appropriate calibration methods, adapting sample preparations or limiting the amount of sample reaching the nebulizer, plasma and sampling devices. (77)

Before beginning the measurements with ICP-MS the instrument requires a calibration to ensure the qualification of the analysis. This is traditionally done using an external standard with known concentrations of elements diluted to match the sample matrix. The measured samples concentrations must be between the known standard solutions to ensure the best results. If the actual samples are unknown it is possible to perform a semi quantitative analysis to quickly estimate the concentrations with an error within 10-30 %. Throughout the measurement the calibration stability is supervised by the use of internal standard and known reference samples. (75)

One way to reduce the interferences during the analysis and gain better resolution is the use of high-resolution (HR) ICP-MS, which utilises strong electromagnets with a varying magnetic field. HR-ICP-MS enables to separation between each different elements with the two swinging gate slits that vary the resolution. HR-ICP-MS also has a high ion transport efficiency, which gives a very high sensitive, and a low background noise from the design, when compared to the traditional ICP-MS. Some of the throwbacks of this method are the slow analysis speed, due to the time that it takes to change the magnetic field between the different masses, and a mass drift at higher resolutions. (78)

11.2.2 Analysis of the trace metal concentrations with ICP-MS

In this study the samples were analysed using Agilent 7800 ICP-MS instrument (Agilent 7800; Agilent Technologies, Santa Clara, CA, USA) in the Department of Geosciences and Geography's in University of Helsinki. Prior to measurements a semi-quantitative run was commenced to clarify the unknown metal concentrations on the different samples, which included natural waters, mining area waters and supernatants from sequential extractions and microwave digestion. The metals were analysed using an ICP-MS method developed to detect Na, Mg, K, Ca, Cr, Mn, Fe, Ni, Co, Cu, Zn, As, Cd, Pb, Th and U. Metals with atomic mass between 30-90 were detected with helium mode, to reduce the interferences, and other metals with non-gas mode. The internal standard used in this study for low-mass metals was ^{72}Ge, for medium-mass ^{103}Rh and ^{125}Te and for heavy-mass metals ^{175}Lu. External calibration was performed by preparing elemental standard solution (bulk solution) from single-element standard solutions (Merck) and then diluting this to attain the desired concentrations. External calibration solutions are presented in the table 23.

Table 23. External calibration solutions (ppb) for ICP-MS.

Bulk solution		**Calibration standards (ppm)**								
Element	ppm	std1	std2	std3	std4	std5	std6	std7	std8	std9
Ca	100	0	0,01	0,1	0,5	1	5	10	25	50
Mg	100	0	0,01	0,1	0,5	1	5	10	25	50
Fe	100	0	0,01	0,1	0,5	1	5	10	25	50
K	20	0	0,002	0,02	0,1	0,2	1	2	5	10
Na	20	0	0,002	0,02	0,1	0,2	1	2	5	10
Cu	20	0	0,002	0,02	0,1	0,2	1	2	5	10
Mn,	10	0	0,001	0,01	0,05	0,1	0,5	1	2,5	5
Zn	10	0	0,001	0,01	0,05	0,1	0,5	1	2,5	5
Ni	10	0	0,001	0,01	0,05	0,1	0,5	1	2,5	5
As	10	0	0,001	0,01	0,05	0,1	0,5	1	2,5	5
Cr	10	0	0,001	0,01	0,05	0,1	0,5	1	2,5	5
Co	10	0	0,001	0,01	0,05	0,1	0,5	1	2,5	5
Cd	5	0	0,0005	0,005	0,025	0,05	0,25	0,5	1,25	2,5
Pb	5	0	0,0005	0,005	0,025	0,05	0,25	0,5	1,25	2,5
Th	5	0	0,0005	0,005	0,025	0,05	0,25	0,5	1,25	2,5
U	5	0	0,0005	0,005	0,025	0,05	0,25	0,5	1,25	2,5

The spectra from the ICP-MS run was analysed using the Masshunter spectral analysis program. To avoid non-spectral interferences all the measured samples were diluted with 1/100 dilution factor with 5 % suprapure HNO_3. All the laboratory glass wear, centrifuge tubes, syringes, syringe filters and pipettes used for sample preparation were acid washed with 5% nitric acid before use to reduce the risk of contamination. Also, the used water was acquired from Milli-Q purification system (Millipore, USA). One reference sample was included to the analysis to check the qualification of the standards: Spectrapure Standards, Reference Material for Measurement of Element in Surface Waters, SPS-SW2, batch 128. The results for the reference water sample are presented in the table 24.

Table 24. Declared and measured values of the studied reference water SPS-SW2. Measured values are averages from all measurements (n = 11).

Element	**SPS-SW2**			
	Declared (ppb)	Measured (ppb)	STDEV	Difference %
Na	10000	9604	293	4,0
Mg	2000	1867	52	6,6
K	1000	934	23	6,6
Ca	10000	10353	282	3,5
Cr	10	9	0,2	9,2
Mn	50	46	1	7,4
Fe	100	92	2	8,4
Co	10	9	0,2	6,5
Ni	50	48	1	4,9
Cu	100	94	2	6,2
Zn	100	96	3	4,0
As	50	47	1	5,5
Pb	25	26	0,4	3,7
Th	2,5	2,3	0,05	6,9
U	2,5	2,3	0,05	7,2

Reagent blank samples were also analysed for the extraction solutions in order to account for the metal concentrations present in the extraction reagents. Blank sample concentrations can be subtracted from the concentrations found in the samples to ensure that the final concentration is representative of the original sample. Also, concentrations from the extraction and washing step, for steps III – VI, were summed together before giving the total concentration. (48)

Trace metal and radionuclide concentrations for the water samples were calculated as an average of duplicate samples. The concentrations for extraction and microwave digestion samples were calculated using formula 2.

$$c(ppm\ or\ ppb) = \frac{c_{avg} \cdot dilution\ factor \cdot V}{m}$$

[2]

Where c_{avg} is the average of duplicate or triplicate samples measured with ICP-MS, V is the total volume of the measured sample and m is the mass of the solid sample. Finally, an error for the average concentrations was calculated by using standard deviation.

11.3 Determination of elements with X-ray techniques

The most commonly used X-ray based techniques for material analysis are X-ray fluorescence (XRF) and X-ray powder diffraction (XRD). X-rays are energetic radiation that may cause the removal of electrons located in the inner orbitals in the target atoms. These vacancies are then filled with electrons from the outer orbitals, leading to emissions of X-ray photons with an energy corresponding to the energy difference of the two orbitals. The produced X-rays are characteristics to different elements, since the emission lines can be linked into the atomic number of the atom, and can therefore be used as a tool for determining the chemical composition of the measured sample.

Both XRF and XRD techniques can be used for qualitative and quantitative elemental analysis of the samples with different approaches. The XRF technique utilizes the diffraction power of a single crystal, or a proportional detector, to separate the polychromatic beam of characteristic radiation exited from the sample into narrow wavelength bands, while the XRD method relies on the diffraction of X-rays. In this study a selected set of solid samples were first analyzed with XRF method in order to obtain the elemental content of the samples and then with the synchrotron XRD method to quantitatively identify the main mineral phases. (79)

11.3.1 Elemental analysis with X-ray fluorecense

In XRF the X-ray source is used to irradiate the sample causing the elements in it to emit discrete fluorescent X-ray radiation, which is characteristic for each element. By measuring the energy differences and intensities of the produced radiation it is possible to determine the present elements and their quantities in the sample. (80) The measured radiation is transformed into elemental values by the use of calibration curves derived from the measurements of standard samples. (81)

XRF analysis is done with X-ray spectrometers, which, as an addition to the spectrometer itself, has a primary source unit (etc. X-ray tube) and the measuring electronics. The used spectrometers are either energy dispersive systems (ED-XRF) or wavelength dispersive systems (WD-XRF). In ED-XRF the radiation coming from the sample is measured directly by the detector, which can separate the radiation from the different elements using

dispersion. In WD-XRF the radiation coming from the sample is directed to analyzing crystals in order to disperse it in different directions before entering the detector. In the XRF method the analyzed elements and their detection limits depend on the type of spectrometer used. The highest elemental range can be achieved with WD-XRF (from Be to U). The elements with a higher atomic number can be detected with better detection limits than the lighter ones. (80)

11.3.1.1 Sample preparation and analysis with WD-XRF

In total 8 solid samples were prepared and analyzed with WD-XRF. Four of these were original samples collected from Rautuvaara tailings and four of them were subsamples of the residues produced in the oxidizable fraction in sequential extractions. The tailings samples were already processed as described in chapter 7.1 and the extraction residues were air dried in the fume cupboard overnight. Approximately 1 g of the sample was weighed into a crucible and then placed into the muffle furnace, ignited at 550 ºC for 2 hours and then placed to cool down in a desiccator for 45 minutes before weighing. The beads for the WD-XRF spectrometer were prepared from the dried samples by weighing 6.0 g of flux (49.75 % $Li_2B_4O_7$ – 49.75 % $LiBO_2$ – 0.5 % LiBr) with 0.6 g of sample into a platinum crucible and processing the mixture with Claisse M4 gas fluxer in 1000 ºC. In this study the XRF measurements were done using WD-XRF PANanalytical Axios mAX spectrometer in the Department of Geosciences and Geography's, University of Helsinki. The measurements were done using both standardized quantitative setting (Bead) and semi-quantitative Omnia 27-3 kW settings. During the method the setup used was 3 kW with an acceleration voltage of 60 kV and probe current of 50 mA. The measured results were analyzed using SuperQ –measure and analyze –program.

11.3.2 Elemental and mineral analysis by X-ray powder diffraction

X-ray powder diffraction (XRD) is a widely used crystallographic technique that can be used for structure and phase characterization of crystalline samples. In this study the samples were analyzed by using the Synchrotron Radiation X-ray Powder Diffraction (SR-XRPD) technique. Synchrotron radiation is created when electrons moving along a curved trajectory and as the speed of the electrons approaches the speed of light the properties of the emitted radiation change due to relativistic effects. (82) Synchrotron radiation is considered as a fundamental tool in many fields of science since it has many desired qualities:

- *Adjustable photon energy* covering a wide range of the spectra.
- *Spectral brightness* that is defined as flux per unit area of the radiation source per unit solid angle of the radiation cone per unit spectral bandwidth.
- *Linear polarization* of the emitted radiation with the electric vector at the point the orbit is parallel to it.
- *Pulsed time structure* of the source, which depends on the size of the ring and by the total number of circulating bunches and is usually defined by the duration and separation time in-between the pulses.
- *Coherence* in the radiation depending on the size of the ring, angular spread of the source and in the wavelength bandwidth. (82)

Each synchrotron facility has its own detailed characteristics and they can be, further on, tuned and improved if insertion devices, like wigglers and undulators, are used to extract the radiation. The latter two consist of multiple magnets that are able to change the path of the electrons from straight into slalom like course causing them to emit radiation every time they oscillate. After the extraction the radiation needs to be conditioned for the specific experiment by appropriate beamline optics. By changing the used beamline optics and magnets it is possible for one facility to host experiments needing a wide range of different energies. The angular (FWHM) resolution of the photon beam is defined by the energy resolution ($\Delta\lambda/\lambda$) and the degree of collimation. In SR-XRPD experiments to achieve high-resolution the beam should be monochromatic and collimated so the beamline optics usually consist of a monochromator and a few mirrors. (82)

In this study the samples were measured in the Material Science (MS) beamline at the Swiss Light Source (SLS) at the Paul Scherrer Institut in Switzerland. This MS-SLS beamline consists of a linear accelerator, booster and storage ring. The linear accelerator has an electron source and two accelerating sections, which are able to increase the energy of the pulled out electrons to 100 MeV with speed close to the speed of light. The booster accelerates the incoming electrons from the linear accelerator to the final energy, which is close to 2.4 GeV. The storage ring allows the accelerated electrons to circulate for hours and undulator magnets are used to make the electrons move in a slalom like course, which concentrates the produced synchrotron light into discrete lines in the spectrum. The distance between electrons slalom turns and the strength of the magnetic field define the desired wavelength. The SLS facility can produce very high quality synchrotron light, with an average power of 200 kW, due to 330 installed magnets, which are designed to keep the electron beam as small as possible.

11.3.2.1 Sample preparation and analysis with SR-XRPD

In total 16 selected samples from Rautuvaara tailings were analyzed quantitatively with SR-XRPD to identify the main mineral phases. Four of these samples were original enrichment sands and the rest subsamples of extraction residues produced in sequential extractions. All samples were manually crushed and homogenized in mortar, and screened to < 20-µm using the equipment shown in Figure 36.

Figure 36. Equipment used to manually prepare the samples for SR-XRPD analysis: mortar, 20-µm screen with collecting pan and brush.

In this study, data was collected using a Dectris Pilatus 6 M single photon counting hybrid detector implemented at the Material Science beamline X04SA at the Paul Scherrer Institut, Swiss Light Source (SLS) using a piezo driven Vibrating Sample Houlder (VHS). (83) The employed wavelength was 0.56462 Å. The distance between sample and detector was 588.136 mm and the X-ray powder diffraction spectra was recorded with 2 θ – coverage between 0,63211° - 22,43711° using 16 s exposure time. The 2D –diffraction patterns were created using Dioptas software. The mineral phases were identified through the Rietveld refinement technique using PanAnalytical High Score+ software equipped with ICDD PDF4 Minerals database using search-match function, the results from XRF analysis and the geological knowledge of the source of the tailings. Figure 36 presents the recorded diffraction patterns for the enrichment sand sample (R-E-1) that were processed with Dioptas software.

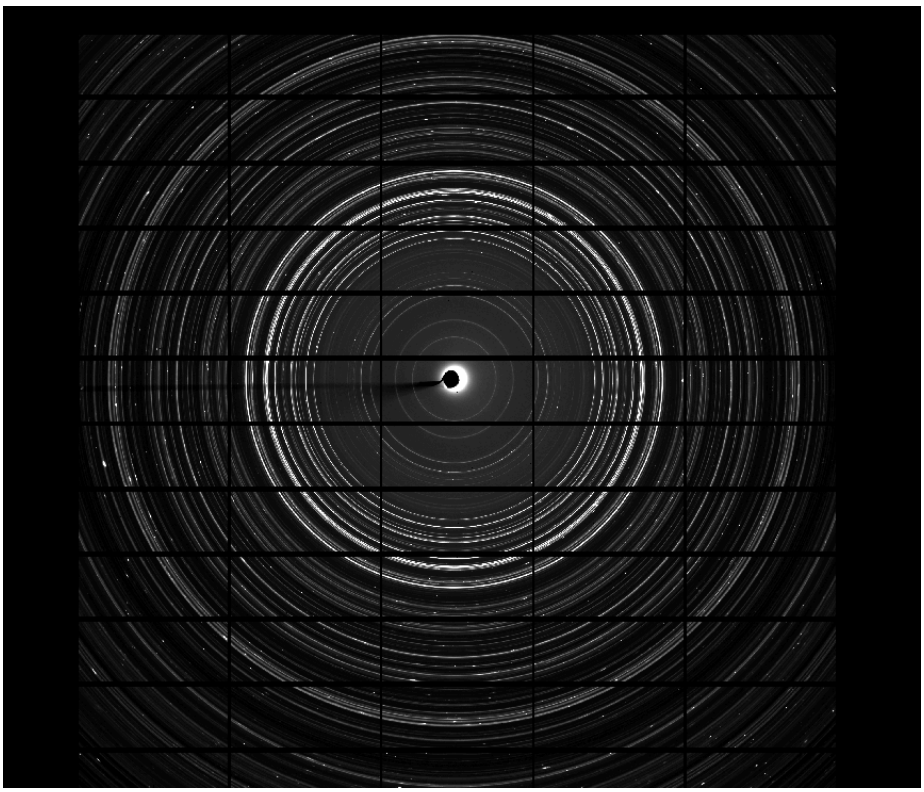

Figure 36. Diffraction patterns of the Rautuvaara enrichment sand sample (R-E-1) recorded with Dectris Pilatus 6 M single photon counting hybrid detector.

12. Results and discussion

12.1 Gamma activities of sediment, enrichment sand, acidic pond sand and waste rock samples

Four different sample types were analyzed by gamma spectrometry, which were the sediment, enrichment sand, acidic pool sand and waste rock. For each sample the observed radionuclides were ^{210}Pb, ^{238}U, ^{226}Ra and ^{232}Th/^{228}Ra, and their activity concentrations are shown in Tables 25, 26, 27 and 28. The activities of ^{232}Th and ^{228}Ra are in secular equilibrium (± 5 years) with their daughter nuclide ^{228}Ac, since the mining activities at the Rautuvaara mine terminated 30 years ago.

Table 25. Activity concentrations (Bq/kg d.w.) ± uncertainty (Bq/kg d.w.) of ^{210}Pb, ^{238}U, ^{226}Ra, ^{232}Th and ^{228}Ra in sediment samples taken from Rautuvaara settling pond.

Sediment sample	Depth (cm)	**U-238** (Bq/kg d.w.)	**Ra-226** (Bq/kg d.w.)	**Pb-210** (Bq/kg d.w.)	**Th-232 / Ra-228** (Bq/kg d.w.)
R-S-1	0 - 1	513	244	747	25
±		82	14	56	4
R-S-2	1 - 2	371	285	495	32
±		53	15	25	3
R-S-3	2 - 7	209	239	184	28
±		17	9	26	2
Mean		364	256	475	28
Range		209 - 513	239 - 285	184 - 747	28 - 32

Table 26. Activity concentrations (Bq/kg d.w.) ± uncertainty (Bq/kg d.w.) of ^{210}Pb, ^{238}U, ^{226}Ra, ^{232}Th and ^{228}Ra in acidic pond sand samples taken from Rautuvaara tailings.

Acidic pond sand sample	**U-238** (Bq/kg d.w.)	**Ra-226** (Bq/kg d.w.)	**Pb-210** (Bq/kg d.w.)	**Th-232 / Ra-228** (Bq/kg d.w.)
R-S-4	< 31,7	36	32	9
±	-	2	6	1
R-S-5	< 38,9	42	47	11
±	-	2	4	1
R-S-6	< 42,5	44	33	12
±	-	2	3	1
R-S-7	83	51	42	15
±	17	3	4	2
Mean	83	43	39	12
Range	-	36 - 43	32 - 47	9 - 15

Table 27. Activity concentrations (Bq/kg d.w.) ± uncertainty (Bq/kg d.w.) of ^{210}Pb, ^{238}U, ^{226}Ra, ^{232}Th and ^{228}Ra in enrichment sand samples taken from Rautuvaara tailings.

Enrichment sand sample	**U-238** (Bq/kg d.w.)	**Ra-226** (Bq/kg d.w.)	**Pb-210** (Bq/kg d.w.)	**Th-232 / Ra-228** (Bq/kg d.w.)
R-E-1	182	163	113	13
±	37	8	7	2
R-E-2	< 70,9	88	79	13
±	-	6	4	1
R-E-3	133	148	114	18
±	34	8	7	2
R-E-4	135	152	117	16
±	15	8	10	1
R-E-5	203	147	99	19
±	38	8	6	2
R-E-6	< 77,6	69	58	14
±	-	4	11	2
R-E-7	127	132	118	18
±	21	7	9	2
R-E-8	107	101	91	16
±	22	6	7	2
R-E-9	81	79	67	10
±	21	4	5	1
R-E-10	< 141,3	111	77	8
±	-	6	5	2
R-E-11	167	95	87	16
±	25	5	7	2
R-E-12	156	125	110	17
±	16	7	9	1
R-E-13	163	176	146	15
±	24	11	26	2
R-E-14	145	117	96	8
±	29	6	6	1
R-E-15A	110	106	102	9
±	22	6	8	1
R-E-15B	115	110	84	11
±	30	6	5	2
R-E-16	97	106	82	16
±	22	5	9	2
Mean	140	119	96	14
Range	81 - 203	69 - 176	58 - 146	8 - 19

Table 28. Activity concentrations (Bq/kg d.w.) ± uncertainty (Bq/kg d.w.) of ^{210}Pb, ^{238}U, ^{226}Ra, ^{232}Th and ^{228}Ra in waste rock samples taken from Rautuvaara mining area.

Waste rock sample	**U-238** (Bq/kg d.w.)	**Ra-226** (Bq/kg d.w.)	**Pb-210** (Bq/kg d.w.)	**Th-232 / Ra-228** (Bq/kg d.w.)
R-R-1A	64	63	53	43
±	20	4	10	4
R-R-1B	83	54	51	43
±	20	3	5	3
Mean	74	59	52	43
Range	64 - 83	54 - 63	51 - 53	-

The mean activity concentration in the sediment for ^{238}U, ^{226}Ra, ^{210}Pb and ^{232}Th/^{228}Ra was 364, 256, 475 and 28 Bq/kg dry weight, respectively. The concentrations of ^{226}Ra and ^{232}Th/^{228}Ra were seen to be similar in all the measured core depths. The concentration of ^{238}U was seen to be highest in the top layer of the sediment core, the activity concentration being twice as high as in the lowest. A similar trend was seen with the ^{210}Pb activity concentration as the top layer had three times as much activity as the deepest part of the core.

In the sample R-S-3, ^{238}U, ^{226}Ra and ^{210}Pb were seen to be in secular equilibrium, which can be seen in Figure 37.

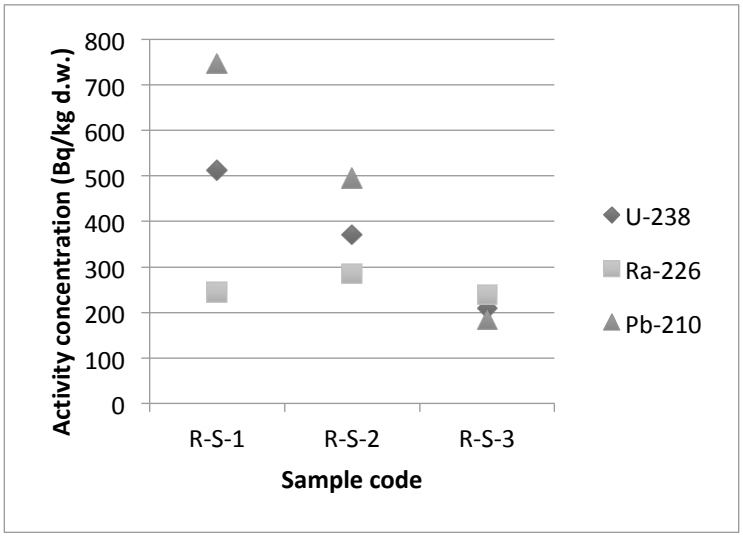

Figure 37. The activity concentrations (Bq/kg d.w.) of ^{238}U, ^{226}Ra and ^{210}Pb in the sediment samples from the Rautuvaara settling pond.

The mean activity concentration of ^{238}U, ^{226}Ra, ^{210}Pb and ^{232}Th/^{228}Ra in the enrichment sand samples was 140, 119, 96 and 14 Bq/kg dry weight, respectively, and their spatial distribution varied only slightly throughout the sampling area. The highest activity concentration of ^{238}U was found at the southern side of the area in the sample R-E-5, where it reached 203 ± 38 Bq/kg dry weight. The highest activity concentrations of ^{226}Ra and ^{210}Pb were found at the northeast side of area in the sample R-E-13, where the activities were 176 ± 11 and 146 ± 26 Bq/kg dry weight, respectively. The activity concentration for ^{232}Th/^{228}Ra stayed moderately low in all the samples and the highest value of 19 Bq/kg dry weight was found in the sample R-E-5. In the acidic pond sand samples the mean activities of ^{238}U, ^{226}Ra, ^{210}Pb and ^{232}Th/^{228}Ra were 83, 43, 39 and 12 Bq/kg dry weight,

respectively. The activity concentration of ^{238}U in the acidic pond sand was below the detection limit in most of the samples.

The mean activity concentrations of ^{238}U, ^{226}Ra, ^{210}Pb and $^{232}Th/^{228}Ra$ in waste rock samples were 74, 59, 52 and 43 Bq/kg dry weight, respectively. The measured values resembled those of the acidic pond samples, apart from the concentration of $^{232}Th/^{228}Ra$ that was three times higher. Figures for the activity concentrations of ^{238}U, ^{226}Ra and ^{210}Pb in the enrichment sand, acidic pond sand and waste rock are presented in Appendix A.

The sediment samples had the highest concentrations of ^{238}U, ^{226}Ra and ^{210}Pb when compared to the values from other sample types, which were 364, 256 and 475 Bq/kg dry weight, respectively. The highest concentration of $^{232}Th/^{228}Ra$ was found in the waste rock samples. Table 29 presents the average activity concentrations of ^{238}U, ^{226}Ra and ^{232}Th in soils in Finland and on average in the world's lithosphere. The concentrations of U are approximately six times higher in the sediment and twice as high in the enrichment sand than on average in Finnish soil. The concentration of ^{226}Ra is also four times higher in the sediment and twice as high in the enrichment sand. All of the measured ^{232}Th activity concentrations, as well as ^{238}U and ^{226}Ra in the acidic pond sand and waste rock, resemble the average activities in Table 29.

Table 29. Average activity concentrations of ^{238}U, ^{226}Ra and ^{232}Th in soil samples. (1) (30)

Radionuclide	**World's average in the lithosphere (Bq kg^{-1})**	**Finland (Bq kg^{-1})**
^{238}U	28	30 - 60
^{226}Ra	-	30 - 60
^{232}Th	33	-

In order to compare the gamma measurement results of ^{238}U and ^{232}Th to those derived from ICP-MS the results were converted into concentrations using the following relations:

$$1\ Bq\ ^{238}U\ kg^{-1} = 81 \cdot 10^{-3}\ mg\ U\ kg^{-1}$$

$$1\ Bq\ ^{232}Th\ kg^{-1} = 246 \cdot 10^{-3}\ mg\ Th\ kg^{-1}$$

The converted results can be found in Appendix A.

12.2 Elemental concentrations in the water samples

Water samples from the Rautuvaara mining area and its surroundings were analysed with ICP-MS for their radionuclide (^{238}U and ^{232}Th) and elemental (Cr, Mn, Fe, Co, Ni, Cu, Zn, As, Cd and Pb) concentrations. The analytical results for the reference water (collected upstream from the mining area), settling pond water, downstream water and reservoir water are given in Figures 38 and 39. The results for the acidic pond water are given in Figures 40 (ppm) and 41 (ppb). The analytical data from ICP-MS measurement can be found in Appendix A.

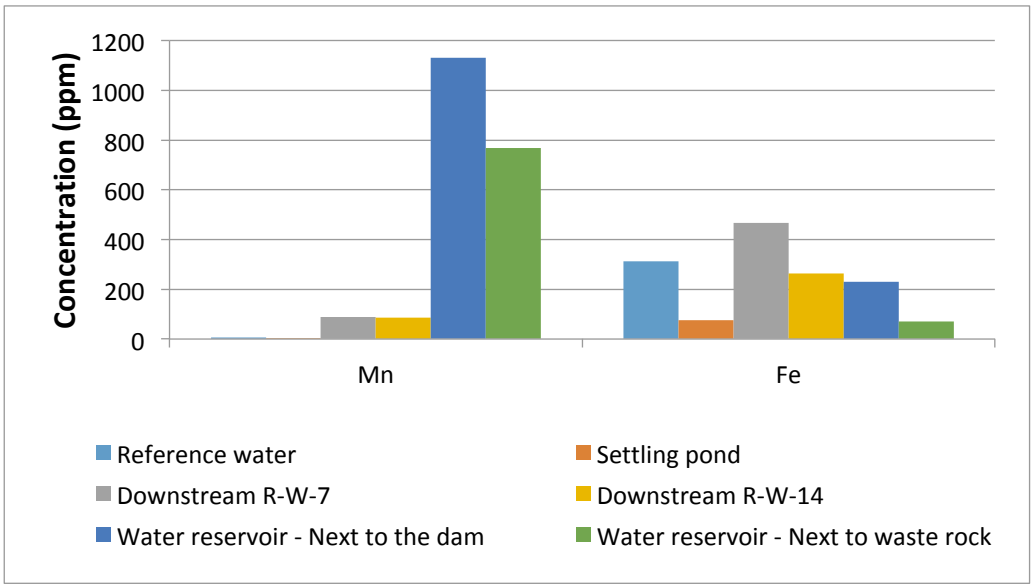

Figure 38. Measured metal concentrations of Fe and Mn (ppm) in the water samples collected from the Rautuvaara mining area and its surroundings, excluding the acidic pond. (R-W = Rautuvaara Water, No. = sampling location)

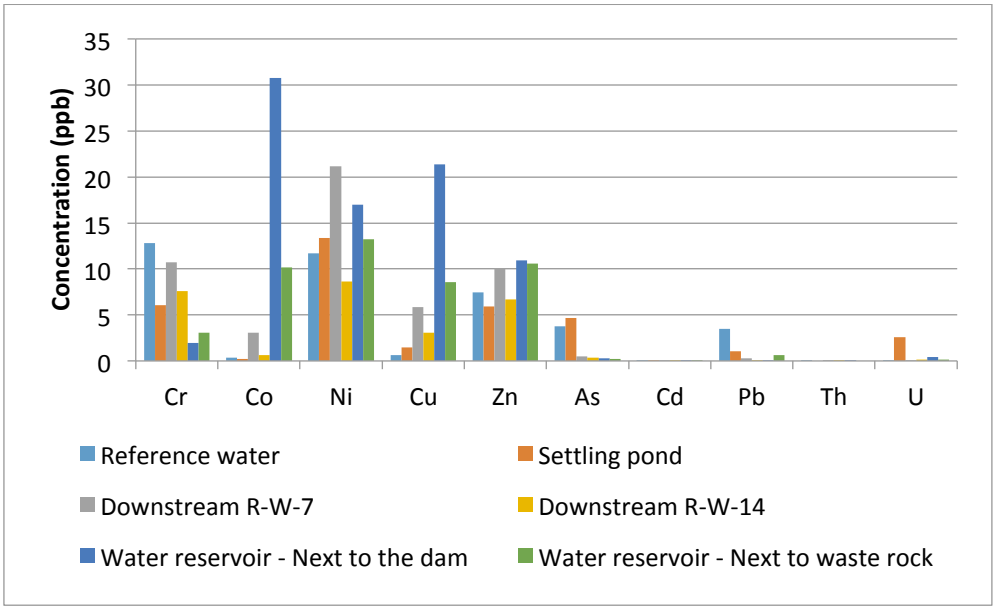

Figure 39. Measured metal concentrations (ppb) of Cr, Co, Ni, Cu, Zn, As, Cd, Pb, Th and U in the water samples collected from the Rautuvaara mining area and its surroundings, excluding the acidic pond. (R-W = Rautuvaara Water, No. = sampling location)

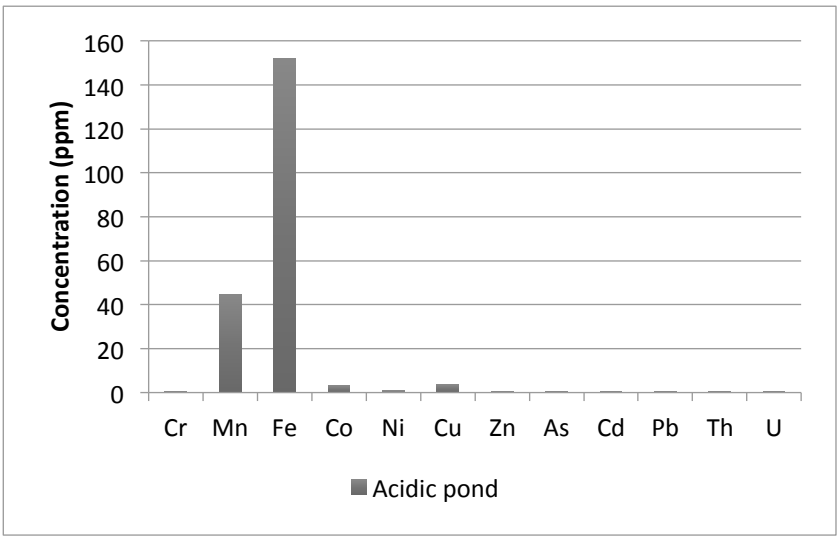

Figure 40. Measured metal concentrations (ppm) in the acidic pond water taken from the Rautuvaara mining area.

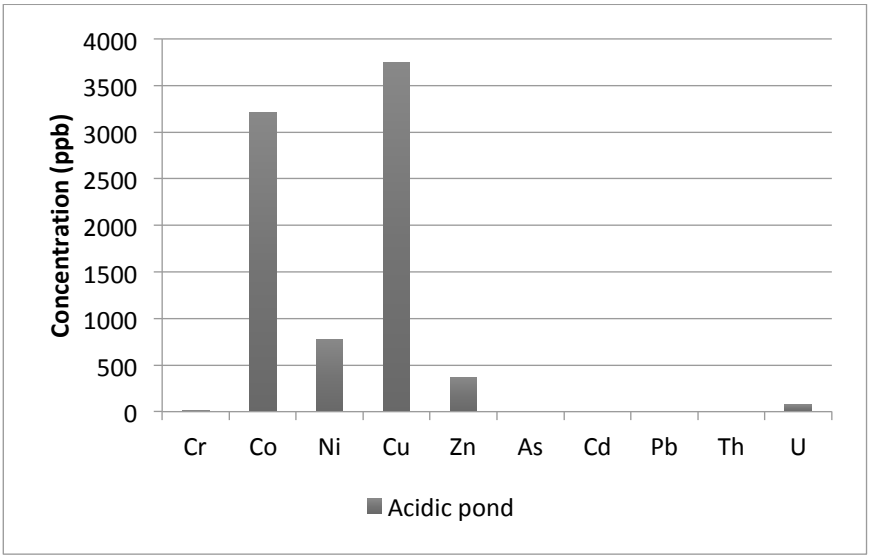

Figure 41. Measured metal concentrations (ppb) of Cr, Co, Ni, Cu, Zn, As, Cd, Pb, Th and U in the acidic pond water taken from the Rautuvaara mining area.

The reference water is seen to fulfil the criteria for drinking water set by WHO (Table 7). The area where the reference water samples were collected is located upstream from the mining area and is not affected by it. Table 30 presents the ratio of other water sample concentrations compared to the reference water sample concentrations. The values below zero represent the situation where the concentration is higher in the reference water sample and vice versa.

Table 30. The ratios of the water sample concentrations to those in the reference water sample collected upstream from the mining area.

	Cr	Mn	Fe	Co	Ni	Cu	Zn	As	Cd	Pb	Th	U
Settling pond	0,47	0,51	0,24	0,67	1,14	2,46	0,80	1,25	0,63	0,30	-	40,32
Downstream (R-W-7)	0,84	17,71	1,50	8,69	1,80	9,76	1,35	0,13	1,44	0,09	2,31	0,80
Downstream (R-W-14)	0,59	17,23	0,84	1,85	0,74	5,14	0,90	0,09	0,68	0,01	1,22	2,81
Water reservoir (close to the acidic pond)	0,15	224,16	0,74	86,83	1,45	35,50	1,47	0,08	2,03	0,01	1,33	6,96
Water reservoir (next to the waste rock)	0,24	152,37	0,23	28,72	1,13	14,20	1,42	0,07	1,60	0,17	-	1,79
Acidic pond	0,63	8806,17	487,59	9068,81	65,82	6225,51	49,32	0,88	117,17	0,25	442,23	1209,91

The radionuclide and metal concentrations measured in the settling pond water resemble those of the reference water, however slightly elevated U concentrations were detected.

Water samples collected downstream from the mining are in the Niesa river (R-W-7 and R-W-14) had mildly elevated levels of Mn, Fe, Co, Ni and Cu, which were seen gradually decrease as the distance from the mining area increased. These results are in line with the former water quality studies of the Niesa river. (84) The radionuclide and metal concentrations in the water reservoir were close to those of the reference water, apart from the elevated levels of Mn, Co and Cu, which were highest close to the acidic pond. Mn levels in the water reservoir exceeded the criteria for drinking water set by WHO (Table 7). The highest concentrations of radionuclides and metals were found in the acidic pond water, where the levels of Mn (44 ppm), Cu (4 ppm), Ni (772 ppb) and U (77 ppb) significantly exceeded the standard value for drinking water set by WHO (Table 7). The level of U in the acidic pond was over a thousand times higher than in the reference water and the corresponding value for Th was three hundred times higher than in the reference water. The average concentration of U in Finnish ground water is 1.6 ppb and in drilled well water 32 ppb. (4) The U concentration in the settling pond resembles that of the ground water, but the concentration in the acidic pond water greatly exceeds the average concentrations in Finland.

12.3 Total concentrations of metals and radionuclides in solid samples

Acid digestion was performed in order to determine the total metal and radionuclide concentrations in the solid sample materials by ICP-MS. Nitric acid (suprapure grade) was used based on the work of Tuovinen et al. (30). The determined radionuclide (^{238}U and ^{232}Th) and metal (Cr, Mn, Fe, Co, Ni, Cu, Zn, As, Cd and Pb) concentrations are presented in Tables 31, 32, 33 and 34. The analytical data of the ICP-MS measurements can be found in Appendix A.

Table 31. The concentrations (ppm) of metals (Cr, Mn, Fe, Co, Ni, Cu, Zn, As, Cd and Pb) and radionuclides (^{238}U and ^{232}Th) in the enrichment sand samples taken from Rautuvaara tailings.

Enrichment sand						
	Concentration (ppm)					
	Cr	**Mn**	**Fe**	**Co**	**Ni**	**Cu**
Average	111	967	69402	105	388	346
Standard deviation	52	218	10941	45	186	178
Range	7 - 204	398 - 14000	46614 - 91798	15 - 178	5 - 673	182 - 915
	Concentration (ppm)					
	Zn	**As**	**Cd**	**Pb**	**Th**	**U**
Average	33	267	0,1	7	2	8
Standard deviation	29	128	0,1	2	1	3
Range	6 - 131	15 - 486	0 - 1	3 - 13	1 - 3	1 - 12

Table 32. The concentrations (ppm) of metals (Cr, Mn, Fe, Co, Ni, Cu, Zn, As, Cd and Pb) and radionuclides (^{238}U and ^{232}Th) in the acidic pond sand samples taken from Rautuvaara tailings.

Acidic pond sand						
	Concentration (ppm)					
	Cr	**Mn**	**Fe**	**Co**	**Ni**	**Cu**
Average	69	441	28468	60	226	310
Standard deviation	101	231	21317	14	4	359
Range	7 -219	547 - 1038	39499 - 87983	15 - 45	5 - 15	493 - 1360
	Concentration (ppm)					
	Zn	**As**	**Cd**	**Pb**	**Th**	**U**
Average	49	159	1	5	1	5
Standard deviation	2	4	-	1	0	2
Range	2 - 6	7 - 16	0 - 1	3 - 6	2 - 3	1 - 5

Table 33. The concentrations (ppm) of metals (Cr, Mn, Fe, Co, Ni, Cu, Zn, As, Cd and Pb) and radionuclides (^{238}U and ^{232}Th) in the waste rock samples taken from Rautuvaara tailings.

Waste rock						
	Concentration (ppm)					
	Cr	**Mn**	**Fe**	**Co**	**Ni**	**Cu**
Average	105	140	46167	16	23	201
Standard deviation	60	22	1103	2	4	61
Range	62 - 147	124 - 155	45387 - 46947	15 - 18	20 - 25	158 - 244
	Concentration (ppm)					
	Zn	**As**	**Cd**	**Pb**	**Th**	**U**
Average	10	0,45	LOD	3	11	4
Standard deviation	5	0,01	-	0	2	0
Range	6 - 14	0,4 – 0,5	-	2 - 3	10 - 12	4 - 4

LOD = below the detection limit.

Table 34. The concentrations (ppm) of metals (Cr, Mn, Fe, Co, Ni, Cu, Zn, As, Cd and Pb) and radionuclides (^{238}U and ^{232}Th) in the sediment samples taken from Rautuvaara tailings.

Sediment						
	Concentration (ppm)					
	Cr	**Mn**	**Fe**	**Co**	**Ni**	**Cu**
Average	139	1184	78878	152	304	1193
Standard deviation	19	144	8991	18	43	141
	Concentration (ppm)					
	Zn	**As**	**Cd**	**Pb**	**Th**	**U**
Average	200	140	1	27	9	23
Standard deviation	31	22	-	5	1	3

Finland's environmental authorities have set screening levels for the metal concentrations in soil indicating possible contamination in the PIMA guideline (guidelines for contaminated soils). (85) The screening levels do not take into account the possible mobilization of elements so they do not completely resemble the actual risk caused by the elevated concentrations. The acid digestion results show that the levels of Cd, Cr, Pb and Zn follow the natural occurring levels in Finland, which are 0.03 ppm, 31 ppm, 5 ppm and 31 ppm, respectively. The levels of As are above the screening level of 100 ppm set for industrial estate in the enrichment sand (289 ppm) and sediment (140 ppm). The screening level for Cu in the industrial estate is 200 ppm and this level is exceeded in the enrichment sand (346 ppm), acidic pond sand (969 ppm), sediment (1193 ppm) and waste rock (201 ppm). The levels of Ni exceed the screening level of 150 ppm in the enrichment sand (388 ppm) and sediment (304 ppm). The results indicate that the concentrations of elements in the samples collected from the Rautuvaara mining area have increased probably as a result of the tailings weathering. The concentration of potentially harmful As is three times the value set for the screening level in the PIMA guideline, which may pose a risk to the surrounding environment.

12.4 Mobilization of elements in the sequential extractions

A potential mobilisation of metals and radionuclides in four different types of sample material from Rautuvaara mining area was studied using a sequential leaching protocol. The supernatants from the extraction procedure were analysed with ICP-MS and the observed elements were base metals Ni, Zn, Cu, Co, Fe and Mn, potentially toxic metals Cr, Cd and Pb, and radionuclides ^{238}U and ^{232}Th. The results are presented separately for the different sample types and the values presented are the averages of all the samples in the same sample matrix, unless otherwise stated. Duplicate samples were analysed and chemical blank sample of the used extraction reagent was added into each set. This ensured the purity of the used chemical reagents and from this a correction factor to the real leached concentrations in sequential extractions was obtained, which was then applied to all analytical results reported. The analytical data for measured blank samples can be found in Appendix A. A correction to dry weight was also performed for all the analytical concentrations reported. The different extraction fractions and their pH values are presented in Table 35.

Table 35. The different extraction fractions and their pH -values in the sequential extraction procedure used for solid samples from Rautuvaara mining area. (I – VI indicates the order of leached fraction)

Extraction fraction	pH
Exchangeable fraction I (I)	7,8
Exchangeable fraction II (II)	5,0
Mild acid-soluble fraction (III)	4,1
Reducible fraction (IV)	2,0
Oxidizable fraction (V)	1,5
Strong acid soluble fraction (VI)	(4 M HNO_3)

The sum of metal concentrations from all the different extraction fractions compared well to those achieved from acid digestion, which were presented in chapter 12.3, and these results are presented in Appendix A. Overall, the measured concentrations are fairly close for Mn, Co, Ni, Cu, Zn, As, Cd, Pb, Th and U. Only in the case of Cr do the values differ between the acid digestion and sequential extractions.

12.4.1 The dissolution of metals from the enrichment sand in the sequential extractions

The results of metal dissolution from the enrichment sand samples collected from Rautuvaara mining area are presented in Figures 42, 43, 44 and 45.

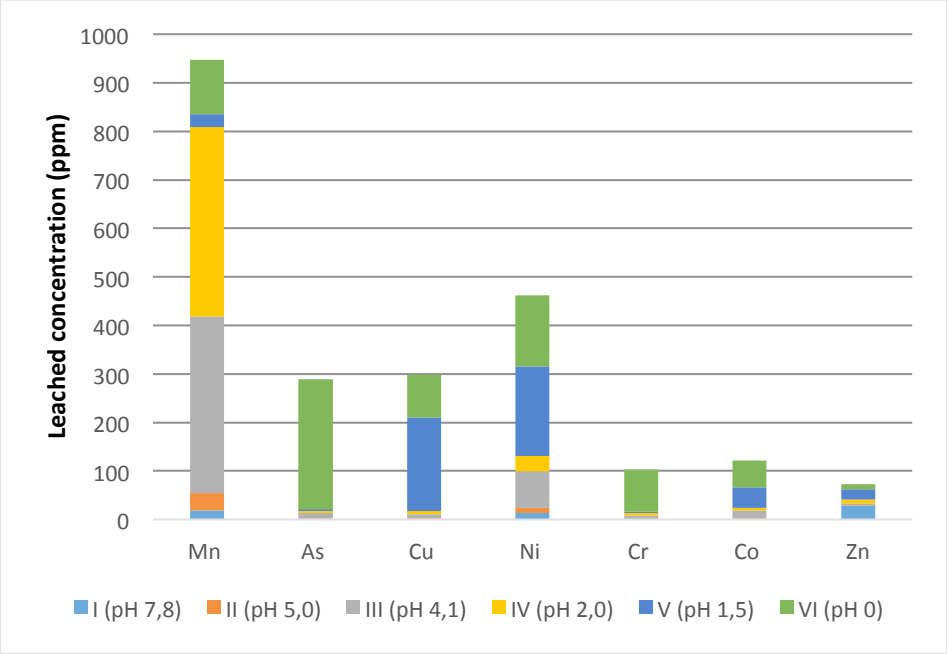

Figure 42. The release of Mn, As, Cu, Ni, Cr, Co and Zn (ppm) from Rautuvaara enrichment sand in laboratory sequential extraction leach tests. (I = Exchangeable fraction I; II = Exchangeable fraction II; III = Mild acid-soluble fraction; IV = Reducible fraction; V = Oxidizable fraction; VI = Strong acid-soluble fraction)

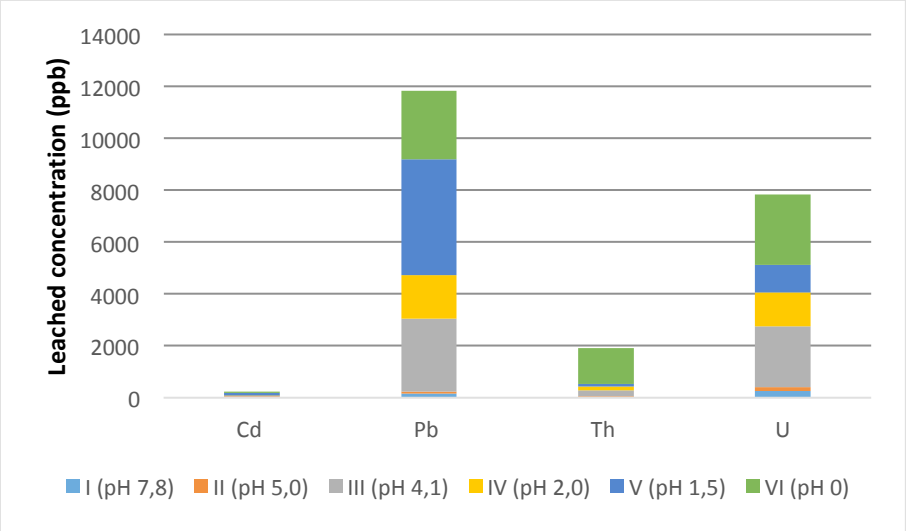

Figure 43. The release of Cd, Pb, Th and U (ppb) from Rautuvaara enrichment sand in laboratory sequential extraction leach tests. (I = Exchangeable fraction I; II = Exchangeable fraction II; III = Mild acid-soluble fraction; IV = Reducible fraction; V = Oxidizable fraction; VI = Strong acid-soluble fraction)

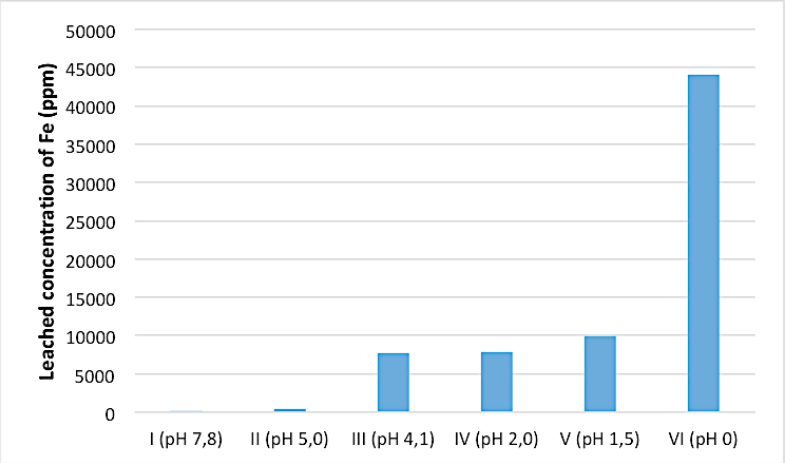

Figure 44. The leached concentrations of Fe (ppm) from Rautuvaara enrichment sand in laboratory sequential extraction leach tests. (I = Exchangeable fraction I; II = Exchangeable fraction II; III = Mild acid-soluble fraction; IV = Reducible fraction; V = Oxidizable fraction; VI = Strong acid-soluble fraction)

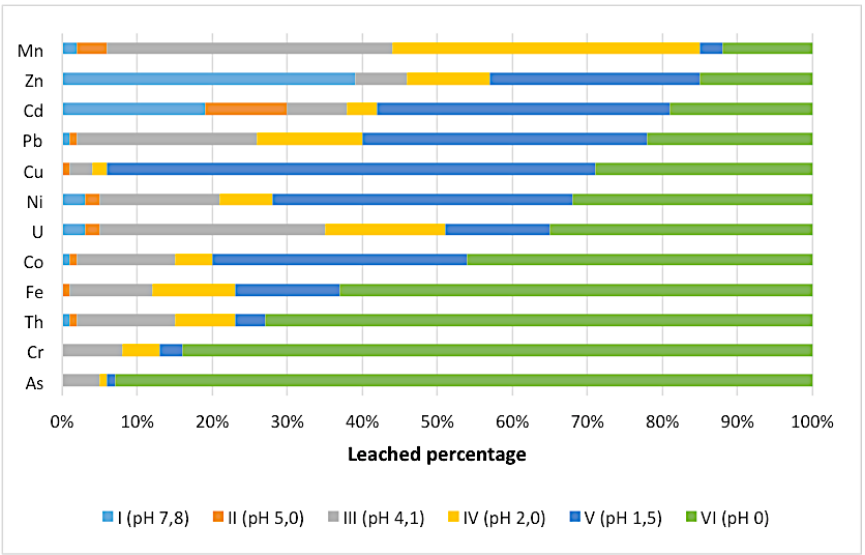

Figure 45. The leached proportions of metals (% from the total) from Rautuvaara enrichment sand in laboratory sequential extraction leach tests. (I = Exchangeable fraction I; II = Exchangeable fraction II; III = Mild acid-soluble fraction; IV = Reducible fraction; V = Oxidizable fraction; VI = Strong acid-soluble fraction)

The results show a large variation in the leached metals in each sequential extraction fraction. In the exchangeable I and II fractions, the proportions of dissolved metals were low, apart from aslightly higher proportions of leached Zn (39 %) and Cd (19 %) in the first step and Cd (11 %) in the latter. High proportions of leached Mn, Pb and U were found in the mild acid-soluble and reducible fractions. The highest proportion of As (93 %), Cr (84 %) and Th (73 %) were leached with concentrated nitric acid in the strong acid-

soluble fraction. Overall, the highest percentage of elements were leached in the last two fractions. In the strong acid-soluble fraction over 50 percent of Fe, Th, Cr and As was leached and over 30 percent of Ni, U and Co. Metals leached out in the exchangeable and mild acid-soluble fractions are considered to be the most mobile and bioavailable, and the combined percentages of dissolved metals for these fractions were highest for Mn (44 %), Zn (46 %), Cd (38 %), Pb (26 %) and U (35 %). However, the total leached concentration of Cd remained low (0.2 ppm) in all of the sample types. The total release of metals from Rautuvaara enrichment sand in sequential leach tests is presented in Table 36. Rautuvaara enrichment sand had the highest amounts of leachable metals of all the solid samples matrixes. The analytical data of the sequential extractions for enrichment sand can be found in Appendix A.

Table 36. The total release of metals (ppm) from Rautuvaara enrichment sand in laboratory sequential leach tests. The concentrations are mean values of the all the samples (n = 34) and the uncertainty (±) is their standard deviation.

Metal	**Total leached concentration (ppm)**	**Metal**	**Total leached concentration (ppm)**
Mn	947 ± 181	Zn	73 ± 124
Fe	70284 ± 13233	As	289 ± 102
Cr	104 ± 30	Cd	0.2 ± 0.2
Co	122 ± 32	Pb	12 ± 15
Ni	462 ± 148	Th	2 ± 0.4
Cu	298 ± 120	U	8 ± 1

12.4.2 The dissolution of metals from the acidic pond sand in the sequential extractions

The results of metal dissolution from acidic pond sand samples collected from Rautuvaara mining area are presented in Figures 46, 47 and 48. The pH in the exchangeable fraction I (I) is in reality lower than 7.8, since the pH of the acidic pond sand is 4.1.

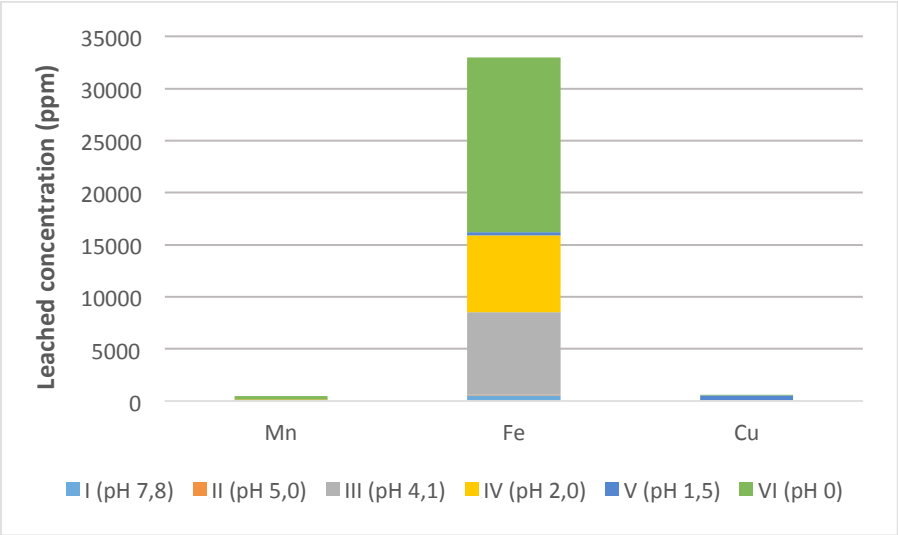

Figure 46. Leached amounts of Mn, Fe and Cu (ppm) from Rautuvaara acidic pond sand in laboratory sequential extraction leach tests. (I = Exchangeable fraction I; II = Exchangeable fraction II; III = Mild acid-soluble fraction; IV = Reducible fraction; V = Oxidizable fraction; VI = Strong acid-soluble fraction)

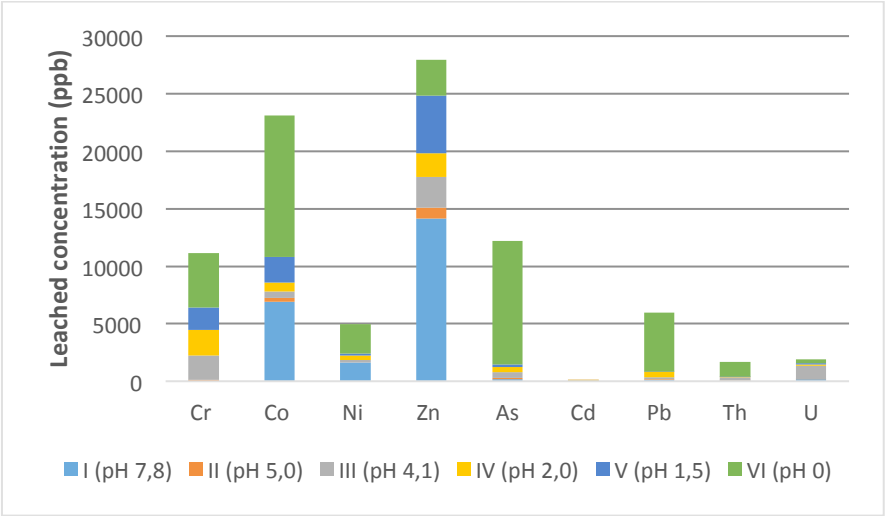

Figure 47. Leached amounts of Cr, Co, Ni, Zn, As, Cd, Pb, Th and U (ppb) from Rautuvaara acidic pond sand in laboratory sequential extraction leach tests. (I = Exchangeable fraction I; II = Exchangeable fraction II; III = Mild acid-soluble fraction; IV = Reducible fraction; V = Oxidizable fraction; VI = Strong acid-soluble fraction)

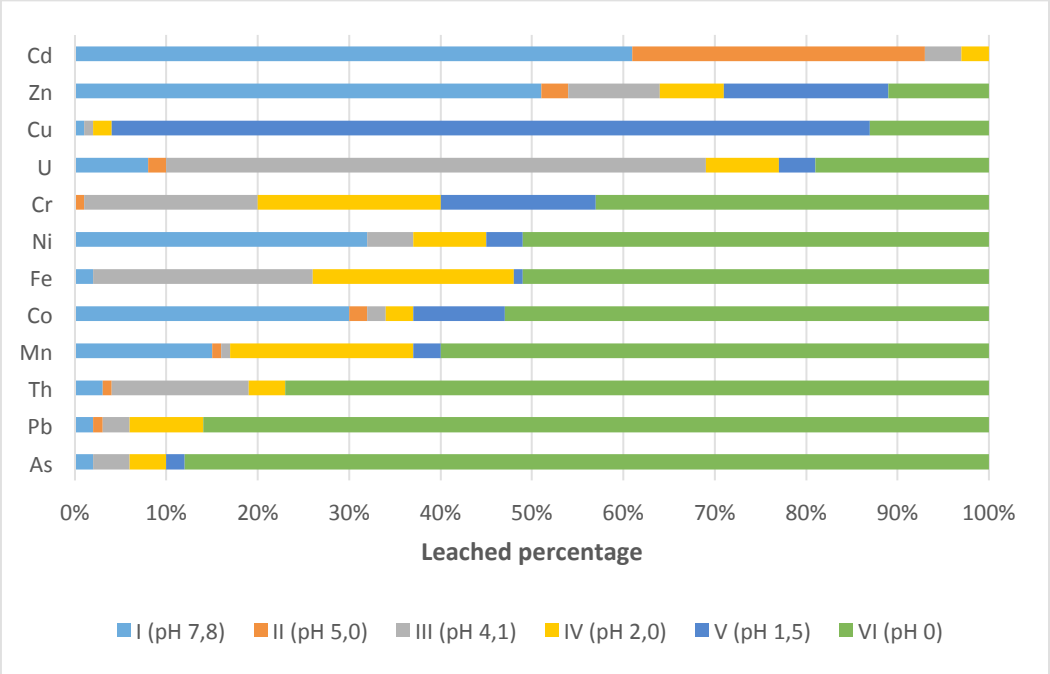

Figure 48. Leached proportions of metals (% from the total) from Rautuvaara acidic pond sand in laboratory sequential extraction leach tests. (I = Exchangeable fraction I; II = Exchangeable fraction II; III = Mild acid-soluble fraction; IV = Reducible fraction; V = Oxidizable fraction; VI = Strong acid-soluble fraction)

The acidic pond sand belongs to Rautuvaara enrichment sand tailings, but since it has been affected by the acid mine drainage it is presented as a separate sample matrix and a few changes in the leaching behaviour of metals can be seen when compared to the enrichment sand samples. The results show that the highest amount of metals was dissolved in the strong acid soluble fraction. The amount of leached metals in the exchangeable I and II fractions was low, apart from the higher concentrations of Cd (69 %), Zn (51 %), Ni (32 %) and Co (30 %) in the first fraction and Cd (32 %) in the latter. In the mild acid-soluble fraction 59 % of U was leached out, where the percentages for other elements stayed below 30 %. Dissolution of metals was also low in the reducible and oxidizable fractions, however, a high percentage of Cu (83 %) leached out in the oxidizable fraction. Cd mainly dissolved in the first two fractions, although, the total concentration of leached Cd was low (0.09 ppm). Metals leached out in the first three fractions, exchangeable fractions I & II and mild acid-soluble fraction, are considered to be possibly mobile. In these labile fractions, high percentages of Cd (97 %), U (69 %), Zn (64 %), Ni (37 %) and Co (30 %) were leached out from the acidic pond sand. As was mainly leached out in a similar manner than from the enrichment sand, but the total concentration of As was relatively

lower in the acidic pond sand (12 ppm). Mn is more available for leaching in the enrichment sand and more tightly bound in the acidic pond sand. From the enrichment sand Cd leached out in several fractions (I, II, III and IV), whereas, from the acidic pond sand it was leached out mainly in the first two. The percentage of labile U was slightly higher in the acidic pond sand (70%), than in the enrichment sand (40 %), however, the total leached U concentration were four times higher in the enrichment sand. The enrichment sand had higher percentage of Ni leached out in the oxidizable fraction and the total leach concentration was considerably lower in the acidic pond sand (5 ppm) than in the enrichment sand (462 ppm). The dissolution of Pb indicated a stronger association in the acidic pond sand than in enrichment sand. Cu, Zn, Co and Th were seen to behave similarly in both sample matrixes. The total leached concentrations of metals were seen to be considerably lower in the acidic pond sand than in the enrichment sand. Only Cu was leached out in higher amount from the acidic pond sand than from the enrichment sand. The total release of leached metals from Rautuvaara acidic pond sand in sequential leach tests is presented in Table 37. The analytical data of the sequential extractions for the acidic pond sand can be found in Appendix A.

Table 37. The total release of metals (ppm) from Rautuvaara acidic pond sand in laboratory sequential leach tests. The concentrations are mean values of all the samples (n = 8) and the uncertainty (±) is their standard deviation.

Metal	Total leached concentration (ppm)	Metal	Total leached concentration (ppm)
Mn	495 ± 145	Zn	28 ± 29
Fe	33013 ± 7700	As	12 ± 3
Cr	11 ± 1	Cd	0.1 ± 0.02
Co	23 ± 16	Pb	6 ± 1
Ni	5 ± 1	Th	2 ± 0.3
Cu	602 ± 183	U	2 ± 2

12.4.3 The dissolution of metals from the sediment in the sequential extractions

The results of metal dissolution from sediment samples collected from Rautuvaara mining area are presented in Figures 49, 50 and 51.

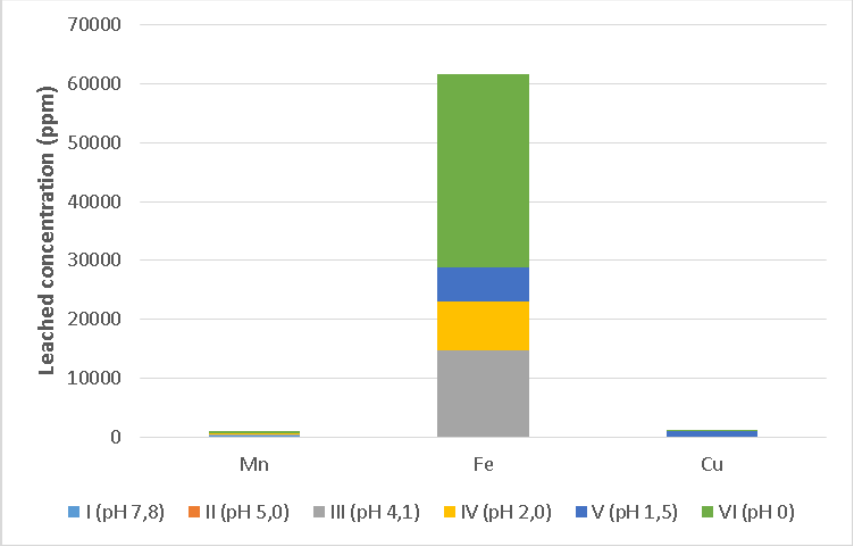

Figure 47. Leached amounts of Mn, Fe and Cu (ppm) from Rautuvaara sediment in laboratory sequential extraction leach tests. (I = Exchangeable fraction I; II = Exchangeable fraction II; III = Mild acid-soluble fraction; IV = Reducible fraction; V = Oxidizable fraction; VI = Strong acid-soluble fraction)

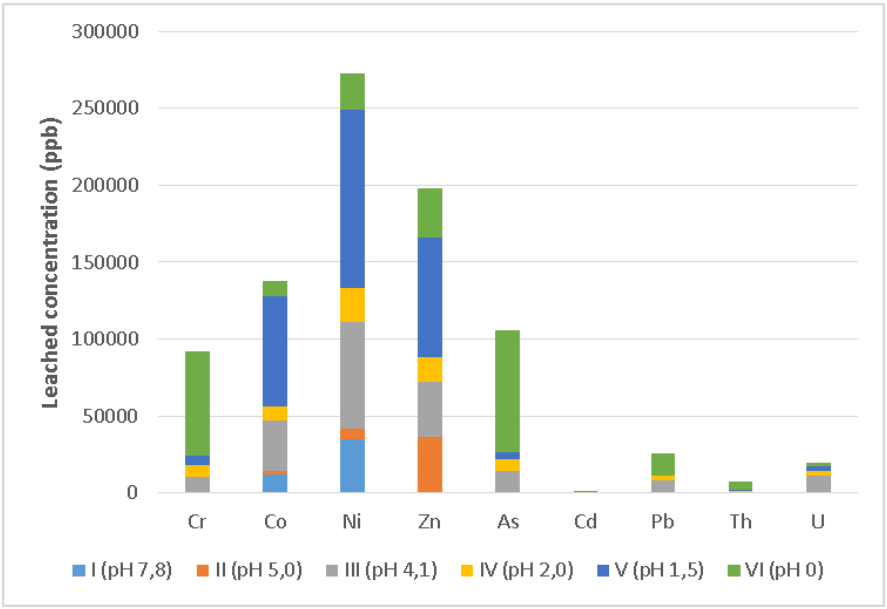

Figure 47. Leached amounts of Cr, Co, Ni, Zn, As, Cd, Pb, Th and U (ppb) from Rautuvaara sediment in laboratory sequential extraction leach tests. (I = Exchangeable fraction I; II = Exchangeable fraction II; III = Mild acid-soluble fraction; IV = Reducible fraction; V = Oxidizable fraction; VI = Strong acid-soluble fraction)

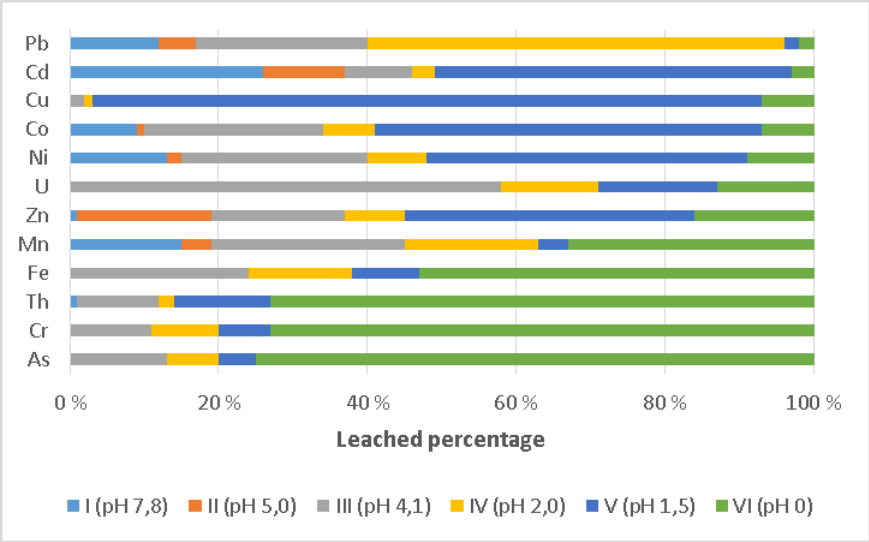

Figure 51. Leached proportions of metals (% from the total) from Rautuvaara sediment in laboratory sequential extraction leach tests. (I = Exchangeable fraction I; II = Exchangeable fraction II; III = Mild acid-soluble fraction; IV = Reducible fraction; V = Oxidizable fraction; VI = Strong acid-soluble fraction)

The results show that metals are mostly leached out from Rautuvaara sediment in the oxidizable fraction and strong acid-soluble fraction. In the first leaching step only a high proportion of Cd (26 %) was dissolved, however, the total leached concentration was minor (0,6 ppm). The proportions of leached metals in the exchangeable fraction II stayed below 20 %. In the mild acid-soluble fraction and reducible fraction the leached proportions varied between 1 – 26 %, the only exception being a high percentage of leached U (58 %) in the first step and Pb in the latter (56 %). High amounts of Cu (90 %), Co (73 %), Cd (48 %) and Zn (39 %) were leached out in the oxidizable fraction. In the strong acid soluble fraction high amounts of As (75 %), Cr (73 %) and Th (73 %) were leached out, as well as slightly smaller amounts of Fe (53 %) and Mn (33 %). In the mobile fractions, including the first three extractions steps, only uranium was leached over 50 %. Dissolution from the Rautuvaara sediment, in different extraction fraction, resembles dissolution of metals from the Rautuvaara enrichment sand. The total leached concentrations are close to those of the enrichment sand, except for Cu, Zn, Cd, Pb and U, which are elevated concentrations when compared. The total release of metals from Rautuvaara sediment in the sequential leach test is presented in Table 38. The analytical data from the sequential extractions for sediment can be found in Appendix A.

Table 38. The total release of metals (ppm) from the Rautuvaara sediment in the laboratory sequential leaching tests. The concentrations are mean values of all the samples (n = 2) and the uncertainty (±) is their standard deviation.

Metal	Total leached concentration (ppm)	Metal	Total leached concentration (ppm)
Mn	935 ± 108	Zn	198 ± 26
Fe	61700 ± 12429	As	105 ± 31
Cr	92 ± 26	Cd	1 ± 0.1
Co	138 ± 26	Pb	25 ± 6
Ni	273 ± 40	Th	8 ± 2
Cu	1130 ± 408	U	20 ± 4

12.4.4 The dissolution of metals from the waste rock in the sequential extractions

The results of metal dissolution from waste rock samples collected from Rautuvaara mining area are presented in Figures 52, 53, 54 and 55.

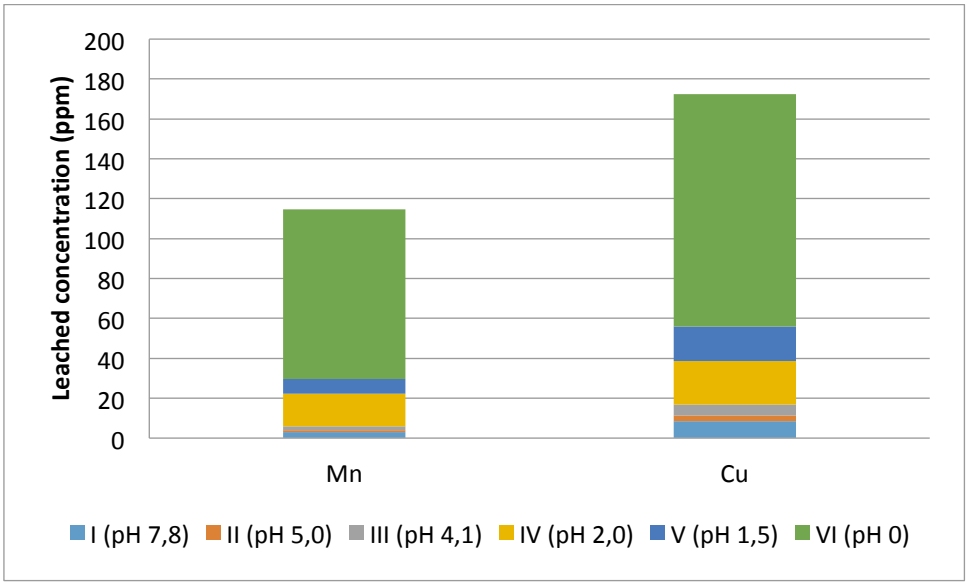

Figure 52. Leached amounts of Mn and Cu (ppm) from Rautuvaara waste rock in laboratory sequential extraction leach tests. (I = Exchangeable fraction I; II = Exchangeable fraction II; III = Mild acid-soluble fraction; IV = Reducible fraction; V = Oxidizable fraction; VI = Strong acid-soluble fraction)

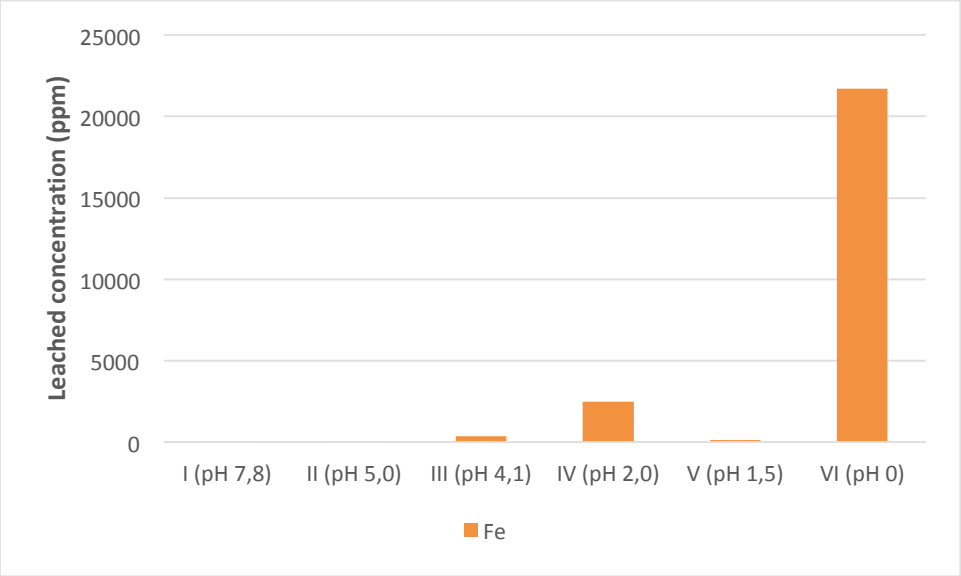

Figure 53. Leached amount of Fe (ppm) from Rautuvaara waste rock in laboratory sequential extraction leach tests. (I = Exchangeable fraction I; II = Exchangeable fraction II; III = Mild acid-soluble fraction; IV = Reducible fraction; V = Oxidizable fraction; VI = Strong acid-soluble fraction)

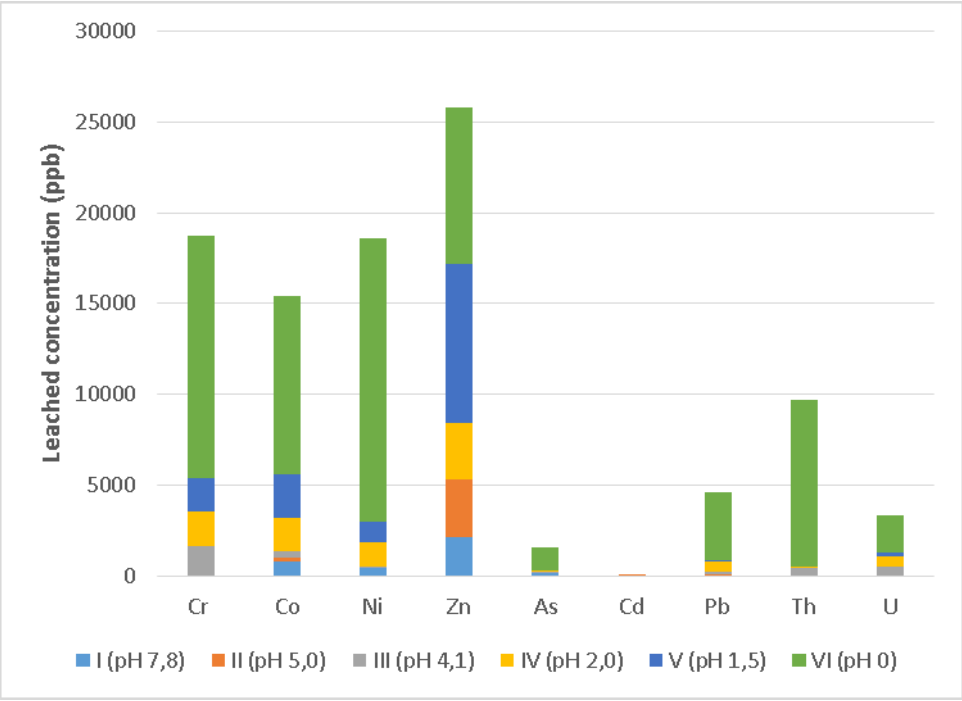

Figure 54. Leached amounts of Cr, Co, Ni, Zn, As, Cd, Pb, Th and U (ppb) from Rautuvaara waste rock in laboratory sequential extraction leach tests. (I = Exchangeable fraction I; II = Exchangeable fraction II; III = Mild acid-soluble fraction; IV = Reducible fraction; V = Oxidizable fraction; VI = Strong acid-soluble fraction)

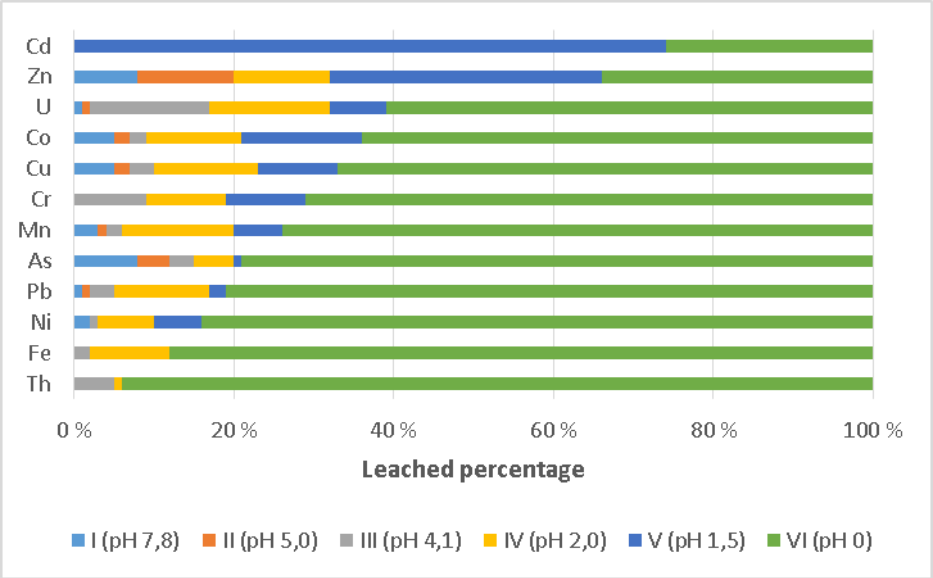

Figure 55. Leached proportions of metals (% from the total) from Rautuvaara waste rock in laboratory sequential extraction leach tests. (I = Exchangeable fraction I; II = Exchangeable fraction II; III = Mild acid-soluble fraction; IV = Reducible fraction; V = Oxidizable fraction; VI = Strong acid-soluble fraction)

Most of the metals from the Rautuvaara waste rock were leached out with concentrated nitric acid in the strong acid-soluble fraction, with percentages between 60 – 95 %. Only Zn and Cd were leached with smaller percentages in the strong acid-soluble fraction, 34 % and 26 %, respectively. Leached concentrations of Cd in all the extraction fractions were low (total 0.03 ppm). In the mobile fractions, which includes the first three leaching steps, the combined percentages of leached elements were minor. In the waste rock the elements seem to be more tightly bound than in the enrichment sand, acidic pond sand and sediment. The waste rock had the lowest amounts of leached elements overall. The total release of metals from the Rautuvaara waste rock in the sequential leach tests is presented in Table 39. The analytical data of the sequential extractions for waste rock can be found in Appendix A.

Table 39. The total release of metals (ppm) from the Rautuvaara waste rock in the laboratory sequential leach tests. The concentrations are mean values of all the samples and the uncertainty (±) is their standard deviation.

Metal	Total leached concentration (ppm)	Metal	Total leached concentration (ppm)
Mn	115 ± 5	Zn	26 ± 13
Fe	24652 ± 250	As	2 ± 0.2
Cr	19 ± 1	Cd	0.03 ± 0.03
Co	15 ± 2	Pb	5 ± 1
Ni	19 ± 3	Th	10 ± 0.2
Cu	172 ± 17	U	3 ± 0.1

12.4.5 The dissolution of Ni in the sequential extractions

The dissolution of Ni in the sequential extraction procedure from different sample matrixes is presented in Figure 56.

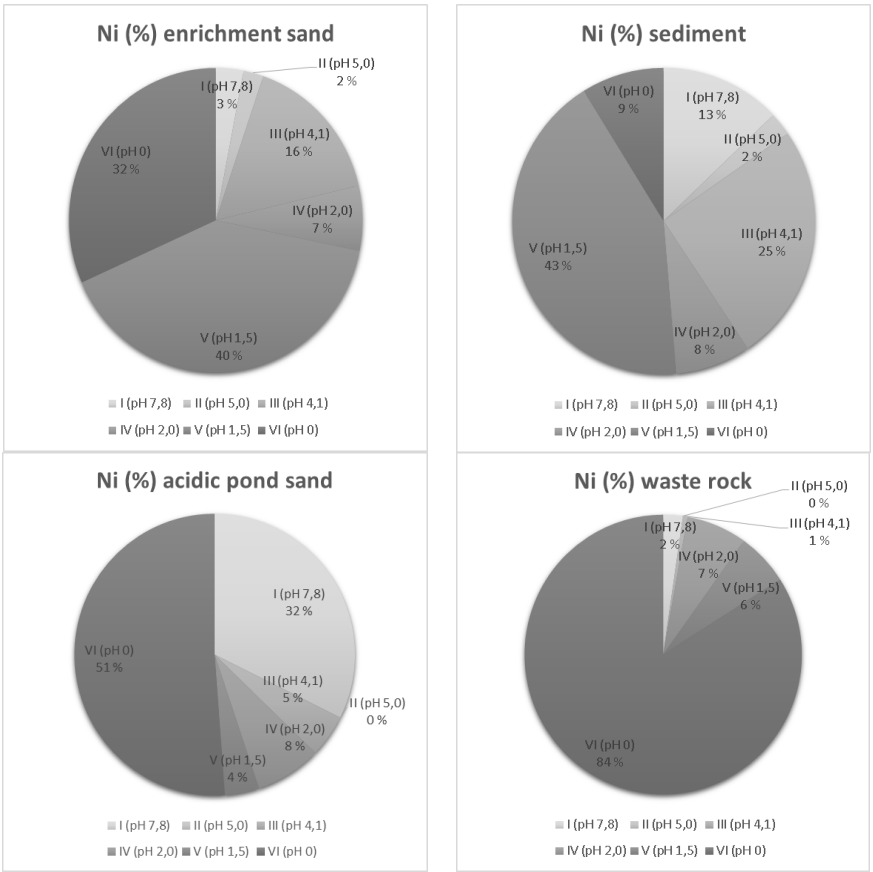

Figure 56. Dissolution of Ni in the sequential extraction procedure for different sample matrixes. I – VI refer to the different extraction fractions: I = Exchangeable fraction I; II = Exchangeable fraction II; III = Mild acid-soluble fraction; IV = Reducible fraction; V = Oxidizable fraction; VI = Strong acid-soluble fraction.

The dissolution of nickel varied from one sample type to another and on the average. The total concentration of leached Ni in different sample types was in order of: enrichment sand (462 ppm), sediment (273 ppm), waste rock (19 ppm) and acidic pond sand (5 ppm). From the enrichment sand and sediment Ni is mainly leached out in the oxidizable fraction (pH 1.5). This fraction traditionally presents the elements bound to organic matter, but the percentage of organic matter in the Rautuvaara tailings samples was assumed to be minimal. Most of the Ni from the waste rock, and a significant amount from the enrichment sand, was leached out in the strong acid-soluble fraction, due to probably occurring in the sulphides. From the acidic pond sand, an elevated proportion of Ni (37%) was leached out in the labile fractions, which includes the exchangeable fractions I & II and the mild acid-soluble fraction. Most of the Ni from the acidic pond sand was dissolved in the strong acid-soluble fraction (51 %). Favas et al. (13) used a seven-step sequential leach test to study the mobility and retention behavior of elements in the mine tailings and soil samples collected from an abandoned Sn-As Everdosa mine. They showed that Ni dissolution in the oxidizable and strong acid-soluble fraction may be due to a partial attack on silicate phases, and that the dissolved Ni in the first three fractions is most likely associated with clay minerals and Fe and Mn oxy-hydroxides. (13)

12.4.6 The dissolution of Zn in the sequential extractions

The dissolution of Zn in the sequential extraction procedure from the different sample matrixes is presented in Figure 57.

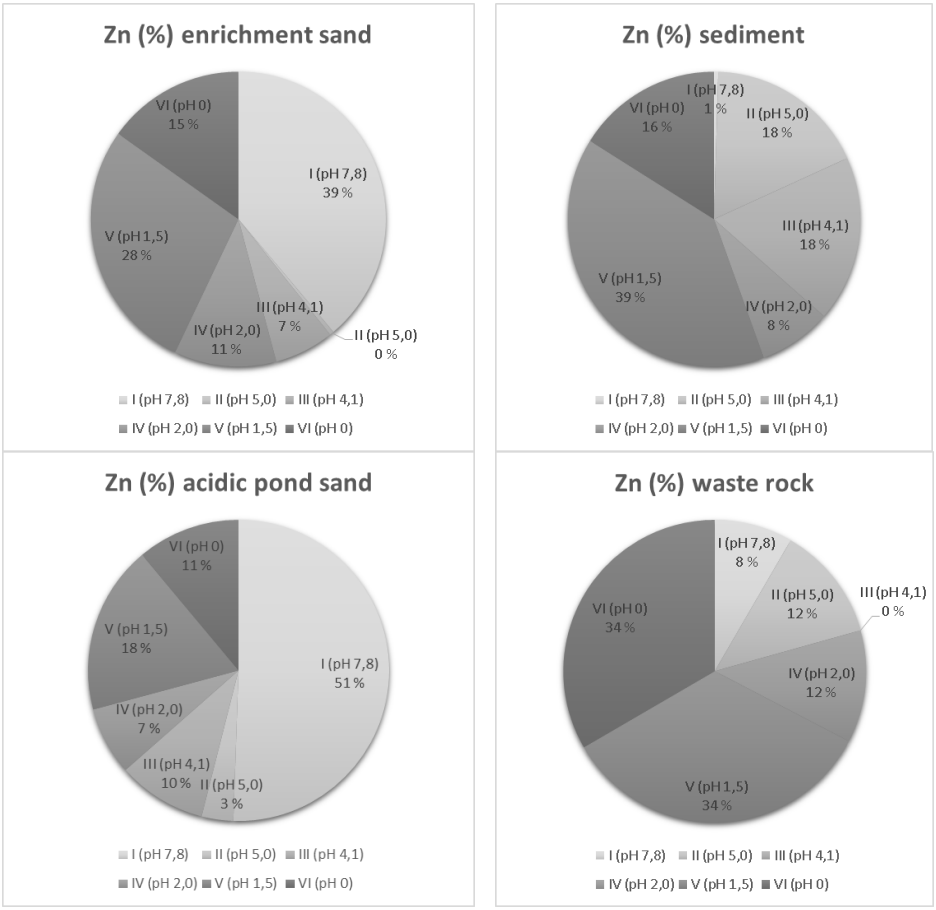

Figure 57. The dissolution of Zn in the sequential extraction procedure for different sample matrixes. I – VI refer to the different extraction fractions: I = Exchangeable fraction I; II = Exchangeable fraction II; III = Mild acid-soluble fraction; IV = Reducible fraction; V = Oxidizable fraction; VI = Strong acid-soluble fraction.

The dissolution of Zn varied greatly between the different extraction fractions in all the sample matrixes. The enrichment sand, sediment and acid pond sand all have a high percentage of labile Zn (leach steps I – III). All of the sample matrixes had high amounts of tightly bound Zn in the last two fractions (V – VI). The total concentration of leached Zn was highest from the sediment (198 ppm) and lowest from the waste rock (26 ppm). The dissolution of Zn in the oxidizable and strong acid-soluble fractions would indicate a strong association with primary sulphides, since the organic matter content can be expected to be minor in the mine tailings from Rautuvaara. Overall, in the different sample types

the total leached concentrations of Zn remained low and the highest concentrations were found in the sediment (mean 200 ppm).

12.4.7 The dissolution of Cu in the sequential extractions

The dissolution of Cu in the sequential extraction procedure from the different sample matrixes is presented in Figure 58.

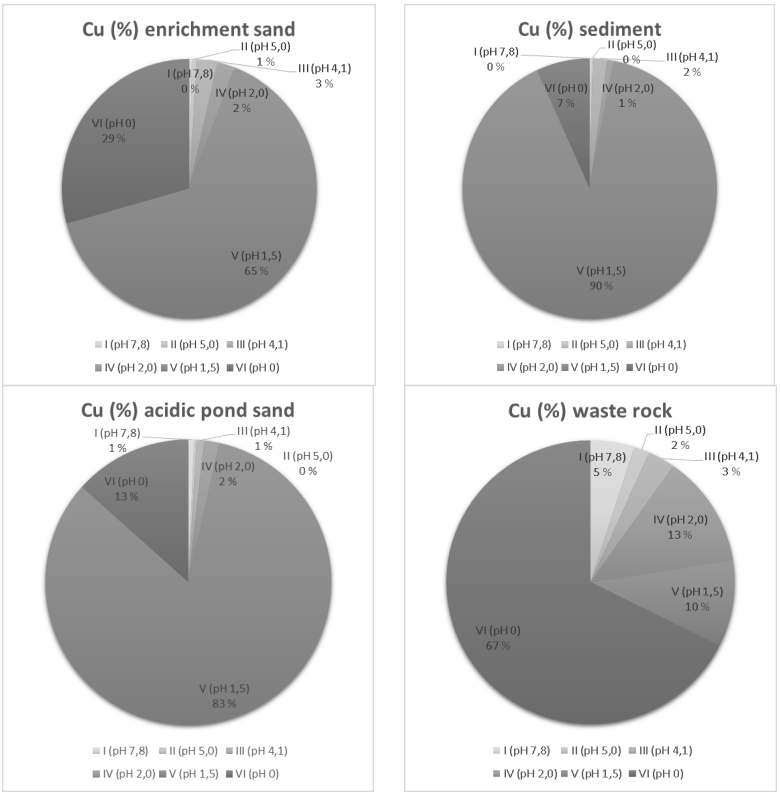

Figure 58. The dissolution of Cu in the sequential extraction procedure from different sample matrixes. I – VI refer to the different extraction fractions: I = Exchangeable fraction I; II = Exchangeable fraction II; III = Mild acid-soluble fraction; IV = Reducible fraction; V = Oxidizable fraction; VI = Strong acid-soluble fraction.

From the enrichment sand a large proportion of Cu was leached out from the oxidizable fraction (65 %) and from the strong acid-soluble fraction (29 %). From the sediment and acidic pond sand samples over 80 percentages of Cu is dissolved in the oxidizable fraction. From the enrichment sand, sediment and acidic pond sand the labile fractions (leach steps I-III), were minor contributors for the proportions of dissolved Cu. From the waste rock, the largest amount of Cu was leached out in the strong acid-soluble fraction (67 %). Waste rock also had 13 % of dissolved Cu in the reducible fraction, which reflects the ability of Cu to bound to Fe-Mn oxides when there is no organic matter available (86). On average,

the total concentration of leached Cu in different sample types was in the order of: sediment (1130 ppm), acidic pond sand (522 ppm), enrichment sand (298 ppm) and waste rock (172 ppm). Overall, it can be said that Cu is tightly bound in all the sample types and does not become easily mobile.

12.4.8 The dissolution of Co in the sequential extractions

The dissolution of Co in the sequential extraction procedure for the different sample matrixes is presented in Figure 59.

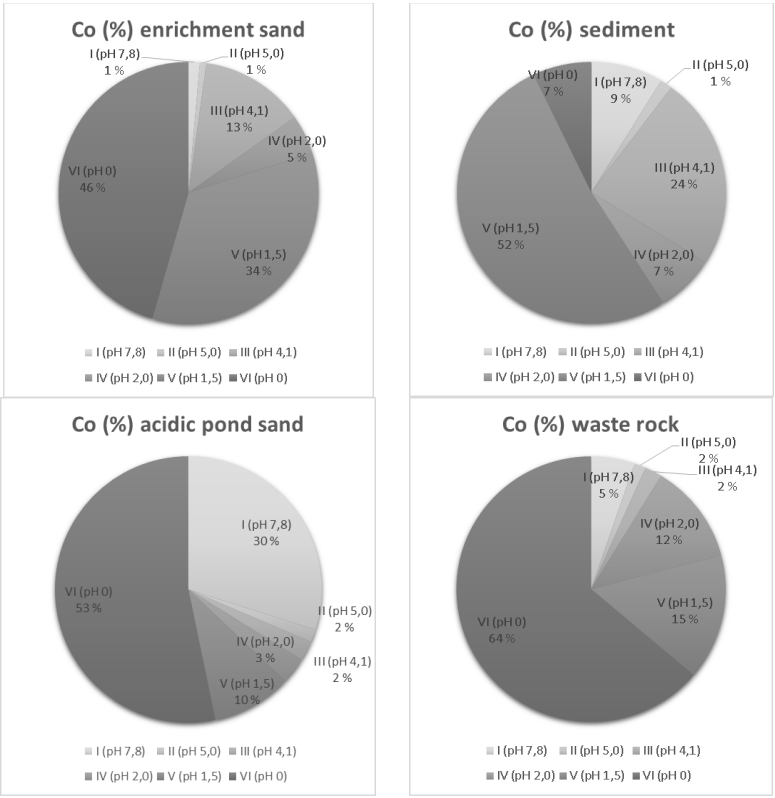

Figure 59. The dissolution of Co in the sequential extraction procedure for the different sample matrixes. I – VI refer to the different extraction fractions: I = Exchangeable fraction I; II = Exchangeable fraction II; III = Mild acid-soluble fraction; IV = Reducible fraction; V = Oxidizable fraction; VI = Strong acid-soluble fraction.

The distribution of dissolved Co varies between the different sample types. Sediment and acidic pond sand had the highest amount of possibly mobile Co (fractions I – III), the percentage was 34 % for both. From the enrichment sand samples the highest amount of Cu was leached out in the strong acid-soluble fraction (46 %) and the second highest in the

oxidizable fraction (34 %). The dissolution of Co from waste rock was similar to that from enrichment sand. From the sediment samples, 52 % of Co was leached out in the oxidizable fraction. From the acidic pond sand Co was leached out in the strong acid-soluble fraction (53 %) and in the exchangeable I fraction (30 %). According to Favas et al. (13), Co leached out in the exchangeable fraction is most likely bound to clay minerals, as was discussed with Ni. (13) On average, the total concentration of leached Co from different sample types was in the order of: sediment (138 ppm), enrichment sand (122 ppm), acidic pond sand (23 ppm) and waste rock (15 ppm).

12.4.9 The dissolution of Fe in the sequential extractions

The dissolution of Fe in the sequential extraction procedure for the different sample matrixes is presented in Figure 60.

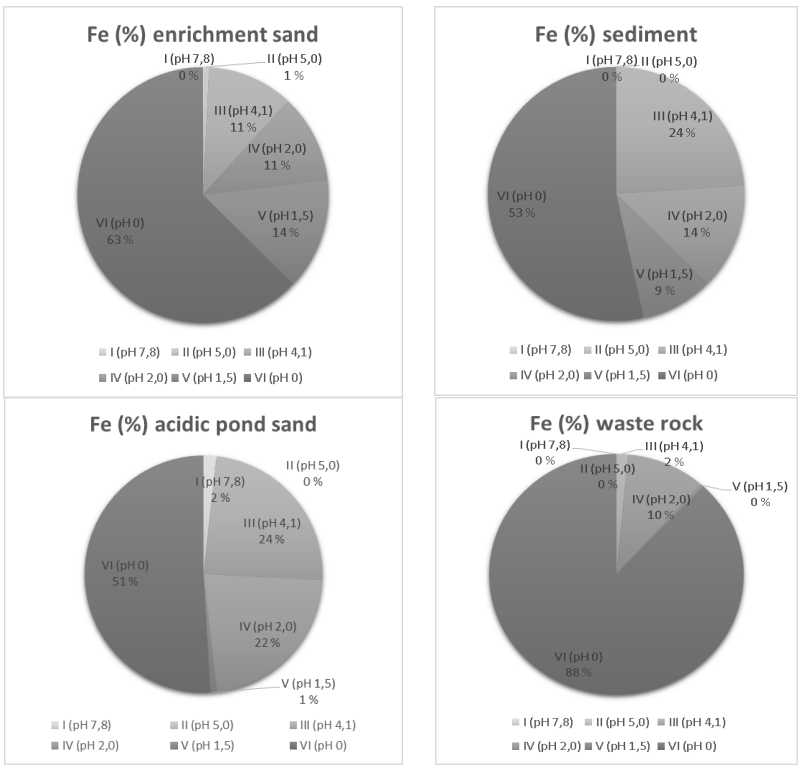

Figure 60. The dissolution of Fe in the sequential extraction procedure for the different sample matrixes. I – VI refer to the different extraction fractions: I = Exchangeable fraction I; II = Exchangeable fraction II; III = Mild acid-soluble fraction; IV = Reducible fraction; V = Oxidizable fraction; VI = Strong acid-soluble fraction.

Fractions of Fe are leached out in every leaching step and the concentrations are high. On average, the total leached concentrations of Fe are in order of: enrichment sand (70 284 ppm), sediment (61 700 ppm), acidic pond sand (33 013 ppm) and waste rock (24 652

ppm). The exchangeable fractions I and II had the lowest percentages of dissolved Fe in all the sample types. The acidic pond sand had a slightly elevated amount of dissolved Fe in the reducible fraction (22 %), while for the other sample types the percentages stayed between 10 – 14 %. Tessier et al. (1985) and Tipping et al. (1986) concluded that the Fe leached out in the reducible fraction might represent the presence of amorphous Fe (III) oxides or hydroxides. (47) (87) Fe was leached out in the oxidizable fraction from the enrichment sand (14 %) and sediment (9 %), while it was of minor importance from the acidic pond sand and waste rock. This behavior indicates the existence of sulfide minerals, such as pyrite (FeS_2) in the samples. (88) From all the sample types the highest percent of Fe was leached out in the strong acid-soluble fraction, indicating that a significant amount of Fe exists in the more resistant mineralogical phases e.g. crystalline Fe oxides. Mikutta et al. showed that using H_2O_2 in the second last extraction fraction only allows partial dissolution of the dissolving phases, which may lead to overestimations of leached metals in the strong acid-soluble fraction. (89) The acidic pond sand has the highest amount of labile Fe (26 %) and the second highest amount can be found from the sediment (24 %).

12.4.10 The dissolution of Mn in the sequential extractions

The dissolution of Mn in the sequential extraction procedure for the different sample matrixes is presented in Figure 61.

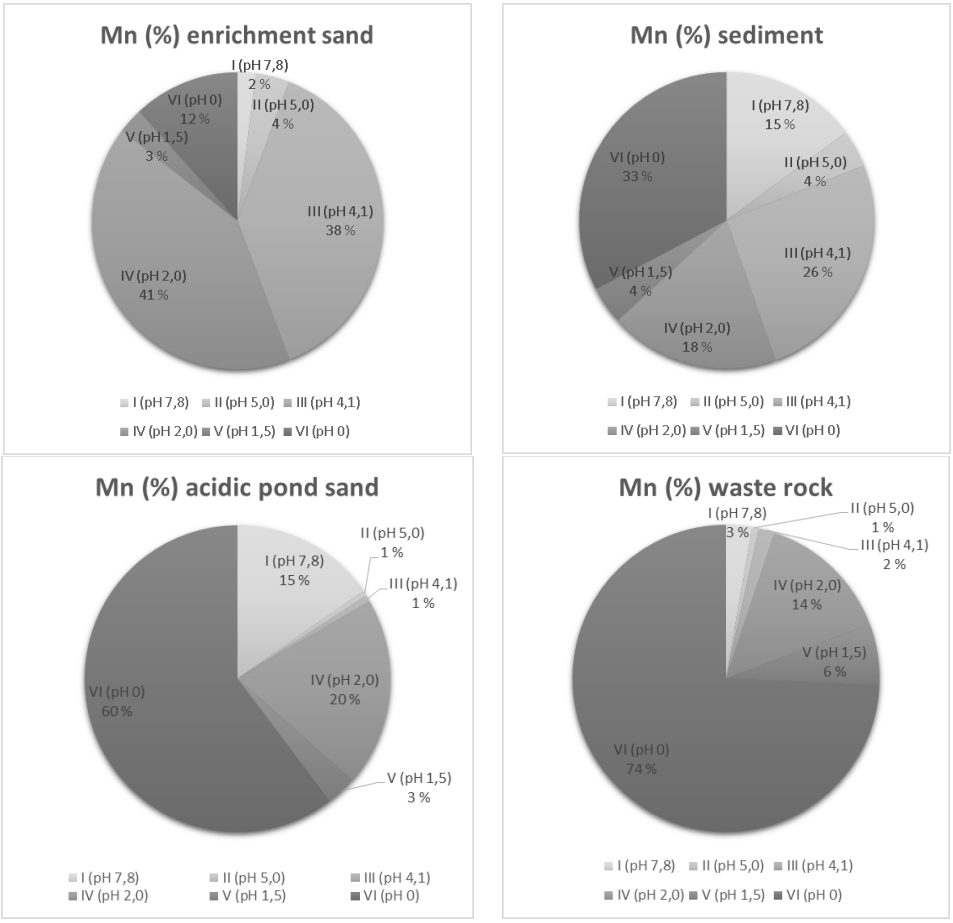

Figure 61. The dissolution of Mn in the sequential extraction procedure for the different sample matrixes. I – VI refer to the different extraction fractions: I = Exchangeable fraction I; II = Exchangeable fraction II; III = Mild acid-soluble fraction; IV = Reducible fraction; V = Oxidizable fraction; VI = Strong acid-soluble fraction.

The dissolution of Mn varies between the different sample types and the total leached concentrations are in the order of: enrichment sand (947 ppm), sediment (935 ppm), acidic pond sand (495 ppm) and waste rock (115 ppm). From the enrichment sand Mn is mainly leached out in the mild acid-soluble fraction (38 %) and the reducible fraction (41 %). From the sediment samples, Mn leached out in all of the fractions and the highest amounts were found in the strong acid-soluble fraction (33 %), mild acid-soluble fraction (26 %), reducible fraction (18 %) and the exchangeable fraction I (15 %). The presence of dissolved Mn in the mild acid-soluble fraction is most likely due to the dissolution of divalent salts, such as $MnCO_3$ or $(Ca,Mn)CO_3$. (88) (47) From the acidic pond sand

samples the dissolution mainly happened in the strong acid-soluble fraction (60 %), reducible fraction (20 %) and the exchangeable I fraction (15 %). The dissolution of Mn from the waste rock mainly happened in the strong acid-soluble fraction (74 %). The amount of leached Mn in the oxidizable fraction was low for all the samples. (90) (91) The enrichment sand and sediment had similar amounts of potentially mobile Mn (42 – 44 %), in fractions I - III, while the percentage for the acidic pond sand and waste rock was relatively low, 17 % and 6 %, respectively.

12.4.11 The dissolution of Pb in the sequential extractions

The dissolution of Pb in the sequential extraction procedure for the different sample matrixes is presented in Figure 62.

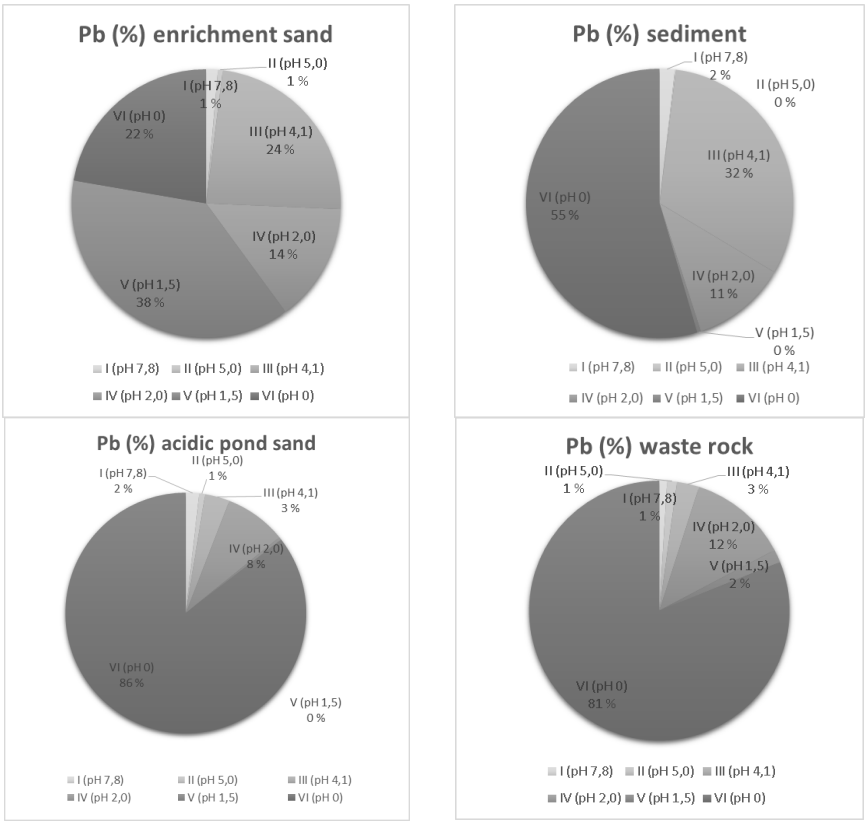

Figure 62. The dissolution of Pb in the sequential extraction procedure for the different sample matrixes. I – VI refer to the different extraction fractions: I = Exchangeable fraction I; II = Exchangeable fraction II; III = Mild acid-soluble fraction; IV = Reducible fraction; V = Oxidizable fraction; VI = Strong acid-soluble fraction.

The results for Pb dissolution vary depending on the sample type. In the enrichment sand Pb seems to be associated with the oxidizable fraction (38 %), mild acid-soluble fraction

(24 %), strong acid-soluble fraction (22 %) and the reducible fraction (14 %). From the sediment samples the dissolution happened in the strong acid-soluble fraction (55 %), mild acid-soluble fraction (32 %) and the reducible fraction (11 %). From the acidic pond sand the highest amount of Pb was leached out from the strong acid-soluble fraction (86 %) and the second highest in the reducible fraction (8 %). From the waste rock, Pb was also mainly leached out in the strong acid-soluble fraction. Increased amounts of Pb in the reducible fraction can be explained by its tendency to co-precipitate with Fe and Mn oxides. (13) The highest amount of potentially mobile Pb (fractions I – III) was found in the sediment (40 %). The total Pb concentrations were moderately low and in the order of: sediment (25 ppm), enrichment sand (7 ppm), acidic pond sand (6 ppm) and waste rock (5 ppm). Reabsorption of Pb is a well-known problem in sequential extractions and it has been proved that most of it happens in the first three fractions: exchangeable fractions I, exchangeable fractions II and the mild acid soluble fractions. (88) Evaluating the amount of reabsorbed Pb is not possible from the sequential extractions results, but the reabsorption might explain why Pb is found in multiply extraction fractions.

12.4.12 The dissolution of Cr in the sequential extractions

The dissolution of Cr in the sequential extraction procedure for the different sample matrixes is presented in Figure 63.

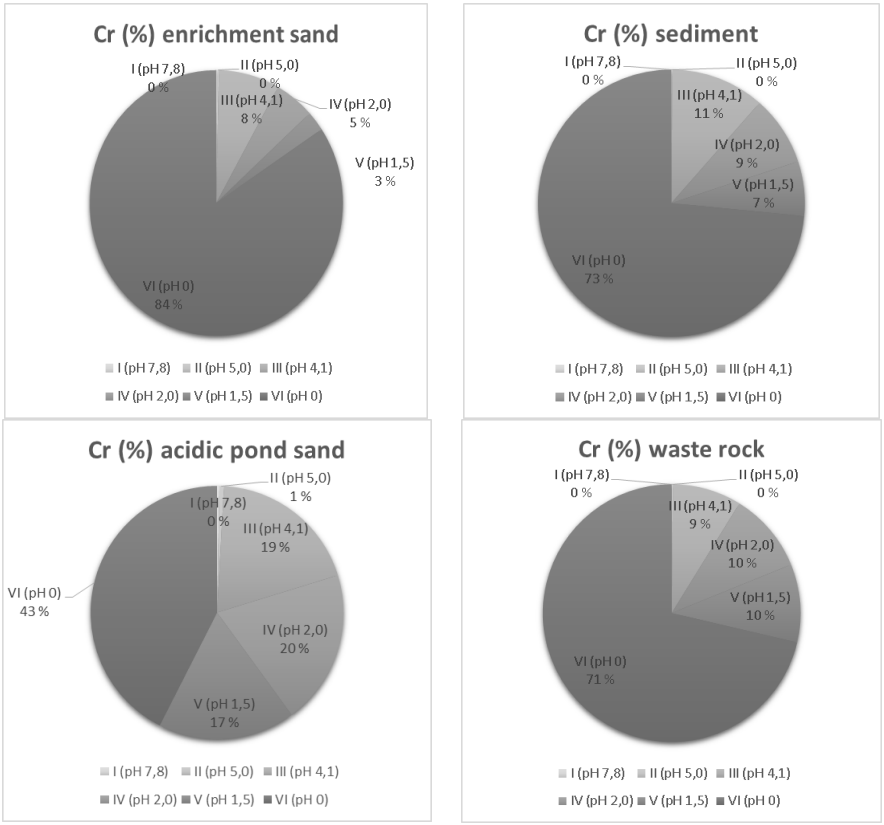

Figure 63. The dissolution of Cr in the sequential extraction procedure for the different sample matrixes. I – VI refer to the different extraction fractions: I = Exchangeable fraction I; II = Exchangeable fraction II; III = Mild acid-soluble fraction; IV = Reducible fraction; V = Oxidizable fraction; VI = Strong acid-soluble fraction.

The dissolution of Cr from the enrichment sand, sediment and waste rock is similar: most of Cr was leached out in the strong acid-soluble fraction (71 – 84 %) and lesser amounts in the mild acid-soluble, reducible and oxidizable fractions (3 – 11 %). From the acidic pond sand, Cr was leached out in the strong acid-soluble fraction (43 %), reducible fraction (20 %), mild acid-soluble fraction (19 %) and the oxidizable fraction (17 %). The dissolution of Cr in both exchangeable fractions was minor for all the sample matrixes. The results indicate that Cr is strongly bound in all the sample materials and it's unlikely for it to become mobile. On average, the total Cr concentrations were in the order of: enrichment sand (103 ppm), sediment (69 ppm), waste rock (18 ppm) and acidic pond sand (11 ppm).

12.4.13 The dissolution of Cd in the sequential extractions

The dissolution of Cd in the sequential extraction procedure for the different sample matrixes is presented in Figure 64.

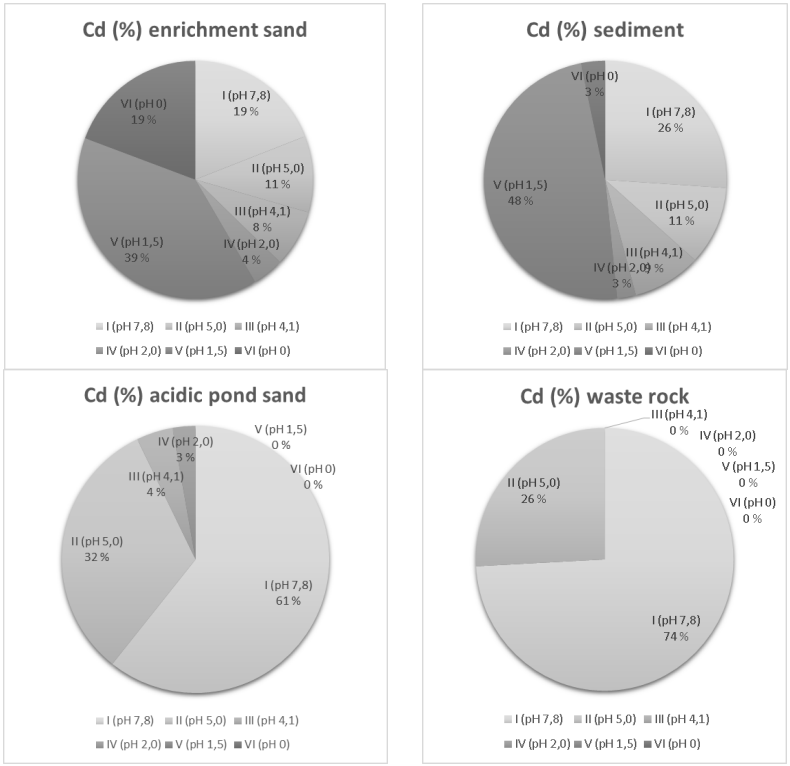

Figure 64. The dissolution of Cd in the sequential extraction procedure for the different sample matrixes. I – VI refer to the different extraction fractions: I = Exchangeable fraction I; II = Exchangeable fraction II; III = Mild acid-soluble fraction; IV = Reducible fraction; V = Oxidizable fraction; VI = Strong acid-soluble fraction.

The dissolution of Cd from the enrichment sand and sediment samples is distributed over all of the extraction fractions, whereas from the acidic pond sand and waste rock Cd is meanly leached out in the exchangeable fractions I and II. The highest proportion of Cd from the enrichment sand and sediment samples were leached out in the oxidizable fraction, 38 % and 48 %, respectively. From the acidic pond sand and waste rock the highest amount was leached out in the exchangeable fraction I, 61 % and 74 %, respectively. The acidic pond sand and sediment had a high content of labile Cd (fractions I – III), the percentage being 97 % and 46 %, respectively. Cd^{2+} has a known tendency to be mobile in the well-drained acid soils since it binds loosely to organic substances, clay and oxide minerals in pH below 6. (92) The pH of the different sample matrixes was lowest in the acidic pond sand (pH 4,1) and this might explain why the mobility was highest from it. Overall, the total concentrations of Cd were low and the combined

concentrations from all the leaching steps ranged between 0,03 – 0,6 ppm. On average, the total leached Cd concentrations were in the order of: sediment (0,6 ppm), enrichment sand (0,2 ppm), acidic pond sand (0,09 ppm) and waste rock (0,03 ppm).

12.4.14 The dissolution of As in the sequential extractions

The dissolution of As in the sequential extraction procedure for the different sample matrixes is presented in Figure 65.

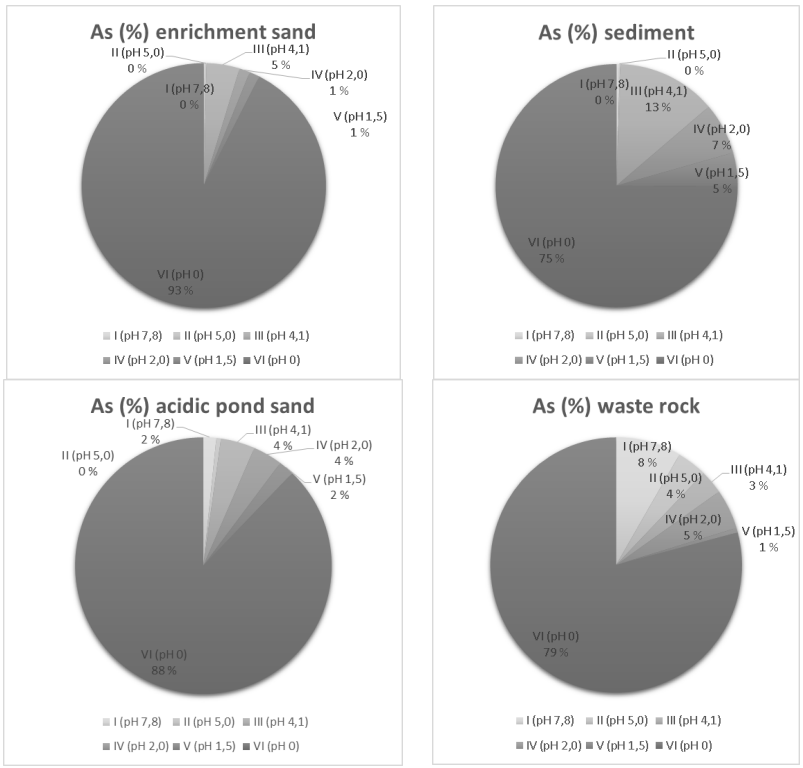

Figure 65. The dissolution of As in the sequential extraction procedure for the different sample matrixes. I – VI refer to the different extraction fractions: I = Exchangeable fraction I; II = Exchangeable fraction II; III = Mild acid-soluble fraction; IV = Reducible fraction; V = Oxidizable fraction; VI = Strong acid-soluble fraction.

The dissolution of As was similar from all the sample types and the highest amount was leached out in the strong acid-soluble fraction, the percentages varying between 75 – 93 %. The As (V) -oxyanion has a known tendency to adsorb with Fe oxy-hydroxides as the pH decreases, in which case most of the leached out As should be found in the reducible fraction. (93) However, this is not the case in this study, since most of the As was seen to be leached out in the strong acid-soluble fraction and this shows that As is tightly bound in the sample matrix e.g. to the primary sulphides like pyrite. Blanchard et al. (94) showed

that a high content of As in pyrite (up to 10 wt%) can have an accelerating effect on pyrite dissolution and in the formation of acid mine drainage. The total leached concentrations of As were in the order of: enrichment sand (289 ppm), sediment (105 ppm), acidic pond sand (12 ppm) and waste rock (2 ppm).

12.4.15 The dissolution of U in the equential extractions

The dissolution of U in the sequential extraction procedure for the different sample matrixes is presented in Figure 66.

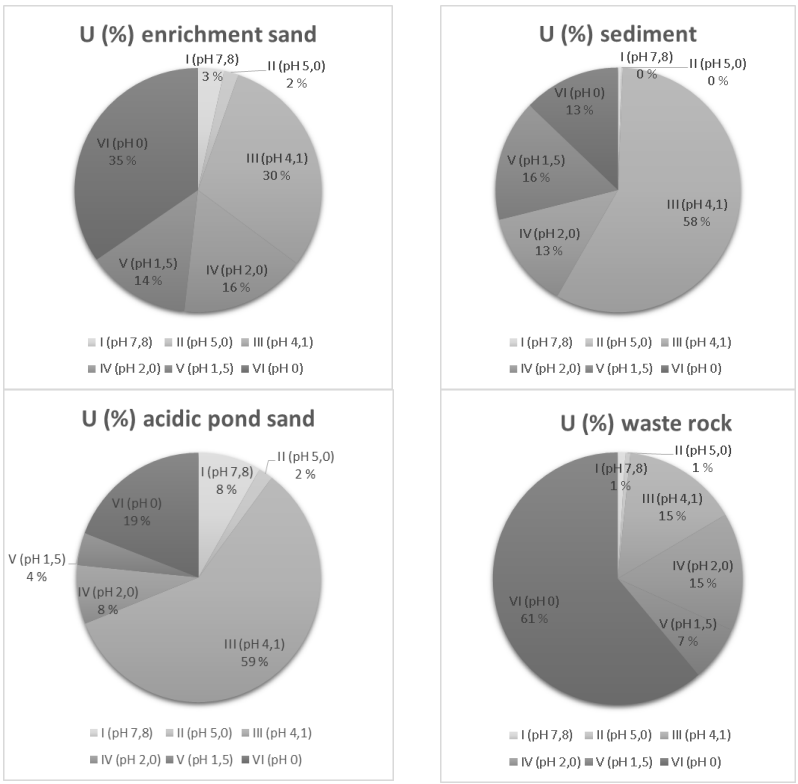

Figure 66. The dissolution of U in the sequential extraction procedure for the different sample matrixes. I – VI refer to the different extraction fractions: I = Exchangeable fraction I; II = Exchangeable fraction II; III = Mild acid-soluble fraction; IV = Reducible fraction; V = Oxidizable fraction; VI = Strong acid-soluble fraction.

Dissolution of U happened in many different leach steps during the sequential extraction procedure. Large proportions of U were leached out in the mild acid-soluble fraction: 68 % from the acidic pond sand, 58 % from the sediment, 30 % from the enrichment sand and 15 % from the waste rock. From the enrichment sand, leached concentrations of U was also found in the strong acid-soluble fraction (35 %), reducible fraction (16 %) and the oxidizable fraction (14 %). Leaching from the sediment resembled that of the enrichment

sand and the percentages for fractions IV – VI were between 13 – 16 %. From the acidic pond sand 59 % of U was leached out in the mild acid-soluble fraction. The dissolution of U in the exchangeable fractions I and II was minor in all the sample matrixes. Large amounts of U were leached out in the strong acid-soluble fraction from the waste rock, which may indicate a strong association with the sulphides. The dissolution of U in the exchangeable fraction I was mainly only seen from the acidic pond sand (10 %). From all the sample matrixes the dissolution of U in the exchangeable fraction II was insignificant. The results indicate that a proportion of U is loosely bound in the enrichment sand, sediment and acidic pond sand, since a large amount of it was leached out in the mild acid-soluble fraction. This result is in agreement with previous studies made by Tuovinen et al. (49) and Virtanen et al. (88). The mobilization of U in the mild acid-soluble fraction may lead to a rapid ecosystem transfer and uptake by plants or organisms. The pH needed for U dissolution was the same that the measured pH of the acidic pond sand (pH 4,1). Large proportions of U were also leached out in the reducible fraction (between 9 – 16 %), which according to Skipperud et al. (15) can refer to existence of the redox and pH sensitive amorphous fractions of U. In the mild acid-soluble fraction, U most likely occurs with an oxidation state U(VI), which is more stable under oxidizing conditions than U(IV). U(VI) hydrolyze in nature and forms uranyl ions (UO_2^{2+}), due to its high charge. UO_2^{2+} can form water-soluble complexes, depending on the pH of the solution and the ligand composition present. The total leached concentrations of uranium for the acidic pond sand and waste rock were at the level of the average in the Finnish bedrock (4 ppm). The U concentrations leached out from the enrichment sand and sediment samples were higher than on average in Finnish bedrock, 8 ppm and 20 ppm, respectively. The amount for enrichment sand is twice as high as the concentration in the Finnish bedrock, and from the sediment five times higher. The total leached concentrations of U in the sequential extractions were compared to those from gamma ray spectrometry. The measured concentrations by the ICP-MS and gamma ray spectrometry for ^{238}U resemble each other and are within the same order of magnitude. The measured results can be found in Appendix A.

12.4.16 The dissolution of Th in the sequential extractions

The dissolution of Th in the sequential extraction procedure for the different sample matrixes is presented in Figure 67.

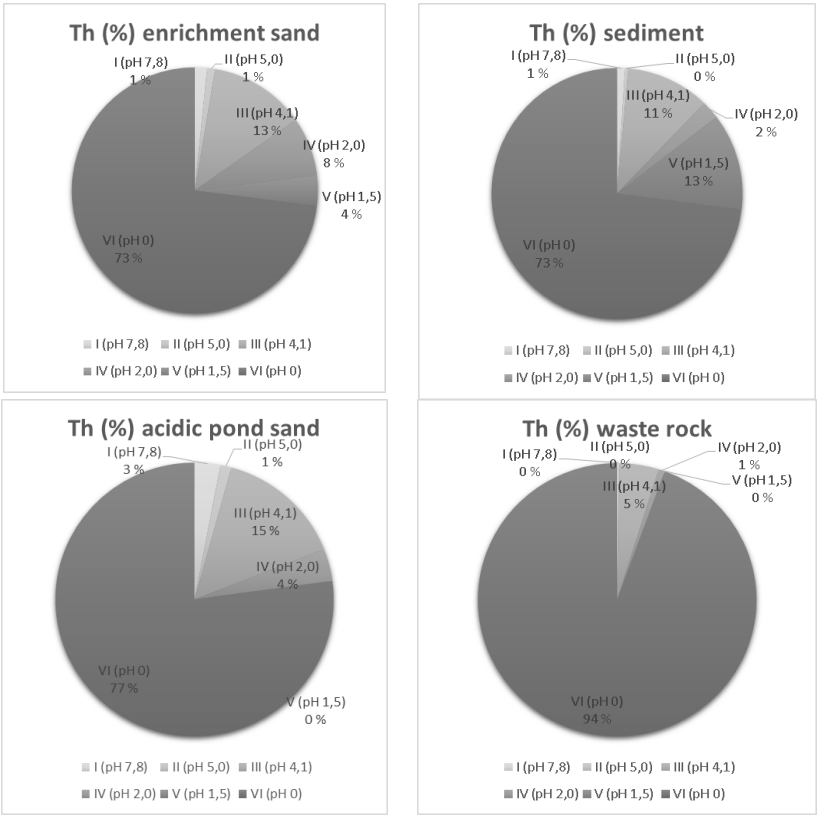

Figure 67. The dissolution of Th in the sequential extraction procedure for the different sample matrixes. I – VI refer to the different extraction fractions: I = Exchangeable fraction I; II = Exchangeable fraction II; III = Mild acid-soluble fraction; IV = Reducible fraction; V = Oxidizable fraction; VI = Strong acid-soluble fraction.

Th is mainly leached out in the strong acid-soluble fraction, which indicates that it is strongly bound to the crystal lattices of minerals. Lesser amount of Th were also leached out in the mild acid-soluble fraction, the percentages varied between 5 – 15 %. The distribution of Th in the sequential extractions showed U to be more mobile than Th in most of the sample types. This result is in agreement with previous studies made by Virtanen et al. (88) and Skipperud et al. (15). The total leached concentrations of Th were low and in the order of: waste rock (10 ppm), sediment (8 ppm), enrichment sand (2 ppm), and acidic pond sand (2 ppm). The total leached amounts of Th are close or below the Finnish average bedrock concentration (8 ppm). Total leached concentrations of ^{232}Th from the sequential extractions were compared to those from the gamma ray spectrometry. The measured concentrations for ^{232}Th resemble each other and are within the same order of magnitude. The measured results can be found in Appendix A.

12.4.17 The uncertainties of the sequential extractions

The uncertainties for the metal and radionuclide concentrations leached out in the different extraction fractions were estimated using standard deviation. The number of used samples (including the duplicates) in the sequential extractions was: 34 enrichment sand samples, 8 acidic pond sand samples, 2 sediment samples and 4 waste rock samples. The estimated uncertainties for each metal in every extraction fraction, together with the analytical data of the leached metal concentrations, are presented in Appendix A. Table 40 presents the range of standard deviations for each metal, regardless of the extraction fraction, in order to give a better understanding of the variety of the leached concentrations.

Table 40. The range of the standard deviations as a percentage of the originally leached elemental concentration in the sequential extraction procedure.

Metal	Enrichment sand (%)	Sediment (%)	Acidic pond sand (%)	Waste rock (%)
Cr	14 … 254	1 … 47	7 … 84	2 … 141
Mn	19 … 145	1 … 2	18 … 60	2 … 87
Fe	16 … 412	1 … 97	28 … 61	1 … 74
Co	32 … 95	1 … 3	20 … 130	9 … 69
Ni	30 … 63	1 … 5	35 … 135	19 … 141
Cu	55 … 406	1 … 7	37 … 110	13 … 55
Zn	122 … 412	3 … 90	68 … 198	48 … 141
As	38 … 350	1 … 17	23 … 53	14 … 141
Cd	69 … 179	1 … 15	27 … 200	0 … 141
Pb	46 … 326	1 … 47	15 … 104	15 … 105
Th	23 … 190	1 … 9	24 … 200	1 … 141
U	30 … 110	1 … 14	24 … 160	4 … 78

The range of the standard deviations in Table 40 may initially look large, since it shows the variation of concentrations from the counted average. The values differ since the composition of the particular sample type is not regular, meaning that each sample has a unique mineral and metal composition. Increasing the number of samples in the sequential extractions in order to obtain the results as the distribution of the Gaussian curve could reduce the range of standard deviations.

However, the overall trends are not affected with scattered results, which can be seen in Figures 67 and 68, which show the overall dissolution of U and Th from enrichment sand samples for each different sample.

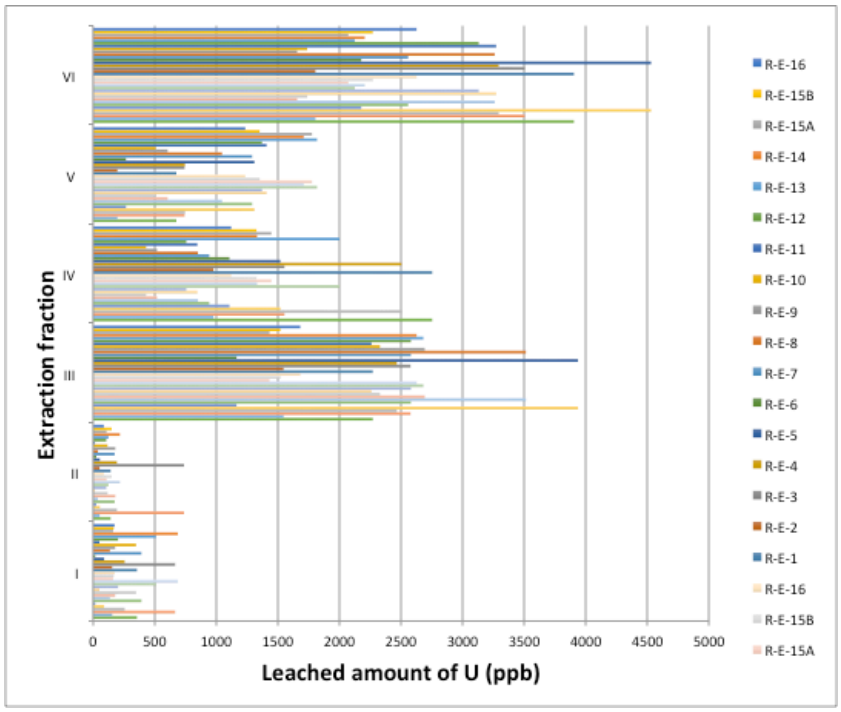

Figure 67. The dissolution of U in the sequential extractions from the Rautuvaara enrichment sand samples.

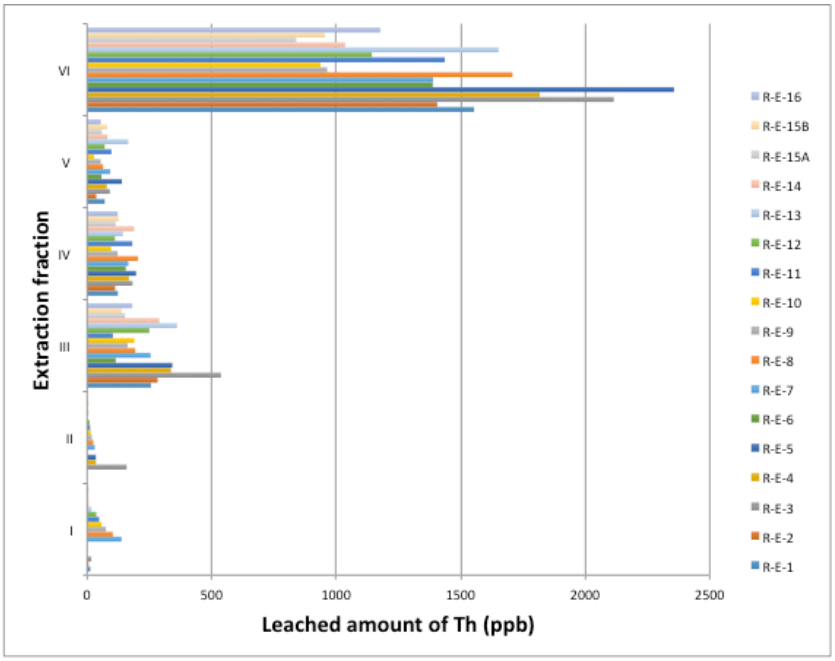

Figure 68. The dissolution of Th in the sequential extractions from the Rautuvaara enrichment sand samples.

12.4.18 Environmental risk assessment from the sequential extractions results

Environmental risk assessment was performed in order to obtain information on the potentially harmful metal and radionuclide concentrations in the Rautuvaara mining area. A risk assessment was performed as Favas et al. (13) described in their work. This method utilized the use of the risk assessment code (RAC), which is based on the bond strength between metals and the geochemical fractions in sample matrixes, and on the ability of metals to be released from them. The RAC code was described more closely in chapter 4.5. The results for the environmental risk assessment are shown in Figure 69.

		<1 % no risk	1-10 % low risk	11-30 % medium risk	31-50 % high risk	> 50 % very high risk	
Samples		(Exchangeable fraction I + Enxchangeable fraction II + Mild acid-soluble fraction)/Total concentration(%)					
Enrichment sand	Cr (ppb)	Mn (ppm)	Fe (ppm)	Co (ppb)	Ni (ppb)	Cu (ppb)	Zn (ppb)	As (ppb)	Cd (ppb)	Pb (ppb)	Th (ppb)	U (ppb)
R-E-1	7	48	11	17	23	1	99	3	41	34	13	27
R-E-2	11	44	12	23	25	5	10	5	34	39	16	37
R-E-3	16	73	28	20	31	8	13	14	31	55	23	41
R-E-4	11	54	13	14	24	1	2	3	30	38	15	31
R-E-5	8	37	10	22	21	18	1	8	49	18	12	36
R-E-6	7	26	7	4	14	0	0	0	14	1	7	25
R-E-7	11	43	11	12	18	0	66	2	80	32	20	40
R-E-8	8	36	9	22	20	7	0	3	75	21	14	42
R-E-9	10	36	11	17	30	0	66	3	75	41	18	52
R-E-10	7	61	21	22	31	5	0	4	87	33	20	51
R-E-11	6	31	8	13	25	1	0	1	49	19	9	30
R-E-12	13	42	14	12	25	0	0	5	57	36	18	35
R-E-13	6	56	18	19	31	5	27	9	63	52	16	36
R-E-14	5	41	10	13	17	2	15	6	22	50	19	40
R-E-15A	5	37	10	12	17	0	30	2	14	42	13	24
R-E-15B	5	35	8	7	13	1	10	2	5	35	11	27
R-E-16	11	30	6	9	12	3	1	3	14	34	12	28
Sediment												
R-S-3	11	45	24	34	41	2	36	14	46	34	12	58
Acidic pond sand												
R-S-4	21	21	15	65	47	1	83	9	100	11	19	34
R-S-5	20	21	28	56	45	4	28	4	100	3	14	65
R-S-6	22	15	32	46	43	1	0	9	88	3	19	41
R-S-7	19	13	22	15	23	2	81	6	100	7	25	79
Waste rock												
R-R-1A	10	3	2	6	1	8	0	13	0	5	6	18
R-R-1B	8	7	1	11	4	11	51	18	100	4	3	16

Figure 69. Environmental risk assessment using RAC code, which combines the leached amounts of metals in the exchangeable fraction I, exchangeable fraction II and mild acid-soluble fraction. The results are presented as percentages (leached concentration / total concentration found in sample * 100 %). Less than 1 % means no risk, low risk for 1 – 10 %, medium risk for 11 – 30 %, high risk for 31 – 50 % and very high risk for over 50 %.

In general, most of the metals have a low risk or medium risk of mobilization to the environment. Cd have the highest calculated risk of being mobile from all the sample matrixes, however its total concentrations are low. As have the lowest risk of mobilization from all the different sample types. Fe, Th and Cr have a low or medium risk of mobilization in all the sample types, whereas Ni and Co have a low or medium risk from the enrichment sand and waste rock and a high risk from the sediment and acidic pond

sand. U have a medium or high risk of mobilization from the enrichment sand, and a high or very high risk from the sediment.

In general, the potentially harmful metals Co, Cr, Cd and Pb and radioactive U are in a more mobile form in the acidic pond sand than in the enrichment sand. This is probably due to the effect of AMD, which alters the pH and redox conditions in the acidic pond sand. The lowered pH attacks the surrounding mineral phases and the out leached metals may end up in the settling pond and accumulate in the bottom sediments. The mobilization from the sediment was mainly of a medium or high risk.

12.5 Comparison of the metal concentrations acquired from different analytical methods: XRF, SD-XRPD, ICP-MS and gamma spectrometry

X-ray methods (XRF and SR-XRPD) were used for the elemental analysis of metal contents of a selected set of enrichment sand samples. The samples were chosen so that they would represent the whole sampling area of the enrichment sand. The analyses were also performed for the enrichment sand subsamples acquired from sequential extractions, e.g. R-E-1 V, in order to study the mineral phase dissolution during the extraction method. The XRF results were used in the identification of the mineral phases in the Rietveld method used for the SR-XRPD data. The results from the XRF and SR-XRPD methods were compared with each other in order to assure that the results from the SR-XRPD are reliable. Table 41 represents the elemental analysis results obtained from the XRF and SR-XRPD methods.

Table 41. Elemental analysis results from the X-ray measurements (XRF and SR-XRPD) of the Rautuvaara enrichment sand samples. The results are given as percentages (%) of the total mineral composition. (R-E = Rautuvaara enrichment sand, No. = Sampling location, V = the oxidizable fraction in the sequential extractions)

	R-E-1		**R-E-3**		**R-E-11**		**R-E-14**	
Phase	XRF	SR-XRPD	XRF	SR-XRPD	XRF	SR-XRPD	XRF	SR-XRPD
Al_2O_3	12.8	12.1	11.7	11.8	11.6	12.0	10.8	10.0
CaO	7.16	7.18	9.15	9.75	7.07	8.49	8.20	8.46
Fe_2O_3	10.3	5.28	9.70	5.25	12.9	8.79	12.6	6.25
K_2O	0.65	0.24	0.71	0.26	0.53	0.32	0.76	0.48
MgO	5.65	4.64	6.17	5.57	4.21	3.33	5.42	5.39
MnO	0.13	0.00	0.16	0.00	0.12	0.00	0.16	0.00
Na_2O	5.27	5.70	4.64	4.99	5.01	5.68	4.29	4.66
SO_3	3.78	0.29	3.22	0.19	5.97	4.27	4.01	0.28
SiO_2	47.5	47.5	44.1	43.0	46.3	41.4	45.0	46.2
TiO_2	0.98	0.91	0.90	1.05	0.93	1.13	0.99	1.22
ZnO	0.00	0.00	0.00	0.00	0.00	0.00	0.01	0.00
	R-E-1 V		**R-E-3 V**		**R-E-11 V**		**R-E-14 V**	
Phase	XRF	SR-XRPD	XRF	SR-XRPD	XRF	SR-XRPD	XRF	SR-XRPD
Al_2O_3	16.0	16.4	16.0	17.4	14.6	16.2	14.2	14.1
CaO	0.52	1.69	0.47	0.44	0.52	0.04	1.82	1.51
Fe_2O_3	8.79	2.74	7.18	1.82	12.3	11.3	11.0	4.56
K_2O	0.71	0.19	0.87	0.37	0.66	0.26	1.00	0.85
MgO	2.71	3.61	3.02	3.58	1.98	1.71	2.72	3.48
MnO	0.02	0.01	0.02	0.03	0.05	0.00	0.07	0.00
Na_2O	6.73	7.49	6.58	7.57	6.52	7.87	5.62	6.39
SO_3	0.91	0.00	0.95	0.54	0.63	0.00	0.74	0.00
SiO_2	60.7	63.7	62.0	65.3	60.6	56.1	60.4	65.6
TiO_2	1.25	1.18	1.23	1.35	1.10	1.21	1.33	1.53
ZnO	0.00	0.00	0.01	0.04	0.01	0.00	0.01	0.00

The results acquired from the XRF and SR-XRPD methods are in a good agreement with each other and prove that the quality of analysis is good. The only exception is seen in the Fe_2O_3 percentages, which are lower from the SR-XRPD method. Table 42 shows the total ^{238}U concentration of the Rautuvaara enrichment sand acquired by three different methods, which were gamma ray spectrometry, ICP-MS and XRF.

Table 42. Total U concentrations (ppm) and their uncertainties (±) in the Rautuvaara enrichment sand samples measured by gamma ray spectrometry, ICP-MS and XRF.

	^{238}U		
Sample	Gamma (ppm)	ICP-MS (ppm)	XRF (ppm)
R-E-1	15	12	14
±	3	4	-
R-E-3	11	11	13
±	3	1	-
R-E-11	14	8	9
±	2	0	-
R-E-14	12	9	14
±	2	1	-

It can be seen from Table 39 that the total uranium concentration in enrichment sand samples are of same order of magnitude, even though there are slight variations. The variations may be caused by the unique mineral and elemental composition of each sample. The Cu, Cr, Ni and Zn concentrations acquired from the XRF analysis were compared to those from the total acid digestion and these results are presented in Table 43.

Table 43. Total Cu, Cr, Ni, and Zn concentrations (ppm) in the Rautuvaara enrichment sand samples from the acid digestion and XRF analysis.

Sample	**R-E-1**			**R-E-3**		
Metal	Acid Digestion (ppm)	XRF (ppm)	Difference (%)	Acid Digestion (ppm)	XRF (ppm)	Difference (%)
Cu	241	264	10	214	233	9
Cr	146	249	71	111	182	64
Ni	330	335	2	372	379	2
Zn	27	26	4	33	20	65
Sample	**R-E-11**			**R-E-14**		
Metal	Acid Digestion (ppm)	XRF (ppm)	Difference (%)	Acid Digestion (ppm)	XRF (ppm)	Difference (%)
Cu	294	314	7	495	493	0.4
Cr	96	151	57	140	227	62
Ni	665	650	2	355	365	3
Zn	19	22	16	131	122	7

The results presented in Table 43 are mostly resemble each other. The only difference is seen in the dissolution of Cr, which has not been dissolved during the acid digestion. For other metals the results from both the acid digestion and the XRF analysis were in good agreement with each other's.

Overall, the compared results agree with each other's and the measured quantities of metals and radionuclides are within the same order of magnitude.

12.6 Mineralogy of Rautuvaara solid samples

Synchrotron Radiation X-ray Power Diffraction (SR-XRPD) was used to study the mineralogical composition of selected enrichment sand samples. The samples were selected in a way that they would be representative of the whole enrichment sand area. The method was used for the enrichment sand samples that were submitted to the first five leaching steps. The mild acid-soluble fraction, reducible fraction and oxidizable fraction residues were measured with SR-XRPD, in order to gain information about the dissolving and precipitating phases. Sequential extractions have been widely criticized about the selectivity of the selected extraction reagents due to the possible formation of secondary mineral phases and their retention of the mobilized elements. The detection limit for SR-XRPD has been reported to be <0.05 wt%, which is very good when compared to the traditional X-ray diffraction that has a detection level of approximately 5 %. (95) (96) This detection limit for SR-XRPD is procurable even with micrograms of sample material. (95) During the extraction the relative concentrations of the remaining, dissolving and precipitating minerals change and due to the low detection level and high resolution of the procedure even the small changes should be considered as an actual change, instead of normal variation of the analytical data between different measurements. Thus, the variations can be due to the heterogeneity of the sample material, as it is a mixture of enrichment sand from several different mines. The results of the SR-XRPD analysis is presented in Tables 44, 45, 46 and 47, and visualized in Figures 70, 71, 71 and 73. In the results, two different polytypes of pyrrhotite ($Fe_{1-x}S$) are presented in the results, which are pyrrhotite-4C (Fe_7S_8) and pyrrhotite-5C (Fe_9S_{10}).

Table 44. The mineral phase content of the R-E-1 sample during the sequential extraction procedure measured with SR-XRPD. The given values are the percentages for each mineral phase of the total sample content (%). The studied extraction fractions were the mild acid-soluble fraction (III), reducible fraction (IV) and oxidizable fraction (V).

	R-E-1	R-E-1 III	R-E-1 IV	R-E-1 V
Dravite	2,7	4,3	4,3	3,7
Clinochlore	6,5	5,9	10	9,4
Dolomite	23,4	13,8	1,3	3,1
Quartz	10,8	11,4	13,5	15,3
Rutile	0,8	0,9	1,2	1,1
Talc	0,4	0,1	0,3	0,1
Pyrrhotite (Fe9S10)	2,4	3,1	3,5	1,1
Pyrite	0,3	0,4	0,4	0,1
Calcite	0,5	LOD	LOD	LOD
Albite	47,6	54,1	60,3	63,6
Bassanite	0,5	0,1	LOD	LOD
Tremolite	0,4	0,3	0,3	0,6
Biotite	2,4	3,7	3,5	1,6
Pyrrhotite (Fe7S8)	1,2	1,9	1,4	0,3

LOD = below the detection limit

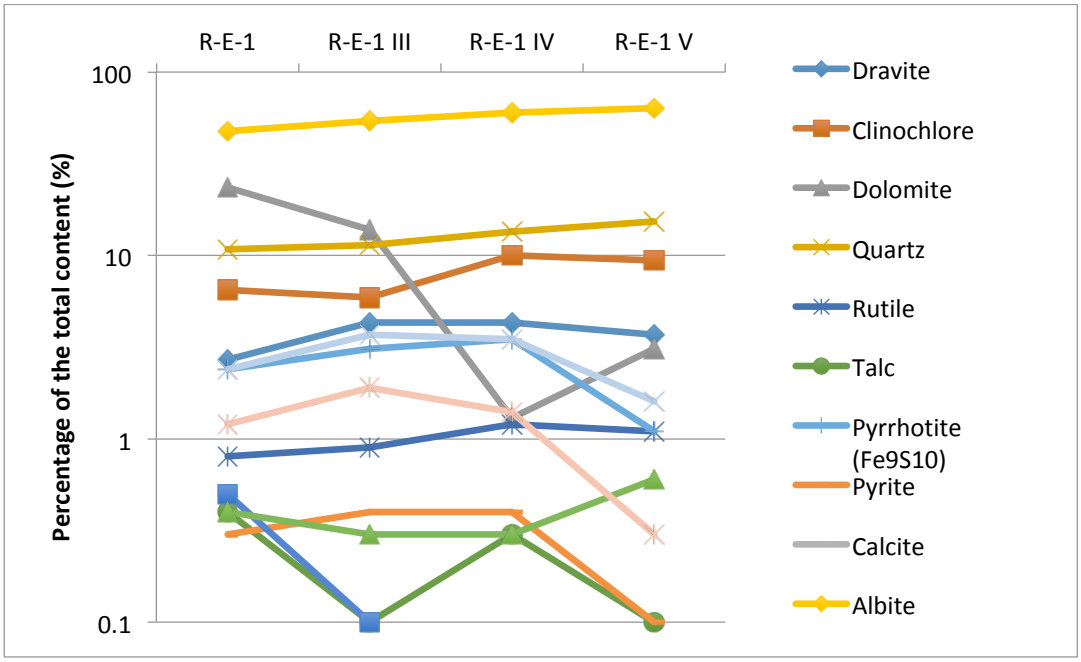

Figure 70. The SR-XRPD results illustrated for R-E-1 bulk sample and for the extraction step samples: the mild acid-soluble fraction (III), reducible fraction (IV) and oxidizable fraction (V). The given values are the percentages for each mineral phase of the total sample content (%).

Table 45. The mineral phase content of the R-E-3 sample during the sequential extraction procedure measured with SR-XRPD. The given values are the percentages for each mineral phase of the total sample content (%). The studied extraction fractions were the mild acid-soluble fraction (III), reducible fraction (IV) and oxidizable fraction (V).

	R-E-3	R-E-3 III	R-E-3 IV	R-E-3 V
Dravite	2,5	2,6	3	3,6
Clinochlore	7,6	6,5	7,5	8,9
Dolomite	26,9	16	1,9	LOD
Quartz	10,3	13,1	14,3	15,6
Rutile	0,9	1	1	1,2
Talc	0,4	1,2	1,7	1,4
Pyrrhotite (Fe9S10)	1,6	1,5	2	LOD
Pyrite	1,3	1,6	1,7	0,6
Calcite	2,9	1,1	0,5	LOD
Albite	41,7	50,3	60,1	64,5
Bassanite	0,4	0,5	0,9	1
Tremolite	0,1	0,1	0,3	LOD
Biotite	2,5	3,4	3,9	3,1
Pyrrhotite (Fe7S8)	0,7	1	1,2	0,2

LOD = below the detection limit

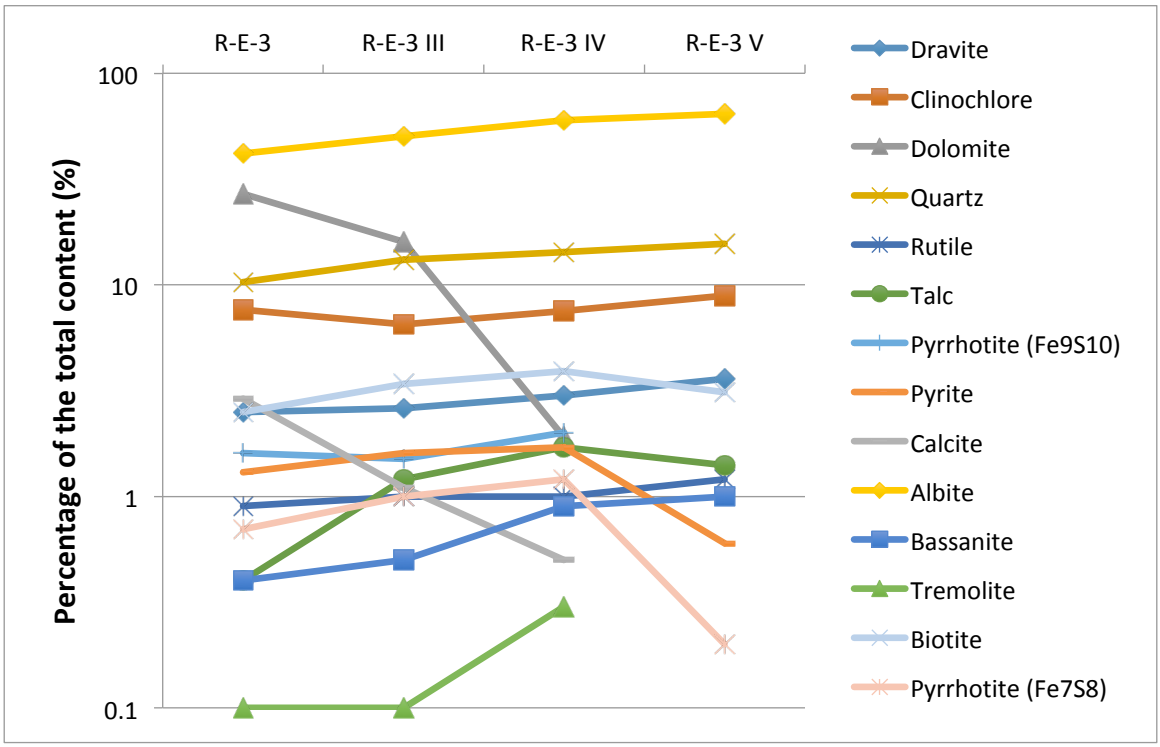

Figure 71. The SR-XRPD results illustrated for R-E-3 bulk sample and for the extraction step samples: the mild acid-soluble fraction (III), reducible fraction (IV) and oxidizable fraction (V). The given values are the percentages for each mineral phase of the total sample content (%).

Table 46. The mineral phase content of the R-E-11 sample during the sequential extraction procedure measured with SR-XRPD. The given values are the percentages for each mineral phase of the total sample content (%). The studied extraction fractions were the mild acid-soluble fraction (III), reducible fraction (IV) and oxidizable fraction (V).

	R-E-11	R-E-11 III	R-E-11 IV	R-E-11 V
Dravite	2,2	2,8	2,8	3,2
Clinochlore	4,6	4,5	5,9	5,5
Dolomite	18,3	14,5	2,6	LOD
Quartz	7	7,2	8,1	9,4
Rutile	0,8	0,8	0,9	1
Pyrite	1,1	1,2	1,2	0,6
Albite	48,5	51,6	60,4	67,1
Bassanite	7,8	LOD	LOD	LOD
Tremolite	0,4	0,3	0,4	0,2
Biotite	3,1	2,2	2,8	2,5
Pyrrhotite (Fe7S8)	0,9	1,3	1,2	LOD
Goethite	4,9	9,1	10,5	10,4
Ilmenite	0,3	0,4	0,3	0,2
Gypsum	LOD	4,1	2,8	LOD

LOD = below the detection limit

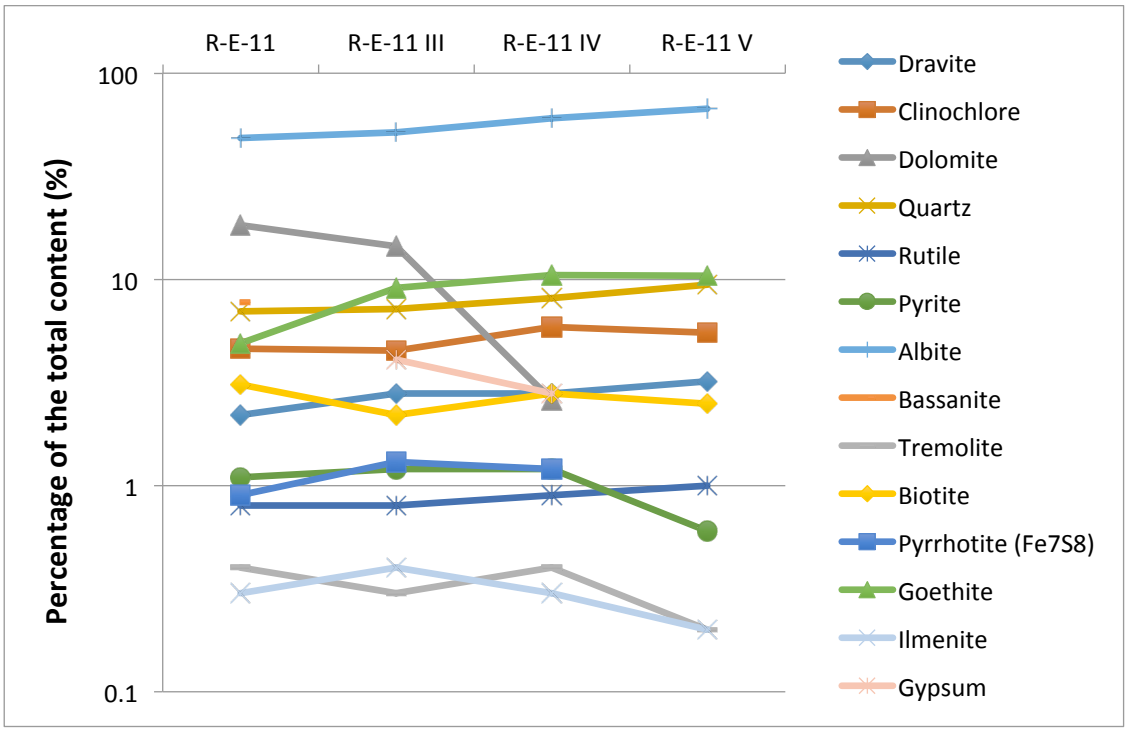

Figure 72. The SR-XRPD results illustrated for R-E-11 bulk sample and for the extraction step samples: the mild acid-soluble fraction (III), reducible fraction (IV) and oxidizable fraction (V). The given values are the percentages for each mineral phase of the total sample content (%).

Table 47. The mineral phase content of the R-E-14 sample during the sequential extraction procedure measured with SR-XRPD. The given values are the percentages for each mineral phase of the total sample content (%). The studied extraction fractions were the mild acid-soluble fraction (III), reducible fraction (IV) and oxidizable fraction (V).

	R-E-14	R-E-14 III	R-E-14 IV	R-E-14 V
Dravite	2,86	2,95	4,33	3,82
Clinochlore	3,08	2,97	3,82	3,97
Dolomite	23,1	13,7	1,37	LOD
Quartz	12,92	15,59	16,39	18,55
Rutile	0,81	0,82	1,03	1,02
Talc	0,18	0,13	0,2	0,18
Pyrrhotite (Fe9S10)	2,6	2,83	2,81	0,4
Pyrite	2,6	0,4	0,61	0,26
Albite	39,19	42,28	54,87	54,42
Bassanite	0,51	0,34	LOD	LOD
Tremolite	1,83	2,15	1,87	3,24
Biotite	4,28	7,55	5,38	7,41
Pyrrhotite (Fe7S8)	2,55	2,7	2,18	0,23
Diopside	2,38	3,25	3,29	3,92
Magnetite	0,94	1,02	0,84	1,42
Ilmenite	0,39	0,47	0,2	0,32
Marialite	0,94	1,02	0,28	0,45
Grunerite	0,35	0,37	0,39	0,38
Calcite	1,14	0,24	0,13	LOD

LOD = below the detection limit

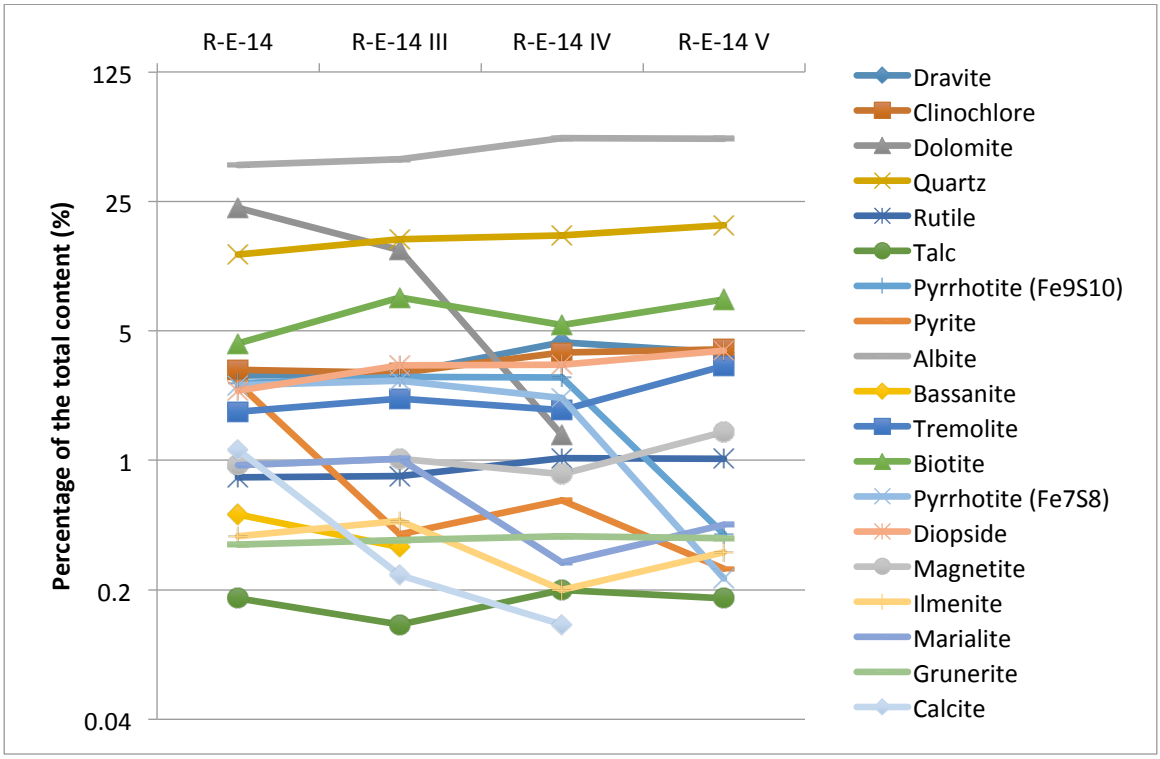

Figure 72. The SR-XRPD results illustrated for R-E-13 bulk sample and for the extraction step samples: the mild acid-soluble fraction (III), reducible fraction (IV) and oxidizable fraction (V). The given values are the percentages for each mineral phase of the total sample content (%).

The results show that more than one mineral is leached out in most of the steps and that some minerals are dissolved completely whereas others only partially. The main minerals in Rautuvaara enrichment sand samples were albite (39 – 48 %), dolomite (18 – 26 %), quartz (7 – 12 %), clinochlore (3 - 7 %) and biotite (2 – 4 %). The mineralogical results are in agreement with a previous study that reported the main ore minerals in Rautuvaara to be magnetite, chalcopyrite, ilmenite, pyrrhotite and pyrite and the gangue minerals to be albite, anthophyllite, biotite and quartz. (97) The minerals that are not present in the Rautuvaara ore may originate from the other deposits presented in Table 11 in Chapter 5.

The mineralogical results of the sequential extractions show the dissolving, precipitating and unaffected mineral phases during the leach test. The completely dissolved mineral phases were bassanite ($CaSO_4 \cdot 2H_2O$), dolomite ($CaMg(CO_3)_2$) and calcite ($CaCO_3$). Bassanite was dissolved between the pH's of 2 – 4.1, calcite between 1.5 – 4.1 and dolomite in pH 1.5. The partially dissolving mineral phases were talc ($Mg_3Si_4O_{10}(OH)_2$), pyrrhotite (Fe_9S_{10}), pyrrhotite (Fe_7S_8), pyrite (FeS_2), tremolite ($Ca_2Mg_5Si_8O_{22}(OH)_2$),

biotite ($(Mg,Fe)_3AlSi_3O(F,OH))_2$), ilmenite ($FeTiO_3$), magnetite ($Fe_3O_4$) and marialite ($Na_4Al_3Si_9O_{24}Cl$). The partial dissolution mainly happened in the reducible fraction (pH 2.0) and in the oxidizable fraction (pH 1.5). Pyrrhotite was seen to dissolve in the reducible fractions and oxidizable fractions, and pyrite and biotite mainly in the oxidizable fraction.

Based on Dold et al. (96) calcite should dissolve completely in the leach step done with NH_4-acetate. From the Rautuvaara samples calcite was found in three of the enrichment sand samples (R-E-1, R-E-3 and R-E-14) and it was dissolved completely before the third step, the mild acid-soluble step (pH 4.1), in only one of the samples (R-E-1). In the others the dissolution continued until the fifth step, which is the oxidizable step (pH 1.5).

During the enrichment sand test a noticeable amount of As was leached out from the enrichment sand (289 ppm), but no As minerals (e.g. arsenopyrite) were detected in the results. According to Rankama and Sahama (98) pyrite may consist notable quantities of arsenic. A partial dissolution of pyrite was witnessed during the extractions, which may be the origin of As.

Gypsum forms as a secondary phase during the extractions, which may affect the selectivity of the sequential extractions since the dissolved elements may be co-precipitate with the formed gypsum. These precipitated elements dissolve again in later fractions once gypsum is dissolved completely. This may lead to a underestimations of dissolved metal phases in the fractions where the gypsum is formed. The formation of gypsum may happen as a result of dissolution of bassanite and/or calcium carbonates (calcite and dolomite). Bassanite can go through an aqueous transformation into gypsum with a process mechanism that is not fully understood yet, but it is thought to be a reconstructive reaction happening in a fluid phase when bassanite dissolves and gypsum precipitates. (99) Calcite and dolomite are dissolved in water when the pH decreases below 5, according to the equations 4 and 5 (100) (101):

$$CaCO_{3(s)} + H^{+}{}_{(aq)} \rightarrow Ca^{2+}{}_{(aq)} + HCO_3{}^{-}{}_{(aq)} \quad (4)$$

$$CaMg(CO_3)_{2(s)} + 2H^{+}{}_{(aq)} \rightarrow Ca^{2+}{}_{(aq)} + Mg^{2+}{}_{(aq)} + 2HCO_3{}^{-}{}_{(aq)} \quad (5)$$

If the dissolved ions are exposed to sulphate ions then the following reaction (6) may happen (100):

$$Ca^{2+}{}_{(aq)} + SO_4{}^{2-}{}_{(aq)} + 2H_2O_{(l)} \rightarrow CaSO_4 \cdot 2H_2O_{(s)} \quad (6)$$

The enrichment sand in Rautuvaara mining area is known to be AMD-forming so the sulphate ions in the latter reaction may originate from the formed sulphuric acid. During the extractions the formation of gypsum was only visible in the R-E-11 –sample, which may be because this sample had the highest amount of bassanite in it. Goethite (FeOOH) was seen in the R-E-11 –sample, which may be a secondary mineral formed when the Fe sulhides are oxidized as a result of AMD. (101) Since the formation of gypsum was only witnessed in one sample and it was seen to re-dissolve during the procedure, then the extraction results can still be considered relevant. Previous studies have shown that the formation of gypsum in the mining processes can happen in the environmental conditions. (30)

Figure 73 gives an example the effect of the sequential extractions on the R-E-1 enrichment sand sample and shows the major dissolving phases in the extraction procedure.

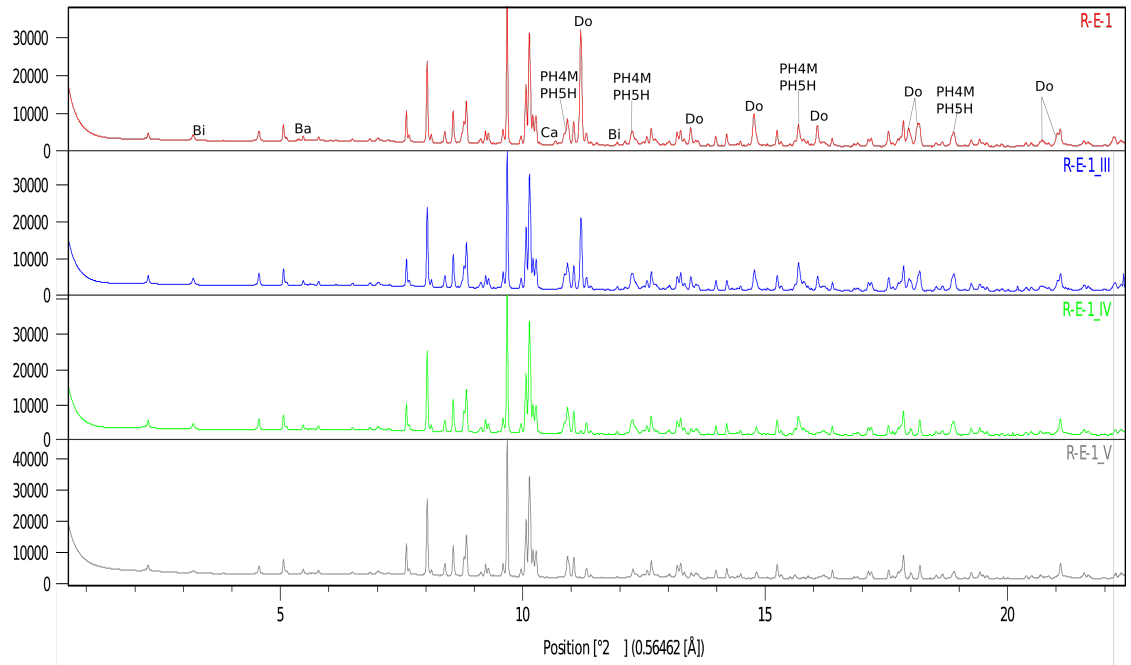

Figure 73. SR-XRPD spectra giving an example of the effect of the third, fourth and fifth extraction fractions on the sample R-E-1. Major visible dissolving phases have been market on the bulk sample. Abbreviations: Bi = biotite, Ba = bassanite, Ca = calcite, PH4M = pyrrhotite (Fe_7S_8), PH5H = pyrrhotite (Fe_9S_{10}), Do = dolomite, R-E = Rautuvaara enrichment sand, III = mild acid-soluble fraction (pH 4.1), IV = reducible fraction (pH 2.0) and V = oxidizable fraction (pH 1.5).

The unaffected mineral phases in the sequential extraction test were dravite ($NaMg_3Al_6Si_6O_{18}(BO_3)_3(OH)_3OH$), clinochlore ($Mg_5Al(AlSi_3O_{10})(OH)_8$), quartz ($SiO_2$), rutile ($TiO_2$), albite ($NaAlSi_3O_8$), goethite (FeOOH), diopside ($MgCaSi_2O_6$) and grunerite ($Fe_7Si_8O_{22}(OH)_2$).

The SR-XRPD results show that a detailed mineralogical study can provide useful information of the used sequential extraction procedure and improve the accuracy and quality of the made geochemical interpretations.

13. Conclusions

The tailings at the old Rautuvaara mining area consists of used enrichment sand, which is known to be AMD producing. The occurrence, mobility and bioavailabity of base metals Mn, Fe, Co, Ni, Cu, Zn, potentially harmful elements Cr, As, Cd and Pb and radioactive elements U and Th was studied in order to assess the risk they might pose to the surrounding area. The applied methods consisted of gamma spectrometry and acid digestion in order to determine the total concentration of elements, ICP-MS to measure the metal concentrations in the liquid samples, sequential extractions to evaluate the possibly mobility of elements from the different sample matrixes and SR-XRPD to assess the mineralogical information of the enrichment sand samples and the dissolving and precipitating mineral phases during the extractions.

Several water samples were collected from the Rautuvaara mining area and its surroundings and the values were compared to the reference water collected upstream from the mining area. The water samples collected downstream from the Niesa river showed slightly elevated concentrations of base metals, which were seen to gradually decrease as the distance from the mining area increased. The water samples collected from the settling pond and water reservoir resembled those of the reference water. The highest concentrations of metals were seen in the acidic pond (pH < 3), where the concentration of U was over thousand times higher than in the reference water sample and it greatly exceeds the average concentration of U in the Finland's ground water.

The total concentrations of radionuclides ^{238}U, ^{226}Ra, ^{210}Pb and ^{232}Th/^{228}Ra were measured with gamma ray spectrometry and the results showed that the highest activity concentrations of ^{238}U, ^{226}Ra and ^{210}Pb were found in the sediment samples. The highest activity concentration of ^{232}Th/^{228}Ra was found in the waste rock. The concentration of ^{238}U in the sediment was seen to be six times higher than the average in Finnish soil. Also the activity of ^{238}U and ^{210}Pb was highest in the top sediment layer and decreased in the deeper in the core layers.

The total concentrations of metals and radioactive elements was assessed with microwave assisted acid digestion and measuring the acquired supernatants with ICP-MS. The results showed that the levels of Cd, Cr, Pb and Zn followed the naturally occurring levels in Finland. The concentration of As and Ni exceeded the screening levels set for industrial

estate indicating soil contamination in the enrichment sand and sediment. Also the concentrations of Cu were over the set levels in all the sample types.

Measuring the total concentrations of metals and radionuclides in solid sample materials is not enough to understand the mobility and bioavailability of different elements and for this purpose a six step sequential extraction protocol was applied for the solid sample materials. The sequential extraction procedure showed that a major amount of the metals and radionuclides were leached in the strong acid-soluble fraction with nitric acid (pH 0). This step is designed to leach out the metals that are tightly bound to the sample matrix e.g. associated in the mineral lattice. In natural conditions similar to the strong acid-soluble step are unlikely to occur and the metals leached out only in this fraction pose a minor risk to the surrounding environment. Although, it is important to notice that Mikutta et al. (89) proved that the use of H_2O_2 in the second last extraction fraction only allows partial dissolution of the dissolving matter, which may lead to an overestimations of leached metals in the strong acid-soluble fraction.

During the extractions, U started to leach out in the mild acid-soluble fraction when the pH decresed and it continued to do so in every following leach step. Approximately 30 % of U was leached out in this step from the enrichment sand and 60 % from the acidic pond sand and sediment. Th was seen to be tightly bound in all the sample matrixes since it did not dissolve before the strong acid-soluble fraction. These results are in agreement with previous studies made by Virtanen et al. (88) and Skipperud et al. (15).

The sequential extraction test showed that the mobilization between the enrichment sand and acidic pond sand had been altered, possibly as an effect of AMD. The acidic pond sand had elements in more mobile forms than the enrichment sand and the total concentrations of metals in acidic pond sand had dramatically decreased, implying that a large amount of elements had already been mobilized from it.

The mild acid-soluble fraction, in this study, was leached out at a pH of 4.1 and this fraction represents metals that become soluble as the pH of the solution decreases. The measured pH's in the enrichment sand, acidic pond sand and sediment are 6.9, 4.1 and 6.5, respectively. The pH in the acidic pond sand had decreased as a result of AMD and it resembles that of the mild acid-soluble fraction. This suggests that all the elements that become mobile in the mild acid-soluble fraction also become mobile in the tailings as the pH decreases when the AMD continues overtime.

An environmental risk assessment was done according to the sequential extraction results and it showed that in general the potentially harmful elements Co, Cr, Cd, Pb and U had a higher risk of mobilization from the acidic pond sand than from the enrichment sand. The elements in the sediment were also seen to have a medium or high risk of mobilization.

The mineralogy of the Rautuvaara enrichment sand and the precipitating and dissolving metal phases during the sequential extractions were studied using the SR-XRPD method. The main minerals in the enrichment sand were albite, dolomite, quartz, clicochlore and biotite. During the sequential extractions the complete dissolution of bassanite, dolomite and calcite was witnessed and a partial dissolution of talc, pyrrhotite, pyrite, tremolite, biotite, ilmenite, magnetite and marialite. The unaffected mineral phases were dravite, clinochlore, quartz, rutile, goethite, diopside and grunerite. Gypsum was seen to form as a secondary mineral during the extraction protocol and it was concluded that this may lead to underestimations of the leached extraction concentrations, since the already dissolved elements may co-precipitate with gypsum and are not witnessed before gypsum is again dissolved later in the leach test. The gypsum formation was only seen in one of the samples and so the sequential extraction results can be considered to be acceptable. Although, it should be kept in mind that the leached concentrations in the first four extraction steps may be underestimates if the formation of gypsum as a secondary mineral does not occur in the Rautuvaara tailings as it did during the extractions protocol in the laboratory.

The U rich layer in the enrichment sand from Juomasuo was not seen in the samples, but it should be noted that if it is located in the area affected by AMD then the lowered pH would over time increase the mobility of U, leading into increased concentrations in the seepage waters and eventually in the surrounding environment.

Overall, it can be concluded that the locally high levels of elements and their increased mobility as a results of AMD could pose a possible threat to the environment and ecosystem surrounding the old Rautuvaara mining area. The on-going AMD formation should be taken into consideration when planning the rehabilitation measures in the future, or if the use of the old tailings area continues.

Bibliography

1. Lehto, J., Hou, X. *Chemistry and Analysis of Radionuclides.* 1st edition, 2011: Wiley-VCH: 978-3-527-32658-7.

2. Choppin, G., Liljenzin, J-O., Rydberg, J., Ekberg, C. *Radiochemistry and Nuclear Chemistry.* 4th edition: Academic Press - Elsevier, 2013. https://doi.org/10.1016/B978-0-12-405897-2.01001-6.

3. Atlas of Eh - pH -diagrams – website. Cited: 20 10 2017. http://www.eosremediation.com/download/Chemistry/Chemical%20Properties/Eh_pH_Diagrams.pdf, Assessed: 30.04.2018.

4. Vesterbacka, P. U-238 -series radionuclides in finnish groundwater-based drinking water and effective doses. *Academic dissertation.* University of Helsinki – Department of Chemistry – Laboratory of radiochemistry, 2005.

5. Crancon, P., Van Der Lee, J. Speciation and mobility of uranium(VI) in humic-containing soils (2003) *Radiochim. Acta* 91 pp. 673-679.

6. Erden, K. E., Donat, R. Removal of thorium(IV) species from aqueous solutions by natural sepiolite (2016) *Radiochimica Acta* 105

7. Virtanen, Sinikka. *Luonnon radionuklidien fraktiointi vaiheittaisten uuttojen avulla maaperä- ja sedimenttinäytteistä – master's thesis.* University of Helsinki – Department of chemistry – Laboratory of radiochemistry, 2011.

8. International Atomic Energy Agency (IAEA) *Technical reports series no. 476: The environmental Behaviour of Radium: Revised Edition*, 2014. STI/DOC/010/476.

9. Vesterbacka, P., Ikäheimo, T.K. Optimization of Pb-210 determination via spontaneous deposition of Po-210 on a silver disk. (2005) *Analytica Chimica Acta* **545** pp. 252-261.

10. Söderlund, M.J. *Sorption and speciation of radionuclides in boreal forest soil - Academic dissertation.* University of Helsinki – Department of chemistry - Laboratory of radiochemistry, 2016.

11. Salbu, B., Fractionation of radionuclide species in the environment.(2009*) Journal of Environmental radioactivity* **100** pp. 283-289.

12. Skipperud, L., Salbu, B. Radionuclides: sources, speciation, transfer and impacts in the aquatic and terrestrial environment, In: Dominick DellaSala Michael Goldstein (Eds), Encyclopaedia of the Anthropocene, Elsevier, 1st edition, 2017, ISBN: 97800128096659.

13. Favas, P.J.C., Pratas, J., Gomes M.E P., Cala, V. Selective chemical extraction of heavy metals in tailings and soils contaminated by mining activity: Environmental implications (2011) *Journal of Geochemical Exploration* **111** pp. 160-171.

14. Popic, J., Salbu, B., Skipperud, L., Ecological tranfer of radionuclides and metals to free-living earthworm species in natural habitats rich in NORM (2012) *Science of the Total Environment* **414** pp. 167-176.

15. Skipperud, L., Salbu, B. Sequential extraction as a tool for mobility studies of radionuclides and metals in soils and sediments (2015) *Radiochim. Acta* **130** pp. 187-197.

16. Salbu, B., Speciation of radionuclides (16.11.2009) - presentation, Cited: 23 10 2017, http://www.nks.org/download/seminar/2009_radworkshop/NKS-B_RadWorkshop_3.pdf, Assessed: 30.04.2018.

17. Salbu, B., Lind, O.C., Skipperud, L. Radionuclide speciation and its relevance in environmental impact assessments (2004) *Journal of Environmental Radioactivity* **74** pp. 233-242.

18. Salbu, B., Speciation of Radionuclides in the Environment - chapter. In: Meyers R. A. *Encyclopedia of Analytical Chemistry: applications, theory and instrumentation.* 1st edition: Wiley, 2000.

19. Surface Science Western. Scanning Electron Microscopy coupled with Energy Dispersive X-ray (SEM/EDX) Spectroscopy - website. http://www.surfacesciencewestern.com/analytical-services/scanning-electron-microscopy-coupled-with-energy-dispersive-x-ray-semedx-spectroscopy/, Cited: 26 03 2018., Assessed: 30.04.2018.

20. International Atomic Energy Agency. Naturally Occurring Radioactive Material (NORM V), IAEA publications 2007, Cited: 25 10 2017, http://www-pub.iaea.org/MTCD/Publications/PDF/Pub1326_web.pdf, Assessed: 30.04.2018.

21. IAEA *Technical Reports Series No. 419: Extent of environmental contamination by naturally occurring radioactive material (NORM) and technological options for mitigation*, 2003. ISBN 92–0–112503–8.

22. IAEA *Naturally occurring racioactive material -website,* Cited: 26 03 2018, https://www.iaea.org/topics/radiation-safety-norm, Assessed: 30.04.2018.

23. Kathren R.L. NORM Sources and Their Origins (1988) *Appl. Radiot. Isot.* **49** pp. 149-168.

24. European commission: Radiation Protection 135 - Effluent and dose control from European Union NORM industries, Volume 1., 2003. Cited: 25 10 2017, https://ec.europa.eu/energy/sites/ener/files/documents/135.pdf, Assessed: 30.04.2018.

25. Michalik, B., NORM contaminated area identification using radionuclides activity concentration pattern in a soil profile (2017) *Journal of Environmental Radioactivity* **173** pp. 102-111.

26. Michalik, B., NORM impact on the environment: An approach to complete environmental risk assessment using the example of areas contaminated due to mining activity (2008) *Applied Radiation and Isotopes* **66** pp. 1661-1665.

27. International Atomic Energy Agency (IAEA) Radiation protection and safety of radiation sources: International basic safety standards, 2014. Cited: 25 10 2017, http://www-pub.iaea.org/MTCD/Publications/PDF/Pub1578_web-57265295.pdf, Assessed: 30.04.2018.

28. Beddow, H., Black, S., Read, D., Naturally occurring radioactive material (NORM) from a former phosphoric acid processing plant (2006) *Journal of Environmental Radioactivity* **86** pp. 289-321.

29. Paschoa A.S., Potential Environmental and Regulatory Implicatios of Naturally Occurring Radioactive Materials (NORM) (1998) *Appl. Radiat. Isot.* **49** pp. 189-196.

30. Tuovinen, H., Mobilization of natural uranium series radionuclides at three mining sites in finland - *Academic dissertation.* University of Helsinki - Faculty of Science - Department of Chemistry - Laboratory of radiochemistry, 2015.

31. Bhattacharyya, D.K., Issues in the Disporal of Waste Containing Naturally Occurring Radioactive Material (1998) *Appl. Radiat. Isot.* **49** pp. 215-226.

32. Solatie, D., Kallio, A., Vaaramaa, K., Venelampi, E., Kyllönen, J., Roos, P., Nielsen, S., Lauri, L., Holmstrand, M., Popic, J. M., Pettersson, H., Pelkonen, M., Rasilainen, T., Leppänen, A-P., NORM-related Mining in Nordic Countries: Legislation, practices and case studies (2015) Nordic nuclear safety research (NKS) – report.

33. Strømman, G., Rosseland, B.O., Skipperud, L., Burkitbaev, L.M., Uralbekov, B., Heier, L.S., Salbu, B. Uranium activity ratio in water and fish from pit lakes in Kurday, Kazakhstan and Taboshas, Tajikistan (2013) *Journal of Environmental Radioactivity* **123** pp. 71-81.

34. Salbu, B., Burkitbaev, M., Stromman, G., Shishkov, I., Kayukov, P., Uralbekov, B., Rosseland, B.O., Environmental impact assessment of radionuclides and trace elements at the Kurday U mining site, Kazakhstan (2013) *Journal of Environmental Radioactivity* **123** pp. 14-27.

35. Strømman, G., Rosseland, B.O., Skipperud, L., Burkitbaev, L.M., Uralbekov, B., Heier, L.S., Salbu, B. Uranium activity ratio in water and fish from pit lakes in Kurday, Kazakhstan and Taboshas, Tajikistan (2013) *Journal of Environmental Radioactivity* **123** pp. 71-81.

36. Skipperud, L., Jorgensen, A.G., Heier, L.S., Salbu, B., Rosseland, B.O. Po-210 and Pb-210 in water and fish from Taboshar uranium mining Pit Lake, Tajikistan (2013) *Journal of Environmental Radioactivity* **123** pp. 82-89.

37. Sipperud, L., Strømman, G., Yunusov, M., Stegnar, P., Uralbekov, B., Tilloboev, H., Zjazjev, G., Heier, L. S., Rosseland, B. O., Salbu, B. Environmental impact assessment of radionuclide and metal contamination at the former U sites Taboshar and Digmai, Tajikistan (2013) Journal of Environmental Radioactivity **123** pp. 50-62.

38. Popic, J., Salbu, B., Skipperud, L. Assessment of radionuclide and metal contamination in a thorium rick area in Norway (2011) *Journal of Environmental Monitoring* **13** pp. 1730-1738.

39. Leopold, K., Michalik, B., Wiegand, J. Availability of radium isotopes and heavy metals from scales and tailings of Polish hard coal mining (2007) Journal of Environmental radioactivity **94** pp. 137-150.

40. Tuovinen, H., Pohjolainen, E., Vesterbacka, D., Kaksonen, K., Virkanen, J., Solatie, D., Lehto, J., Read, D. Release of Radionuclides from Waste Rock and Tailings at a former pilot Uranium mine in Eastern Finland (2015) *BOREAL ENVIRONMENT RESEARCH* **21** pp. 471-480.

41. Salbu, B. Challenges in radioecology (2009) Journal of Environmental Radioactivity **100** pp. 1086-1091.

42. Storer, J.B., Harris, P.S., Furchner, J. E., Langham, W.H. The Relative Biological Effectiveness of Various Ionizing Radiations in Mammalian Systems (1957) *Radiation Research* **6** pp. 188-288.

43. World Health Organization (WHO): *Guidelines for Drinking-water quality -report,* 2011.

44. Hooda, P.S., *Trace elements in Soils,* Blackwell Publishing Ltd., 2010. pp. 3-7.

45. Okoro, H.K., Fatoki, O.S., Adekola, F.A., Bhekumusa, J.X., Snyman, R.G. A Review of Sequential Extraction Procedures for Heavy Metals Speciation in Soils and Sediments (2012) Open Access Scientific Reports **1**

46. Niskala, K., Kaivannaisjätealueiden kartoitus - Kartoitusohjeen sekä tietojen saatavuuden arviointi. *Master's thesis.* Lahden ammattikorkeakoulu, 2011.

47. Tessier, A., Campbell, P.G.C., Bisson, M. Sequential extraction procedure for the speciation of particulate trace metals (1979) *Analytical Chemistry* **51** pp. 884-851.

48. Oughton, D.H., Salbu, B., Riise, G., Lien, H., Ostby, G., Noren, A. Radionuclide Mobility and Bioavailability in Norweigian and Soviet Soils. (1992) *ANALYST.* **117**

49. Tuovinen, H., Pelkonen, M., Lempinen, J., Pohjolainen, E., Read, D., Solatie, D., Lehto, J. Behaviour of heavy metals during bioheap leaching at the talvivaara mine, Finland (2017) *Geoscience* **8**, doi:10.3390.

50. Tuovinen, H, Pohjolainen, E., Lempinen, J., Vesterbacka, D., Read, D., Solatie, D., Lehto, J. Behavious of radionuclides during mictobially-induced mining of nickel at Talvivaara, Eastern Finland (2016) *Journal of Environmental radioactivity* **151** pp. 105-113.

51. Gleyzes, C., Tellier, S., Astruc, M. Fractionation studies of trace elements in contaminated soils and sediments: a revier of sequential extraction precedures (2002) *Trends in analytical chemistry* **21**

52. Riise,G., Bjørnstad, H.E., Lien, H.N., Oughton, D.H., Salbu B. A study on radionuclide association with soil components using a sequential extraction procedure (1990) *Journal of Radioanalytical and Nuclear Chemistry* **142** pp. 531-538.

53. Outola, I., Inn, K., Ford, R., Markham, S. & Outola, P. Optimizing standard sequential extraction protocol with lake and ocean sediments (2009) J Radioanal Nucl Chem **282** pp. p. 321-327.

54. *The impact of Pu speciation on distribution coefficients in Mayak soil* s.l. : The Science of the Total Environment, 2000, Vol. 157, pp. 81-93.

55. Skipperud, L., Oughton, D., Salbu, B., Kheboian, C., Bauer, C. F. Accuracy of selective extraction procedures for metal speciation in model aquatic sediments (1987) *Anal. Chem* **59** pp. 1417-1423.

56. Martin, N., Schuster, I., Peiffer, St., Two experimental methods to determine the speciation of cadmium in sediment from the River Nectar (1996) *Acta Hydrochim Hydrobiol*. **24**

57. Rodriguez, L., Ruiz, E., Alonso-Azcarate, J., Rincon, J. Heavy metal distribution and chemical speciation in tailings and soils around a Pc-Zn mine in Spain (2009) *Journal of Environmental management* **90** pp. 1106-1116.

58. Närhi, P., Räisänen, M. L., Sutinen, M-L., Sutinen, R. Effect of tailings on wetland vegetation in Rautuvaara, a former iron-copper mining area in northern Finland (2012) *Journal of Geochemical Exploration* **116-117** pp. 60-65.

59. Savolainen, T. A hydrogeological and environmental study of the Niesajokivalley in Rautuvaara, Kolari and its suitability as a future tailings disposal area. *Master's thesis.* University of Helsinki - Faculty of Science - Department of Geosciences and Geography, 2013.

60. Pöyry Finland Oy. *Hannukainen Mining Oy: Hannukaisen kaivoksen ympäristölupahakemus.* 2016.

61. Räisänen, M. L., Väisänen, U., Lanne, E., Turunen, P., Väänänen, J. Rautuvaaran suljetun kaivoksen rikastushiekan jätealueen kemiallinen nykytila, vaikutukset pinta ja pohjavesiin vuosina 2005-2006 sekä suositukset jälkihoidolle, Geologian tutkimuskeskus - Pohjois-Suomen yksikkö & Itä-Suomen yksikkö, 2015. Arkistoraportti 64/2015.

62. Pöyry Finland Oy. *Hannukaisen kaivoshanke: Kaivannaisjätteen jätehuoltosuunnitelma.* 2015.

63. Howett, P.J, Salonen, V-P., Hyttinen, O., Korkka-Niemi, K., Moreau, J. A hydrostratigraphical approach to support environmentally safe siting of a mining waste facility at Rautuvaara, Finland (2015) *Bulletin of the Geological Society of Finland* **87** pp. 51-66.

64. Akcil, A., Koldas, S. Acid Mine Drainage (AMD): causes, treatment and case studies (2006) *Journal of Cleaner Production* **14** pp. 1139-1145.

65. Maanmittauslaitos. *Karttapaikka - website.* Cited: 07 06 2017. http://www.maanmittauslaitos.fi/asioi-verkossa/karttapaikka, Assessed: 30.04.2018.

66. Säteilyturvakeskus (STUK). Maaperä- ja sedimenttinäytteiden esikäsittely. *Ohje VALO 4.4.6.4.,* 2011.

67. ISO 10390. *International Organization for Standardization.* Cited: 16 06 2017.] https://www.iso.org/standard/40879.html, Assessed: 30.04.2018.

68. Säteilyturvakeskus (STUK). Ympäristönäytteiden märkäpoltto MARS-5 -mikroaaltouunipolttolaitteella. *Ohje VALO 4.6.5.1B.* 2016.

69. Gaines, P.R. ICP Operations Guide - A Guide for using ICP-OES and ICP-MS. *Instrument Solutions Benelux B.V. - website* Cited: 13 09 2017, https://www.instrument-solutions.com/wp-content/uploads/ICP-Operations-Guide.pdf, Assessed: 30.04.2018.

70. Tuovinen, H., Vesterbacka, D., Pohjolainen, E., Read, D., Solatie, D., Lehto, J. A comparison of analytical methods for determining uranium and thorium in ores and mill tailings (2015) *Journal of Geochemical Exploration* **148** pp. 174-180.

71. Lehto, J. Basics of nuclear physics and of radiation detection and measurement. *An open-access textbook for nuclear and radiochemistry students.* Laboratory of Radiochemistry - Department of Chemistry - University of Helsinki, 2015.

72. Read D., Read G. D., Thorne M.C. Background in the contect of land contaminated with naturally occurring radioactive material (2013) *Journal of Radiological Protection* **33** pp. 367-380.

73. Guidotti, L., Carina, F., Rossi, R., Gatti, M., Cenci, R.M., Beone, G.M. Gamma-spectrometric measurement of radioactivity in agricultural soils of the Lombardia region, northern Italy (2015) *Journal of Environmental Radioactivity* **142** pp. 36-44.

74. Virkanen, J., Reijola, H., Vaahtojärvi, T. Geotieteiden ja maantieteen laitoksen ympäristölaboratorion toimintakäsikirja 24.10.2014, University of Helsinki, 2014.

75. Virkanen, J. ICP-MS -analyysi geologisessa ja maantieteellisessä tutkimuksessa (2007) *TERRA* **119** 2

76. The principles of ICP-MS – webpage, Cited: 13 10 2017, http://www.agilent.com/cs/Satellite?assettype=GSA_C&assetid=1404943730259&d=&formassembly=false&pagename=Agilent/GSA_C/GenericInnerTemplateWithFourZones_New, Assessed: 30.04.2018.

77. Dams, R.F.J., Goossens, J., Moens, L. Spectral and Non-Spectral Interferences in Inductively Coupled Plasma Mass-Spectrometry (1995) *Mikrochim. Acta* **119** pp. 227-286.

78. University of Missouri Research Reactor Center. ICP-MS - Comparison of Techniques: High-Resolution -website, Cited:30.04.2018, http://www.murr.missouri.edu/ps_analytical_ICP_comparison_highres.php, Assessed: 30.04.2018.

79. Jenkins, R. X-ray techniques: Overview. *Encyclopedia of Analytical Chemistry,* 2006.

80. Brouwer, P. Theory of XRF. *PANanalytical – website,* Cited: 22 01 2018, https://www.chem.bg.ac.rs/~grzetic/predavanja/Nedestruktivna%20hemijska%20analiza%20-%20odabrana%20poglavlja/XRF/Literature/PANanalytical%20XRF%20theory.pdf, Assessed: 30.04.2018.

81. Heikkilä, P., Reijola, H., Ruth, O., Virkanen, J. Geotieteiden ja maantieteen laitoksen geokemian laboratorion toimintakäsikirja 29.10.2009, Cited: 22.01.2018. http://www.helsinki.fi/geo/files/labrojen_toimintakasikirja.pdf, Assessed: 30.04.2018.

82. Gozzo. F., Synchrotron X-ray powder diffraction. In: U., Shankland, K., Meshi, L., Avilov, A., David, W.I.F Kolb. *Uniting Electron Crystallography and Powder Diffraction, NATO Science for Peace and Security Series B. Physics and Biophysics,* Springer, Dordrecht, pp. 65-83.

83. Sarrazin, P., Chipera, S., Bish, D., Blake, D., and Vaniman, D.Vibrating sample holder for XRD analysis with minimal sample preparation (2005) *JCPDS - International Centre for Diffraction Data 2005, Advances in X-ray Analysis*, **48**.

84. Pöyty Finland Oy. *Hannukaisen rautakaivoshanke - Ympäristövaikutusten arviointiohjelma - Northland Mines Oy.* 2010.

85. Suomen ympäristökeskus - Jussi Reinikainen. *Maaperän kynnys- ja ohjearvojen määritysperusteet,* 2007. ISSN 1796-1637.

86. Stumm, W., Morgan, J.J. *Aquatic chemistry: An introduction emphazing chemical equilibria in natura waters. 2nd ed.* New York : John Wiley & Sons, 1981.

87. Tipping, E., Thompson, D.W., Ohnstad, M., Hetherington, N.B. Effect of pH on the release of metals from naturally-occurring oxides of Mn and Fe (1986) *Environ. Technol.Lett.* **7** pp. 109-114.

88. Virtanen, S., Vaaramaa, K., Lehto Fractionation of U, Th, Ra and Pb from boreal forest soils by sequential extractions (2013) Applied geochemistry **38** pp. 1-9.

89. Mikutta, R., Kleber, M., Kaiser, K., Jahn, R. Review: organic matter removal from soils using hydrogen peroxide, sodium hypochlorite, and disodium peroxidisulfate (2005) Soil Science Society of America Journal **69** pp. 120-135.

90. Kabata-Pendias, A. *Trace Elements in Soils and Plants, fourth ed.* Boca Raton, Florida, USA : CRC PRESS, 2010.

91. Arenas-Lago, D., Andrade, M., Lago-Vila, M.L., Rodriguez-Seijo, A., Vega, F.A. Sequential extraction of heavy metals in soils from a copper mine: Distribution in geochemical fractions (2014) Geoderma **230-231** pp. 108-118.

92. McBride. *Environmental Chemistry of Soil.* New York : Oxford university press, 1994. p. 406.

93. Dzombak, D.A., Morel, F.M.M. *Surface Complexation Modeling: Hydrous Ferric Oxide.* New York : John Wiley and sons, 1990.

94. Blanchard, M., Alfredsson, M., Brodholt, J., Wright, K., Catlow, C.R.A. Arsenic incorporation into FeS2 pyrite and its influence on dissolution: A DFT Study (2007) *Geochimica et Cosmochimica* **71** pp. 624-630.

95. Cheng, H., Lu, C., Liu, J., Yan, Y., Han, X., Jin, H., Wang, Y., Liu, Y., Wu, C. Synchrotron radiation X-ray powder diffraction techniques applied in hydrogen storage materials - A review (2017) *Progress in Natural Science: Materials International* **27** pp. 66-73.

96. Dold, B., Speciation of the most soluble phases in a sequential extraction procedure adapted for geochemical studies of copper sulfide mine waste (2003) *Journal of Geochemical Exploration* **80** pp. 55-68.

97. Heinänen, K. *Kupari-Rautuvaaran malmin mineraloginen tutkimus,* Rautaruukki Oy:n raportit, 1976.

98. Rankama, K., Sahama, Th.G. *Geochemistry*, University of Chicago Press, 1955.

99. Brandt, F., Bosbach, D. Bassanite (CaSO4*0.5H2O) dissolution and gypsum (CaSO4*2H2O) precipitation in the presence of cellulose ethers (2001) Journal of Crystal **233** pp. 837-845.

100. Bouchelaghem, F. A numerical and analytical study on calcite dissolution and gypsum precipitation (2010) Applied mathematical modelling **34** pp. 467-480.

101. Blowes, D.W., Ptacek, C.J., Jambor, J.L., Weisener, C.G., Paktunc, D., Gould, W.D., Johnson, D.B. 11.5 The Geology of Acid Mine Drainage. *Treatise on Geochemistry 2nd edition.* s.l. : Elsevier Science, 2013.

102. United Nations Scientific Committee on the Effects of Atomic Radiation. *UNSCEAR 2000 Report to the General Assembly, with Scientific Annexes: Sources and Effects of Ionizing Radiation.* New york : United Nations, 2000.

Appendix A

Appendix 1. Acid digestion by MARS 5: quantities of digested and undigested samples. (R-E = Rautuvaara enrichment sand, R-S = Rautuvaara Sediment / Acidic pond sand, R-R = Rautuvaara waste rock, No. = sampling location, A/B = duplicates)

Sample	Weight (g)	Undigested residue (g)	Undigested residue (%)	Digested sample (%)
R-E-1	1,508	1,037	68,8	31,2
R-E-2	1,543	0,899	58,3	41,7
R-E-3	1,508	0,827	54,8	45,2
R-E-4	1,529	0,844	55,2	44,8
R-E-5	1,516	1,187	78,4	21,6
R-E-6	1,537	1,290	83,9	16,1
R-E-7	1,545	0,897	58,0	42,0
R-E-8	1,517	0,810	53,4	46,6
R-E-9	1,527	0,833	54,6	45,4
R-E-10	1,513	0,809	53,5	46,5
R-E-11	1,541	0,891	57,8	42,2
R-E-12	1,534	0,864	56,3	43,7
R-E-13	1,538	0,837	54,4	45,6
R-E-14	1,586	0,878	55,4	44,6
R-E-15A	1,611	0,879	54,6	45,4
R-E-15B	1,571	0,875	55,7	44,3
R-E-16	1,679	0,932	55,5	44,5
R-S-3	1,545	0,986	63,8	36,2
R-S-4	1,613	1,415	87,8	12,2
R-S-5	1,541	1,127	73,1	26,9
R-S-6	1,588	1,368	86,2	13,8
R-S-7	1,679	1,397	83,2	16,8
R-R-1A	1,580	1,289	81,6	18,4
R-R-1B	1,625	1,135	69,8	30,2

Appendix 2. Activity concentrations of ^{238}U, ^{226}Ra and ^{210}Pb in enrichment sand, acidic pond sand and waste rock samples from Rautuvaara mining area. Results are obtained from gamma measurements and given in Bq kg-1 dry weight.

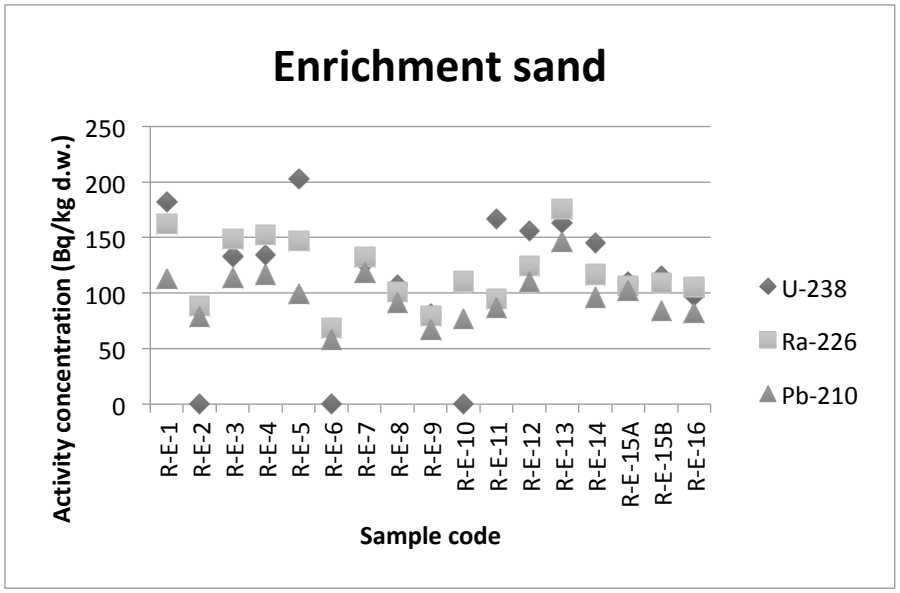

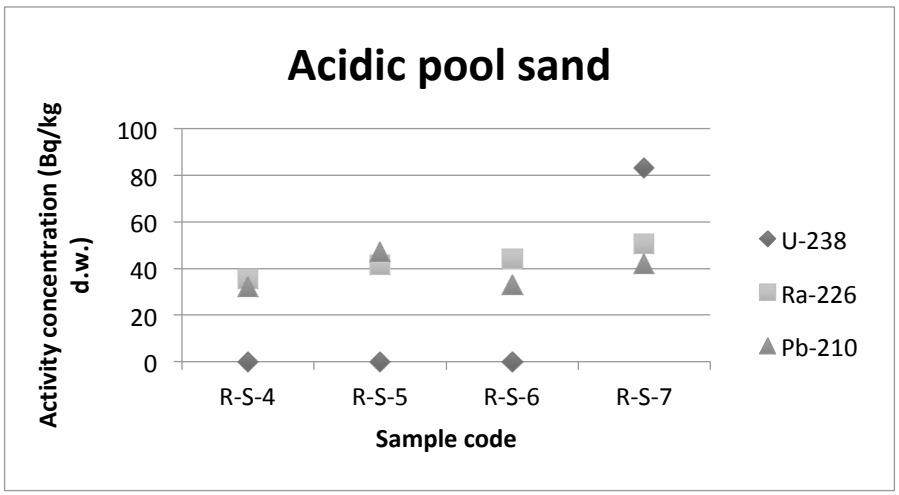

v

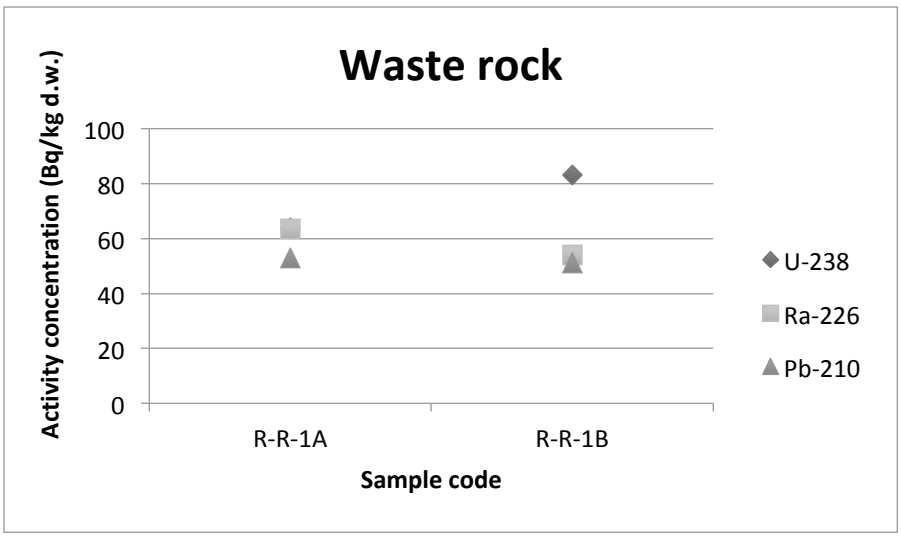

Appendix 3. Concentrations of ^{238}U and ^{232}Th in solid samples collected from Rautuvaara mining area. Results are obtained from gamma measurements and given in Bq kg^{-1} dry weight and in ppm.

Sample	Activity (Bq / kg d.w.) ± Unc. (Bq / kg d.w.)				Concentration (ppm) ± Unc.(ppm)	
	U-238	**Ra-226**	**Pb-210**	**Th-232/ Ra-228**	**U-238**	**Th-232**
R-S-1	513 82	244 14	747 56	25 4	42 7	6 1
R-S-2	371 53	285 15	495 25	32 3	30 4	8 1
R-S-3	209 17	239 9	184 26	28 2	17 1	7 1
R-S-4	< 31,708 -	36 2	32 6	9 1	- -	2 0,2
R-S-5	< 38,878 -	42 2	47 4	11 1	- -	3 0,2
R-S-6	< 42,519 -	44 2	33 3	12 1	- -	3 0,2
R-S-7	83 17	51 3	42 4	15 2	7 1	4 0,4
R-E-1	182 37	163 8	113 7	13 2	15 3	3 0
R-E-2	< 70,853 -	88 6	79 4	13 1	- -	3 0
R-E-3	133 34	148 8	114 7	18 2	11 3	4 1
R-E-4	135 15	152 8	117 10	16 1	11 1	4 0
R-E-5	203 38	147 8	99 6	19 2	16 3	5 1
R-E-6	< 77,592 -	69 4	58 11	14 2	- -	3 0
R-E-7	127 21	132 7	118 9	18 2	10 2	4 0
R-E-8	107 22	101 6	91 7	16 2	9 2	4 0
R-E-9	81 21	79 4	67 5	10 1	7 2	2 0
R-E-10	< 141,29 -	111 6	77 5	8 2	- -	2 0
R-E-11	167 25	95 5	87 7	16 2	14 2	4 0
R-E-12	156 16	125 7	110 9	17 1	13 1	4 0
R-E-13	163 24	176 11	146 26	15 2	13 2	4 0
R-E-14	145 29	117 6	96 6	8 1	12 2	2 0
R-E-15A	110 22	106 6	102 8	9 1	9 2	2 0
R-E-15B	115 30	110 6	84 5	11 2	9 2	3 0
R-E-16	97 22	106 5	82 9	16 2	8 2	4 0
R-R-1A	64 20	63 4	53 10	43 4	5 2	11 1
R-R-1B	83 20	54 3	51 5	43 3	7 2	11 1

Appendix 4. Measured ICP-MS data for water samples collected from Rautuvaara mining area and its surroundings. Sampling locations for water samples are presented in figures 20, 21, 22 and 23.

Reference water samples (R-E-15A/B/C/D)			**Downstream water sample (R-W-7A/B)**		
	Measured (ppb)	stdev		Measured (ppb)	stdev
Cr	13	12	Cr	10,7	4,4
Mn	5	2	Mn	89,4	1,2
Fe	311	126	Fe	466,1	24,4
Co	0,4	0,2	Co	3,1	0,1
Ni	12	10	Ni	21,2	0,8
Cu	1	-	Cu	5,9	0,2
Zn	7	2	Zn	10,1	0,2
As	4	2	As	0,5	0,04
Cd	0,01	0,004	Cd	0,01	0,001
Pb	3	6	Pb	0,3	0,3
Th	0,01	0,001	Th	0,01	0,0001
U	0,06	0,01	U	0,1	0,0
Settling pond water samples (R-E-1A/B … R-E-6A/B)			**Downstream water sample (R-W-14A/B)**		
	Measured (ppb)	stdev		Measured (ppb)	stdev
Cr	6,0	5,4	Cr	7,6	1,9
Mn	2,6	2,0	Mn	87,0	1,2
Fe	76,2	73,9	Fe	263,1	8,6
Co	0,2	0,2	Co	0,7	0,01
Ni	13,3	6,9	Ni	8,7	1,3
Cu	1,5	0,2	Cu	3,1	0,05
Zn	6,0	0,6	Zn	6,7	0,3
As	4,7	1,2	As	0,3	0,0005
Cd	0,004	0,0005	Cd	0,004	0,001
Pb	1,0	0,5	Pb	0,03	-
Th	LOD	-	Th	0,01	0,001
U	2,6	0,2	U	0,2	0,004

LOD = below the detection limit.

Appendix 5. Measured ICP-MS data for water samples collected from Rautuvaara mining area and its surroundings. Sampling locations for water samples are presented in figures 20, 21, 22 and 23.

Acidic pond water samples (R-W-8A/B … R-W-11A/B)		
	Measured (ppb)	stdev
Cr	8	3
Mn	44449	628
Fe	151848	2351
Co	3210	79
Ni	772	21
Cu	3745	100
Zn	367	9
As	3	0,2
Cd	1	0,03
Pb	1	0,3
Th	3	0,2
U	77	0,2

Water reservoir – Next to the dam (R-W-12A/B … R-W-13A/B)		
	Measured (ppb)	stdev
Cr	2,0	0,8
Mn	1131,5	31,1
Fe	229,1	29,1
Co	30,7	3,8
Ni	17,0	0,4
Cu	21,4	1,8
Zn	11,0	0,3
As	0,3	0,02
Cd	0,01	0,004
Pb	0,04	0,01
Th	0,01	0,004
U	0,4	0,2

Water reservoir – Next to waste rock (R-W-16A/B)		
	Measured (ppb)	stdev
Cr	3,0	3,1
Mn	769,1	8,4
Fe	70,4	44,7
Co	10,2	0,2
Ni	13,2	3,5
Cu	8,5	0,5
Zn	10,6	2,1
As	0,2	0,03
Cd	0,01	0,0002
Pb	0,6	0,8
Th	LOD	-
U	0,1	0,0

LOD = below the detection limit.

Appendix 6. Total concentrations (ppm) of metals (Cr, Mn, Fe, Co, Ni and Cu) in solid samples taken from Rautuvaara tailings acquired from acid digestion. Concentrations are mean values of three samples and the uncertainty is their standard deviation.

(R = Rautuvaara /Rock, W = Water, E = Enrichment sand, S = Sand / Sediment, A/B = Dublicates, No. = Sampling location)

Concentration (ppm)	**Cr**	**Mn**	**Fe**	**Co**	**Ni**	**Cu**
R-E-1	146 ± 6	977 ± 37	63893 ± 2065	88 ± 3	330 ± 12	241 ± 10
R-E-2	90 ± 3	986 ± 29	64949 ± 2525	92 ± 3	379 ± 11	281 ± 10
R-E-3	111 ± 2	1204 ± 27	60702 ± 1131	140 ± 4	372 ± 8	214 ± 3
R-E-4	84 ± 2	1082 ± 8	64715 ± 1003	92 ± 1	318 ± 5	290 ± 9
R-E-5	9 ± 0,4	398 ± 18	73993 ± 5846	19 ± 5	7 ± 0,3	473 ± 49
R-E-6	7 ± 0,1	628 ± 40	46614 ± 1143	15 ± 1	5 ± 0,2	915 ± 112
R-E-7	96 ± 6	884 ± 60	72930 ± 4838	136 ± 12	479 ± 34	225 ± 20
R-E-8	100 ± 6	906 ± 53	67773 ± 4162	127 ± 8	482 ± 30	257 ± 18
R-E-9	101 ± 7	1085 ± 81	74873 ± 5660	162 ± 12	488 ± 38	182 ± 16
R-E-10	145 ± 4	1400 ± 61	58744 ± 2363	97 ± 5	299 ± 12	516 ± 14
R-E-11	96 ± 4	927 ± 46	83581 ± 4222	178 ± 7	665 ± 34	294 ± 13
R-E-12	86 ± 6	942 ± 58	82382 ± 4849	159 ± 11	620 ± 41	268 ± 11
R-E-13	183 ± 6	1084 ± 34	57030 ± 1492	103 ± 3	336 ± 9	304 ± 8
R-E-14	140 ± 5	1110 ± 44	75105 ± 3108	106 ± 4	355 ± 17	495 ± 20
R-E-15A	204 ± 7	987 ± 48	72585 ± 3999	75 ± 4	417 ± 22	285 ± 18
R-E-15B	169 ± 7	915 ± 28	68169 ± 1412	80 ± 1	379 ± 7	227 ± 6
R-E-16	116 ± 3	931 ± 27	91798 ± 3088	119 ± 1	673 ± 14	409 ± 8
R-S-3	139 ± 19	1184 ± 144	78878 ± 8991	152 ± 18	304 ± 43	1193 ± 141
R-S-4	36 ± 7	547 ± 100	39499 ± 7309	17 ± 3	9 ± 2	1360 ± 299
R-S-5	219 ± 11	554 ± 17	87983 ± 4478	21 ± 1	15 ± 0,4	493 ± 19
R-S-6	7 ± 1	654 ± 30	47025 ± 1354	15 ± 1	5 ± 0,3	983 ± 86
R-S-7	12 ± 2	1038 ± 104	56721 ± 5881	45 ± 3	10 ± 1	1042 ± 178
R-R-1A	147 ± 2	124 ± 1	46947 ± 1182	15 ± 0,3	20 ± 0,5	158 ± 5
R-R-1B	62 ± 2	155 ± 3	45387 ± 2143	18 ± 0,3	25 ± 0,3	244 ± 5

Appendix 7. Total concentrations (ppm) of metals (Zn, As, Cd and Pb) and radionuclides (^{238}U and ^{232}Th) in solid samples taken from Rautuvaara tailings acquired from acid digestion. Concentrations are mean values of three samples and the uncertainty is their standard deviation.

(R = Rautuvaara /Rock, W = Water, E = Enrichment sand, S = Sand / Sediment, A/B = Dublicates, No. = Sampling location)

Concentration (ppm)	**Zn**	**As**	**Cd**	**Pb**	**Th**	**U**
R-E-1	27 ± 7	193 ± 7	0,1 ± 0,01	7 ± 1,2	3 ± 1	12 ± 4
R-E-2	36 ± 5	236 ± 11	0,1 ± 0,02	5 ± 0,4	2 ± 0,04	6 ± 0,5
R-E-3	33 ± 27	396 ± 12	0,02 ± 0,01	8 ± 0,6	3 ± 0,2	11 ± 1
R-E-4	48 ± 6	201 ± 6	0,2 ± 0,03	7 ± 0,2	3 ± 0,1	10 ± 0,1
R-E-5	30 ± 41	16 ± 1	LOD	6 ± 1	2 ± 0,1	2 ± 0,1
R-E-6	14 ± 12	15 ± 0,4	LOD	5 ± 1	2 ± 0,1	1 ± 0,04
R-E-7	25 ± 14	315 ± 33	0,01 ± 0,01	5 ± 1	3 ± 0,3	10 ± 1
R-E-8	21 ± 3	347 ± 23	0,03 ± 0,01	6 ± 0,1	3 ± 0,1	10 ± 1
R-E-9	7 ± 0	424 ± 33	LOD	3 ± 0,4	2 ± 0,1	6 ± 1
R-E-10	13 ± 0,4	283 ± 18	LOD	5 ± 0,3	2 ± 0,2	6 ± 1
R-E-11	19 ± 3	486 ± 20	0,02 ± 0,02	6 ± 0,2	3 ± 0,1	8 ± 0,2
R-E-12	6 ± 0	339 ± 12	LOD	8 ± 1	3 ± 0,2	11 ± 1
R-E-13	17 ± 6	257 ± 8	0,003 ± 0,004	7 ± 0,4	3 ± 0,2	12 ± 0,4
R-E-14	131 ± 8	381 ± 10	0,6 ± 0,05	13 ± 1	1 ± 0,04	9 ± 1
R-E-15A	57 ± 7	221 ± 12	0,2 ± 0,02	8 ± 1	1 ± 0,1	8 ± 0,3
R-E-15B	41 ± 2	224 ± 5	0,1 ± 0,03	6 ± 1	2 ± 0,1	8 ± 0,6
R-E-16	39 ± 5	211 ± 14	0,1 ± 0,01	8 ± 1	2 ± 0,1	8 ± 0,2
R-S-3	200 ± 31	140 ± 22	1 ± 0	27 ± 5	9 ± 1	23 ± 3
R-S-4	3 ± 2	7 ± 2	LOD	3 ± 1	2 ± 0,3	1 ± 0,4
R-S-5	4 ± 1	16 ± 1	LOD	5 ± 0,3	2 ± 0,04	3 ± 0,1
R-S-6	2 ± 0	16 ± 0,1	LOD	5 ± 0,2	2 ± 0,1	1 ± 0,03
R-S-7	6 ± 3	16 ± 0,2	LOD	6 ± 1	3 ± 0,3	5 ± 1
R-R-1A	6 ± 0,3	0,5 ± 0,2	LOD	3 ± 0,1	12 ± 0,5	4 ± 0,1
R-R-1B	14 ± 4	0,4 ± 0,2	LOD	2 ± 1	10 ± 0,4	4 ± 0,2

LOD = below the detection limit.

Appendix 8. Comparison of total concentrations of metals (ppm) acquired from acid digestion to those from sequential extraction steps for Cr, Mn, Ni, Cu, Cd and Pb. Concentrations for acid digestion are mean of three samples. Concentrations for combined sequential extraction steps are means of all the samples in different sample type. (MARS = Acid digestion, I – VI = Combined concentration from sequential leach tests)

	Cr			**Mn**		
	MARS	I – VI	Difference (%)	MARS	I – VI	Difference (%)
Enrichment sand	111	104	7	967	947	2
Sediment	139	92	52	1184	935	27
Acid pool sand	69	11	515	698	495	41
Waste rock	105	19	458	140	115	22
	Ni			**Cu**		
	MARS	I – VI	Difference (%)	MARS	I – VI	Difference (%)
Enrichment sand	388	462	19	346	298	16
Sediment	304	273	11	1193	1131	5
Acid pool sand	10	5	95	969	602	61
Waste rock	23	19	23	201	172	17
	Cd			**Pb**		
	MARS	I – VI	Difference (%)	MARS	I – VI	Difference (%)
Enrichment sand	0.1	0.2	86	7	12	75
Sediment	1	1	21	27	25	8
Acid pool sand	LOD	0.1	-	5	6	22
Waste rock	LOD	0.1	-	3	5	80

LOD = Below the detection limit

Appendix 9. Comparison of total concentrations of metals (ppm) acquired from acid digestion to those from sequential extraction steps for Fe, Co, Zn, As, Th and U. Concentrations for acid digestion are mean of three samples. Concentrations for combined sequential extraction steps are means of all the samples in different sample type. (MARS = Acid digestion, I – VI = Combined concentration from sequential leach tests)

	Fe			**Co**		
	MARS	I – VI	Difference (%)	MARS	I – VI	Difference (%)
Enrichment sand	69402	70284	1	105	122	16
Sediment	78878	61700	28	152	138	10
Acid pool sand	57807	33013	75	24	23	6
Waste rock	46167	24652	87	16	15	6
	Zn			**As**		
	MARS	I – VI	Difference (%)	MARS	I – VI	Difference (%)
Enrichment sand	33	88	166	267	289	8
Sediment	200	198	1	140	106	32
Acid pool sand	4	28	596	14	12	13
Waste rock	10	26	154	0.4	2	250
	Th			**U**		
	MARS	I – VI	Difference (%)	MARS	I – VI	Difference (%)
Enrichment sand	2.4	1.9	24	8	8	2
Sediment	9	8	17	23	20	16
Acid pool sand	2	2	19	2	2	29
Waste rock	11	10	9	4	3	19

LOD = Below the detection limit

Appendix 10. ICP-MS data of the analytical blank samples in sequential extractions. The given values are mean of all the blank samples. From this a correction to real leached concentrations in sequential extraction was obtained, which was then applied to all analytical results reported. I – VI refer to extraction fractions: I = Exchangeable fraction I; II = Exchangeable fraction II; III = Mild acid-soluble fraction; IV = Reducible fraction; V = Oxidizable fraction; VI = Strong acid-soluble fraction.

	I		**II**		**III**	
Metal	Concentration (ppb)	Stdev	Concentration (ppb)	Stdev	Concentration (ppb)	Stdev
Cr	1.215	0.068	1.179	0.035	1.216	0.029
Mn	0.000	-	0.582	0.067	0.000	-
Fe	1.327	0.564	1.064	0.423	2.756	0.928
Co	0.037	0.000	0.000	-	0.000	-
Ni	0.000	-	0.000	-	0.000	-
Cu	0.393	0.209	0.129	0.042	0.059	0.000
Zn	4.234	4.906	3.263	-	1.059	0.000
As	0.000	-	0.000	-	0.000	-
Cd	0.006	0.001	0.000	-	0.000	-
Pb	0.057	0.028	0.026	0.003	0.020	0.000
Th	0.000	-	0.001	0.000	0.002	0.000
U	0.002	0.000	0.002	0.000	0.002	0.000
	IV		**V**		**VI**	
Metal	Concentration (ppb)	Stdev	Concentration (ppb)	Stdev	Concentration (ppb)	Stdev
Cr	1.204	0.043	1.398	0.052	1.212	0.053
Mn	0.000	-	0.000	-	0.000	-
Fe	2.319	0.832	3.394	2.958	5.187	4.268
Co	0.000	-	0.032	0.000	0.000	-
Ni	0.000	-	0.204	0.102	0.000	-
Cu	0.079	0.000	0.034	0.000	0.000	-
Zn	0.896	0.683	5.440	4.017	9.300	8.633
As	0.000	-	0.052	0.000	0.032	0.021
Cd	0.000	-	0.000	-	0.000	-
Pb	0.040	0.000	0.023	0.000	0.019	0.007
Th	0.000	-	0.000	-	0.010	0.015
U	0.000	-	0.001	0.000	0.004	0.004

Appendix 11. ICP-MS data of the analytical blank samples in acid digestion method. The given values are mean of all the blank samples. From this a correction to real dissolved metal concentrations was obtained and applied to all analytical results reported.

Metal	Mean concentration (ppb)	Stdev
Cr	1.239	0.000
Mn	0.000	-
Fe	0.000	-
Co	0.029	0.010
Ni	0.000	-
Cu	0.182	0.000
Zn	0.000	-
As	0.303	0.083
Cd	0.013	0.005
Pb	0.519	0.077
Th	0.009	0.002
U	0.014	0.001

Appendix 12. The analytical data of the sequential extractions performed for the Rautuvaara enrichment sand measured with ICP-MS. I – VI refer to extraction fractions: I = Exchangeable fraction I; II = Exchangeable fraction II; III = Mild acid-soluble fraction; IV = Reducible fraction; V = Oxidizable fraction; VI = Strong acid-soluble fraction. The error is given as a standard deviation (stdev).

Enrichment sand									
Metal		**Concentration (ppm)**	**Stdev**	**Stdev (%)**	**Metal**		**Concentration (ppm)**	**Stdev**	**Stdev (%)**
Cr	I	154	185	120	**Zn**	I	28275	116580	412
	II	188	479	254		II	332	1232	371
	III	8065	2292	28		III	4759	9077	191
	IV	5263	771	15		IV	8147	13323	164
	V	2525	593	23		V	20206	36856	182
	VI	87370	30207	35		VI	11024	13476	122
Mn	I	19	11	56	**As**	I	262	260	99
	II	36	51	145		II	710	2484	350
	III	364	138	38		III	12744	13238	104
	IV	390	76	19		IV	4061	5307	131
	V	26	26	100		V	3969	4546	115
	VI	112	68	61		VI	267652	100522	38
Fe	I	81	333	412	**Cd**	I	45	46	103
	II	473	1950	412		II	24	17	69
	III	7790	2393	31		III	18	19	104
	IV	7906	1301	16		IV	10	13	131
	V	9930	5193	52		V	91	164	179
	VI	44104	11697	27		VI	45	35	77
Co	I	1691	707	42	**Pb**	I	168	171	102
	II	985	939	95		II	68	100	148
	III	15840	9338	59		III	2803	2214	79
	IV	5883	4111	70		IV	1690	778	46
	V	41859	13528	32		V	4467	14583	326
	VI	55326	27360	49		VI	2635	1405	53
Ni	I	14037	4155	30	**Th**	I	31	41	133
	II	10205	3515	34		II	20	38	190
	III	74290	31842	43		III	244	110	45
	IV	31696	12381	39		IV	148	34	23
	V	185048	110669	60		V	78	34	44
	VI	146272	92244	63		VI	1404	429	31
Cu	I	891	3617	406	**U**	I	267	200	75
	II	1849	2921	158		II	149	163	110
	III	7918	13395	169		III	2344	724	31
	IV	6691	6462	97		IV	1293	640	49
	V	192944	105563	55		V	1062	512	48
	VI	87487	55603	64		VI	2712	825	30

Appendix 13. The analytical data of the sequential extractions performed for the Rautuvaara sediment measured with ICP-MS. I – VI refer to extraction fractions: I = Exchangeable fraction I; II = Exchangeable fraction II; III = Mild acid-soluble fraction; IV = Reducible fraction; V = Oxidizable fraction; VI = Strong acid-soluble fraction. The error is given as a standard deviation (stdev).

Sediment									
Metal		Concentration (ppm)	Stdev	Stdev (%)	Metal		Concentration (ppm)	Stdev	Stdev (%)
Cr	I	63	30	47	Zn	I	920	832	90
	II	47	20	41		II	35144	0	0
	III	10443	125	1		III	36078	920	3
	IV	7767	182	2		IV	15884	2755	17
	V	6054	127	2		V	78037	3816	5
	VI	67428	706	1		VI	31848	14322	45
Mn	I	140	1	1	As	I	351	58	17
	II	38	1	1		II	165	3	2
	III	240	4	2		III	14054	209	1
	IV	174	2	1		IV	7265	64	1
	V	38	0	1		V	4752	179	4
	VI	306	6	2		VI	79199	1001	1
Fe	I	0	-	-	Cd	I	182	2	1
	II	0,5	0,5	97		II	74	2	2
	III	14782	244	2		III	64	10	15
	IV	8318	198	2		IV	17	1	4
	V	5622	43	1		V	337	15	4
	VI	32978	519	2		VI	22	2	8
Co	I	11953	201	2	Pb	I	468	171	37
	II	2004	22	1		II	29	14	47
	III	32789	632	2		III	8050	120	1
	IV	9725	310	3		IV	2916	124	4
	V	71420	1067	1		V	115	19	17
	VI	9740	116	1		VI	13891	160	1
Ni	I	35137	484	1	Th	I	77	7	9
	II	6681	363	5		II	31	0	0
	III	69098	1114	2		III	813	11	1
	IV	21932	1185	5		IV	176	8	5
	V	116014	1166	1		V	940	73	8
	VI	24111	44	0		VI	5487	121	2
Cu	I	2546	65	3	U	I	88	3	3
	II	2106	17	1		II	37	5	14
	III	20067	888	4		III	11338	209	2
	IV	9483	633	7		IV	2521	164	6
	V	1019833	37529	4		V	3162	211	7
	VI	76841	1282	2		VI	2525	36	1

Appendix 14. The analytical data of the sequential extractions performed for the Rautuvaara acidic pond sand measured with ICP-MS. I – VI refer to extraction fractions: I = Exchangeable fraction I; II = Exchangeable fraction II; III = Mild acid-soluble fraction; IV = Reducible fraction; V = Oxidizable fraction; VI = Strong acid-soluble fraction. The error is given as a standard deviation (stdev).

Acidic pond sand									
Metal		**Concentration (ppm)**	**Stdev**	**Stdev (%)**	**Metal**		**Concentration (ppm)**	**Stdev**	**Stdev (%)**
Cr	I	34	28	84	**Zn**	I	14132	27953	198
	II	64	48	75		II	952	1459	153
	III	2156	207	10		III	2672	2523	94
	IV	2202	160	7		IV	2041	2550	125
	V	1949	164	8		V	5061	3423	68
	VI	4739	932	20		VI	3095	2512	81
Mn	I	76	14	18	**As**	I	197	52	26
	II	3	1	31		II	70	16	23
	III	3	2	60		III	526	277	53
	IV	99	62	63		IV	455	209	46
	V	16	7	43		V	237	116	49
	VI	298	130	43		VI	10696	3125	29
Fe	I	566	156	28	**Cd**	I	53	14	27
	II	37	19	50		II	28	8	29
	III	7912	4837	61		III	4	5	118
	IV	7402	3710	50		IV	2	5	200
	V	287	151	53		V	0	0	-
	VI	16809	4699	28		VI	0	0	-
Co	I	6899	1376	20	**Pb**	I	106	74	70
	II	362	121	33		II	47	12	26
	III	557	727	130		III	199	196	99
	IV	739	630	85		IV	493	407	82
	V	2237	2108	94		V	22	23	104
	VI	12293	15280	124		VI	5095	764	15
Ni	I	1608	570	35	**Th**	I	50	14	28
	II	0	0	-		II	22	7	31
	III	244	330	135		III	249	132	53
	IV	378	357	94		IV	63	27	43
	V	197	252	128		V	1	2	200
	VI	2542	997	39		VI	1301	311	24
Cu	I	3958	4337	110	**U**	I	159	94	59
	II	1577	1679	106		II	37	24	66
	III	5161	5121	99		III	1124	1794	160
	IV	10280	4255	41		IV	146	179	122
	V	500833	180687	36		V	81	20	24
	VI	80544	29453	37		VI	367	115	31

Appendix 15. The analytical data of the sequential extractions performed for the Rautuvaara waste rock measured with ICP-MS. I – VI refer to extraction fractions: I = Exchangeable fraction I; II = Exchangeable fraction II; III = Mild acid-soluble fraction; IV = Reducible fraction; V = Oxidizable fraction; VI = Strong acid-soluble fraction. The error is given as a standard deviation (stdev).

Waste rock									
Metal		**Concentration (ppm)**	**Stdev**	**Stdev (%)**	**Metal**		**Concentration (ppm)**	**Stdev**	**Stdev (%)**
Cr	I	0	-	-	**Zn**	I	2162	3058	141
	II	26	37	141		II	3174	4488	141
	III	1626	32	2		III	0	-	-
	IV	1885	159	8		IV	3100	1498	48
	V	1838	124	7		V	8768	9680	110
	VI	13380	1317	10		VI	8624	6104	71
Mn	I	3	3	87	**As**	I	132	33	25
	II	1	0	2		II	60	8	14
	III	2	1	34		III	48	7	14
	IV	16	2	14		IV	79	15	19
	V	7	0	5		V	9	13	141
	VI	85	4	5		VI	1240	172	14
Fe	I	1	1	74	**Cd**	I	20	28	141
	II	3	1	38		II	7	10	141
	III	355	134	38		III	0	-	-
	IV	2485	188	8		IV	0	-	-
	V	103	41	40		V	0	-	-
	VI	21705	88	0		VI	0	-	-
Co	I	812	561	69	**Pb**	I	44	46	105
	II	213	19	9		II	55	19	34
	III	322	180	56		III	127	20	15
	IV	1882	840	45		IV	567	128	23
	V	2368	883	37		V	74	20	27
	VI	9853	1004	10		VI	3718	751	20
Ni	I	424	372	88	**Th**	I	18	24	131
	II	0	-	-		II	5	6	141
	III	99	140	141		III	444	223	50
	IV	1318	594	45		IV	69	17	25
	V	1134	215	19		V	3	4	141
	VI	15638	3252	21		VI	9137	89	1
Cu	I	8483	4255	50	**U**	I	33	3	10
	II	3021	411	14		II	21	16	78
	III	5301	2926	55		III	496	25	5
	IV	21943	4685	21		IV	502	23	5
	V	17129	4086	24		V	237	8	3
	VI	116439	15303	13		VI	2032	81	4